metals

MDPI

Review

Friction Stir Welding/Processing of Various Metals with Working Tools of Different Materials and Its Peculiarities for Titanium Alloys: A Review

Andrey Chumaevskii *, Alihan Amirov, Aleksey Ivanov, Valery Rubtsov and Evgeny Kolubaev

Institute of Strength Physics and Materials Science, Siberian Branch of Russian Academy of Sciences, 634055 Tomsk, Russia; amirov@ispms.ru (A.A.); ivan@ispms.ru (A.I.); rvy@ispms.ru (V.R.); eak@ispms.ru (E.K.)
* Correspondence: tch7av@gmail.com; Tel.: +7-(3822)-28-68-63

Abstract: A review of the state of research in the field of friction stir welding and processing has been carried out. The features of plastic flow in friction stir welding and their connection with the processes of adhesion friction are shown. The main direction of research is related to the features of friction stir welding of titanium alloys. Special attention is paid to the selection of working tool materials from various alloys for friction stir welding and the processing of titanium alloys. The main advantages and disadvantages of applying different types of tools for friction stir welding of titanium alloys are shown. Different mechanisms of tool wear in friction stir welding associated with the interaction of processed material and tools are demonstrated. Information on the influence of tool and material interaction at welding on the mechanical properties and operational characteristics of obtained joints is given.

Keywords: friction stir welding; friction stir processing; titanium alloys; working tools materials; tool wear mechanism

Citation: Chumaevskii, A.; Amirov, A.; Ivanov, A.; Rubtsov, V.; Kolubaev, E. Friction Stir Welding/Processing of Various Metals with Working Tools of Different Materials and Its Peculiarities for Titanium Alloys: A Review. *Metals* **2023**, *13*, 970. https://doi.org/10.3390/met13050970

Academic Editors: Hailin Yang and Masahiro Fukumoto

Received: 2 March 2023
Revised: 18 April 2023
Accepted: 9 May 2023
Published: 17 May 2023

1. Introduction

In recent decades, technologies of solid-phase production of inseparable joints and surface treatment of metallic materials [1–3], based on adhesion heating, frictional heating, and intensive thermomechanical mixing of materials described in a rather wide range of research studies have been intensively developed [4–6] et al.

The most intensively developed types of such technologies are friction stir welding [2] and processing [3], as evidenced by an increasing number of publications in recent years. Less in demand are friction drilling technology, friction stir additive technology, friction stir internal channel technology, friction stir soldering, etc. [7–10]. All these technologies are similar to the friction welding technology widely used in industry [11], but differ from it in purpose, plastic flow geometry, applied technological equipment, and tools.

Friction stir welding makes it possible to obtain permanent joints of aluminum [12–14], copper [15,16], titanium [17], and magnesium [18] alloys and steels [19,20], including those that are weldable within limits or not weldable by conventional fusion welding. Welding provides high-strength and defect-free permanent joints of high-strength heat-strengthened aluminum alloys used in the aerospace industry [21–25], heterogeneous metals, and alloys [26], including joints of the "titanium–aluminum" system [27–29], "aluminum–copper" system [30–32], "aluminum–steel" system [26,33], "aluminum–magnesium" system [34], "magnesium–titanium" system [35–37], and "magnesium–steel" system [38], etc. The possibilities of regulating process parameters and changing the configuration and material of welding tools allow us to obtain permanent joints of different metals and alloys of large thicknesses by friction stir welding [39–44].

Friction stir processing makes it possible to modify surface layers with the formation of a fine grain structure [45] of items made of materials with intense unstrengthening under

excessive heat input or melting [46–48]. By using friction stir processing, a modification of the structure of aluminum [49], copper [50–53], titanium [54–56], magnesium [57–59] alloys, steels [60], and titanium nickelide [61] is possible. It is also possible to obtain composite materials on this basis by introducing powder particles of metals [62,63], alloys [64], ceramics [65–67], graphite [68], oxides [69], MAX-phases [70], or their compositions [71–73] during processing. Friction stir processing is widely used to obtain hybrid composites for tribological purposes [74–76]. Additionally, friction stir processing is used to obtain workpieces for subsequent pressure forming using the effect of superplasticity [77]. The combined use of friction stirring processing and additive technologies makes it possible to obtain materials with different combinations of structure and functional characteristics, as well as to enhance structurally homogeneous and defect-free products obtained by 3D printing methods [78–81].

One of the present research directions is the application of friction stir welding or processing technologies to modify the structure and joining of products made of titanium alloys [17,81–86]. Since titanium alloys have a high specific strength, heat resistance, and high corrosion resistance, they are widely used in various industries and medicine [87]. Medium-strength titanium alloys can be used for the production of propeller shafts, cladding, pump parts, and propellers for shipbuilding needs. High-alloy titanium can be used for the production of diesel engine silencers for submarines, thin-walled tubes for condensers and heat exchangers, and disks for measuring instruments [88]. In addition, the use of titanium alloys makes it possible to significantly reduce the total weight, thereby increasing the cargo capacity and mobility of marine ships [89]. In the automotive industry, titanium alloys can be used to produce load-bearing steel structures, most critical engine parts, chassis components, heat exchangers, etc. The use of titanium high-strength alloys in aircraft construction contributes to aircraft weight reduction [90].

Conventional methods of jointing titanium alloys are traditional types of fusion welding, such as electron-beam welding [91], laser welding [92], plasma welding [93], arc welding with non-consumable and consumable electrodes in an inert gas environment [94,95], and electroslag welding [96], etc. Traditional types of welding are characterized by uneven heating of material and the formation of a wide zone of thermal influence. During welding, elastoplastic deformations and residual stresses occur in a material. Therefore, when welding titanium alloys by traditional methods, heat treatment of welded joints is recommended [97]. The application of friction stir welding of titanium alloys allows us to get rid of typical problems typical of traditional technologies as the process develops at low temperatures.

2. Friction Stir Welding and Processing

As stated previously, friction stir welding and processing are based on the effect of adhesive friction between tool and material, plastic deformation, superplastic metal flow, and other related processes [98–108]. Welding and processing processes are almost identical, and the main difference is the junction line between the plates during welding (Figure 1). Various modifications of the welding process with the formation of angle, lap, or T-joints [109–113] or processing to obtain coatings with complex composition are possible [114]. It is also possible to develop these processes by using bobbin tools [115–117], multi-pin tools [118], square or triangular profile tools [119,120], etc. Both friction stir welding and processing remain unchanged in their basic concepts, although they differ in some respects from the scheme shown below. Both friction stir welding and processing involve a stage when a rotating tool is introduced into a material (Figure 1a,d). This step involves initial heating, plastic deformation, and fragmentation of the material until it reaches a grain size sufficient to initiate a material transfer process along a tool contour. As achieving this grain size is necessary for friction stir welding or processing, these techniques are well suited for forming products with high superplastic properties [120–122]. After plunging the tool into the material until it touches the surface, the tool is moved longitudinally in the direction of welding or processing (Figure 1b,e). In order to perform

welding or processing, the tool is provided with a loading axial force Fz, which presses it against the surface of the material. The reaction of the material to the forces resulting from the tool friction against the material results in a torque Mz. The reaction of the material to the forces occurring as the tool moves longitudinally in the material results in a drag force, Fx. Friction stir welding or processing processes are accompanied by heat generation, which causes heating and cooling of the material area adjacent to the tool [123–126]. This creates relatively stable conditions for plastic deformation and heat generation in the material, compensated by heat dissipation from the tool area and movement of the tool to a lower material temperature. Heat is generated continuously in the tool area, and the material behind the tool cools down relatively quickly. The material deformed by the tool is carried behind the tool and forms the stir zone. Along the edges of the stir zone, zones of thermomechanical effects are formed, differentiated on the advancing AS and retreating RS sides. When welding or processing is complete, the longitudinal movement of the tool in the material is stopped and the rotating tool is moved to the material exit phase (Figure 1c,f). As the material cools, recrystallization processes occur, accompanied by grain growth and structural-phase changes.

The result of friction stir welding or processing is a specific structure in a material, with typical basic structural zones formed by various processes of a thermal or deformation nature [127]. A schematic representation of the subdivision of the material into these zones is shown in Figure 1g. The central area, the stir zone SZ, is a material with a fine-dispersed structure and recrystallized equiaxed grains. At a macro level, the structure of this zone is represented by concentric rings of irregularly shaped material, mostly referred to as "onion rings" in the modern literature [128]. The grain size in this zone may be in the nanocrystalline [79], ultrafine [129], or microcrystalline [130] range. Steels may form various martensitic or bainitic structural states instead of an equiaxial grain structure [131]. Depending on the type and physical nature of the base metal, the mechanical properties of the material in the formed stir zone may increase [132], decrease [105,133], or remain practically unchanged [130] from the initial ones. In order to control the structure of the stir zone, various methods of treatment can be applied: cooling with water [134,135], a mixture of water and ethanol [136], dry ice, liquid nitrogen, compressed air [137], or a mixture of dry ice and ethanol [138], ultrasound application [139–141], the introduction of additional materials [142,143], thermal and thermomechanical post-treatment [144–146], or performing several passes with a tool in succession [147]. Above the stir zone is the thin stir zone, the size of which can vary over a wide range. Its formation is caused by contact of the tool shoulder with the material surface with force Fz and their adhesion interaction. The tool shoulder prevents the extrusion of material from the contact zone with the tool and forms constrained conditions of deformation of the material. Under conditions of interaction between tool pins and material, intensive friction results in the extrusion of material, while under conditions of contact between the material and the tool shoulder friction is less intensive, so that extrusion of material does not occur.

Along the edges of the stir zone is the zone of thermomechanical affection TMAZ, in which the material is represented by grains deformed and stretched in the direction of deformation [148]. This zone can be conventionally divided into two parts. In the part in contact with the stir zone, the fragmentation of grains prevails with the formation of a fine-dispersed structure. In the part remote from the stir zone, plastic deformation of the material with the formation of relatively coarse and elongated, partially fragmented grains is observed [127,149]. The zone of thermomechanical affection differs significantly on the advancing AS and retreating RS sides [150].

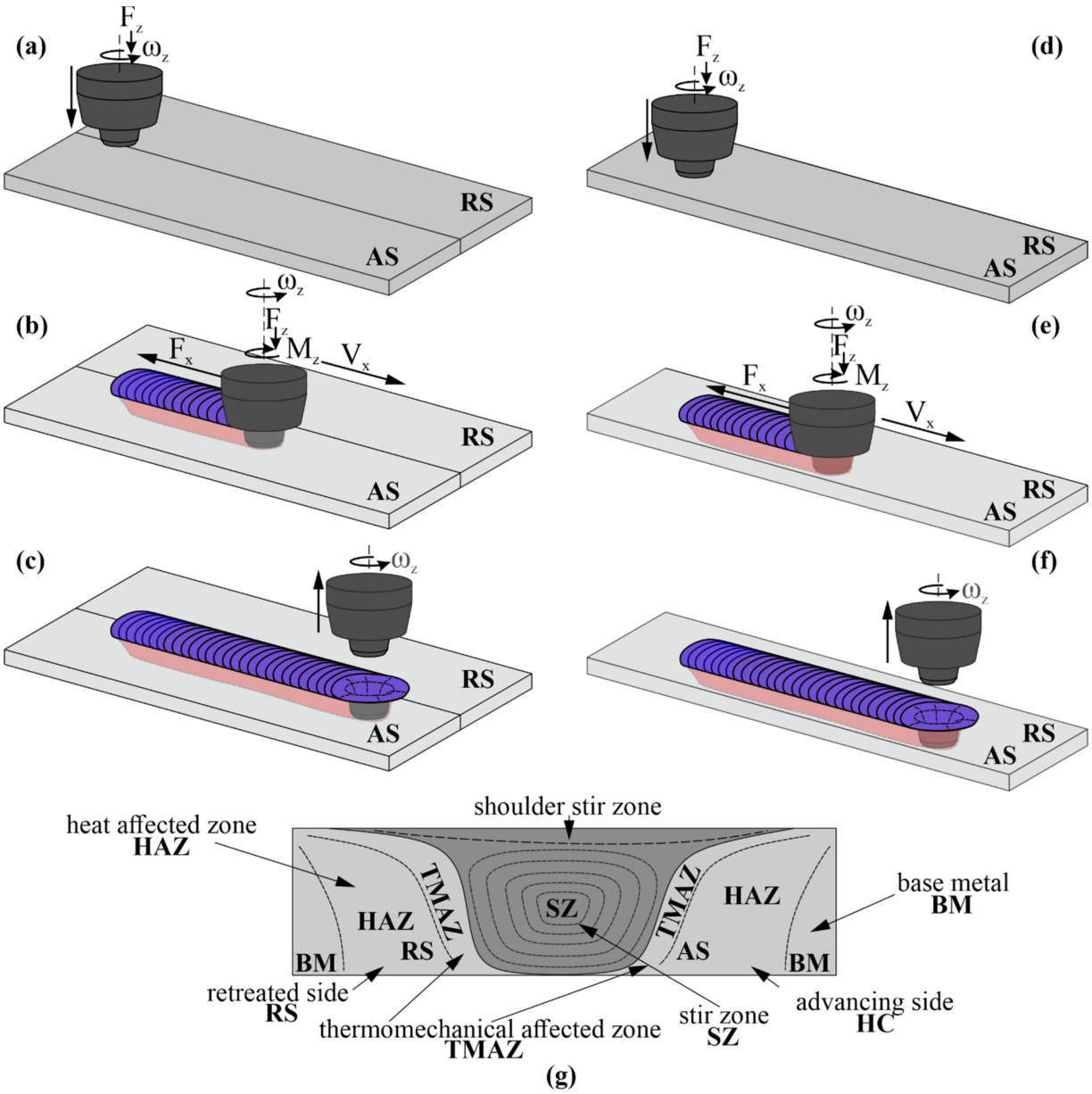

Figure 1. Typical process schemes for friction stir welding (**a**–**c**) and processing (**d**–**f**) and the division of the welding/processing area into characteristic cross-sectional areas (**g**).

The advancing side is the one on which the rotary direction of the point on the surface of the tool coincides with its longitudinal movement. Correspondingly, the retreating side is the opposite side. From the viewpoint of plastic deformation and material transfer, the difference between these sides is of key importance. On the advancing side, metal flow in front of the tool is obstructed because of its interaction with an unheated metal in the longitudinal movement of the tool. On the retreating side, metal flow is in the opposite direction to that of the tool, so that extrusion and adhesion transfer are complementary and mutually reinforcing. The material from the area in front of the tool flows behind the tool through the retreating side; for this reason, the zone of thermomechanical affect on the advancing side is usually considerably smaller than on the retreating side [149]. In composite materials, for example, this leads to an inherently inhomogeneous distribution of the hardening phases in the material volume on the advancing and retreating sides [102]. Therefore, a uniform distribution of strengthening phases in the stir zone requires multiple passes by the tool along the processing line, and the number of necessary passes may vary,

depending on the amount of hardening material introduced [51,118,142,143,151–158]. In addition, such material behavior results in an uneven temperature distribution within the machined volume, which may cause differences in the structural-phase changes and final structure of the material on the advancing and retreating sides.

Outside the zone of thermomechanical affect, there is a zone of thermal affect HAZ, containing undeformed grains of the base metal with traces of thermal influence [159]. In thermally strengthening alloys, the presence of this area causes the disintegration of supersaturated solid solutions, the formation of large incoherent precipitations of secondary phases, or other structural-phase changes. All this may lead to a reduction in material properties and a need for additional material cooling during welding [160,161]. The heat-affected zone will seamlessly transition to the base material (BM) with its structure unaffected by deformation and temperature.

3. Adhesion Friction and Material Flow in Friction Stir Welding and Processing

It was established as early as the middle of the 20th century that frictional interaction without a lubricating layer occurs along individual weld bridges [4,6]. The similarity of material interaction processes in welding and adhesion friction was already known at that stage of research, and a short time later friction welding technology was developed [162–165] and is still being developed today [166]. Later, at the end of the 20th century, the technology of friction stir welding was developed [167].

There was also intensive research into the adhesive interaction of metals and alloys under friction in the absence of a lubricant. At the initial stages of such friction processes, there is mainly plastic deformation of material with the subsequent reorientation of the crystal lattice and formation of a fine grain structure, which was shown using monocrystalline materials [168–171]. With an increase in the degree of deformation of the materials under adhesive friction, the features of plastic flow in the near-surface friction zone become more complicated [5,172–174]. The results of [5,175] indicate the formation of a surface layer with a nanoscale grain structure and low shear stability in adhesive friction conditions. Metal flow in such a layer can be similar to that of a viscous fluid and occur in both laminar and turbulent modes [174,175] (Figure 2). A higher degree of deformation of the material as the loading force increases leads to a more intense outflow of the material from the friction zone and transition to the extrusion friction mode [176]. A number of simulations show that material extrusion conditions occur in the tool–material contact zone [177,178], but the processes inherent to adhesion contact are often not taken into account. Other works describe the process of welding or friction stir welding as a stepwise process of plastic deformation of the material, formation of the ultrafine-dispersed structure of the transfer layer, and its movement from the zone in front of the tool to the stir zone due to its adhesion to the tool [130]. In [127], it was shown that in friction stir processing of aluminum alloy 2024, the formation of structural elements similar to those observed in adhesion friction occurs (Figure 2b). There is also the formation of the heat-affected zone I with a slightly changed structure of the base metal; the plastic deformation zone II; the fragmentation zone III and zone IV or zone of thermomechanical affect; and the zone of metal flow along the contour of the counterbody or tool V and VI (Figure 2b). These zones differ both in the degree of plastic deformation of the material and in the intensity of its structural-phase changes. For example, when a high degree of deformation occurs in layers III–VI, secondary phase particles refine and dissolve in the aluminum matrix and are released from the supersaturated solid solution upon cooling. At the same time in zones I and II, the thermal and strain effects are insufficient for either the process of intensive dissolution of particles or their separation from the solid solution. At the boundary of zones II and III, the secondary phase particles precipitate and enlarge with the formation of large incoherent S-phase precipitates due to relatively high thermal and low strain effects. In layers V and VI, the metal flows along the contour of the tool or counterbody, with the layers closest to the friction surface being set in motion by adhesive bonds with the tool, and those further away by cohesive and extrusive forces [127].

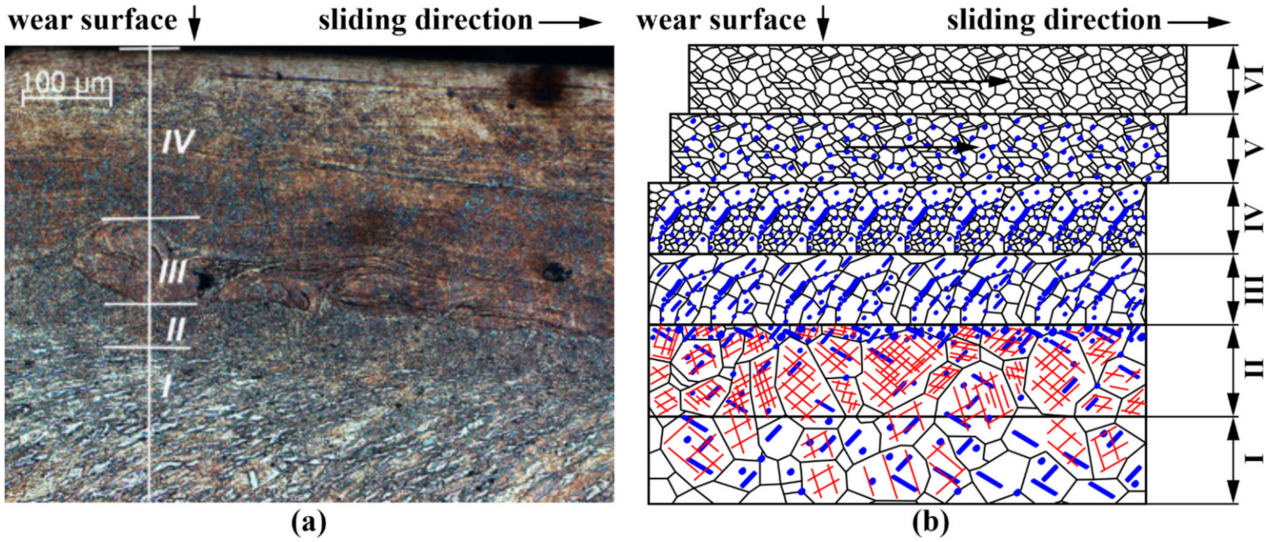

Figure 2. Structure of metal in the friction zone with high loading force: (I) plastic strain zone; (II) fragmentation zone; (III) turbulent flow zone; (IV) laminar flow zone Reprinted with permission from [175] 2010, Elsevier (**a**), a schematic representation of plastic deformation, material fragmentation, and transfer layer formation in adhesion friction, friction stir welding and processing: (I)—base metal, heat affected zone; (II)—plastic strain zone (TMAZ II); (III, IV)—fragmentation zone (TMAZ I); (V, VI)—material flow zone, stir zone (**b**). Data are based on the paper [127].

Thus, the processes of plastic deformation, fragmentation, and material flow in frictional stirring are similar to those realized in adhesive high-load friction. The processes include both metal transfer through superplastic flow initiated by the adhesion of the material to the tool and the phenomenon of metal extrusion from the friction zone as the tool moves in the material. In the process of frictional stirring, the structural-phase changes of the material, caused by its intensive plastic deformation along the tool's contour, additionally occur. These processes may be initiated either by the composition of the material itself [103–105], or by its interaction with the components of the inserted material in the creation of composites [179–184].

Adhesion friction processes of metals and alloys involve both material deformation and fragmentation and structural-phase interactions in the materials. In friction with high loading force, there are ideas about the formation of layers with mechanically mixed material of samples with oxide particles in the conditions of contact of surfaces of rubbing parts, and in friction of dissimilar metals and alloys—basic components, oxides, and results of their interaction, etc. [185–188]. In a number of works, the wear mechanism of materials in friction pairs is described as the sequential formation and destruction of a mechanically mixed layer. This is important for understanding tool–material interaction processes in friction stir welding or machining. Research suggests that frictional interaction and wear processes with the formation of a mechanically mixed layer in frictional stir welding or machining are close to those realized in high-load adhesion friction [106,107]. The typical sequence of the process of self-organization in the materials of rubbing parts with the formation of a mechanically mixed MML layer and its subsequent destruction is true for both adhesion friction and friction stirring action. The material–tool interaction process will be considered in more detail in the final part of the paper. Thus, the processes of material–tool interaction, deformation, and material flow along the tool contour in friction stir welding are similar to those in adhesion friction with high loading force.

The problem of describing the mechanics of the complexly organized plastic flow of a material under frictional action with stirring arose as early as the end of the 20th century [189]. The material in the area of its contact with the tool moves in accordance with both the adhesive and extrusion nature of the flow process. Its transfer along the tool

contour occurs with a clear dependence on the mechanics of the process, associated with the presence of advancing and retreating sides and the difference in the flow of metal in the vertical direction [100–102,177,190–194]. Even in early works on friction stir welding, the material around the tool was separated into an extrusion zone (material transfer zone, superplastic flow zone), a plastic deformation initiation zone (thermomechanically affected zone), a preheating zone, and a cooling zone [2,177]. Later works using mathematical modeling [192] and experimental studies [190] show the peculiarities of material flow both on the advancing and retreating sides and in local areas of the tool action zone. It should be noted that the works show an identical character of metal flow during the welding of both titanium [192] and aluminum [190] alloys.

In [98] it was shown that in the contact zone of the material and the tool, metal flow with the realization of upward flows takes place (Figure 1a). On the retreating side, through which the material enters the zone behind the tool, a downward flow of the material is realized. In general, such flow also occurs in the zone of thermomechanical affect on the advancing and retreating sides. The difference between the metal flow processes on the sides is related to the presence of a point on the advancing side called the pseudo stagnation point [99] (Figure 3b). In this point, material flow can be inhibited and defects can form, for example, in the form of channels or wormholes [195]. In general, the material flow in front of the tool tends to realize downward flows [100] (Figure 3c).

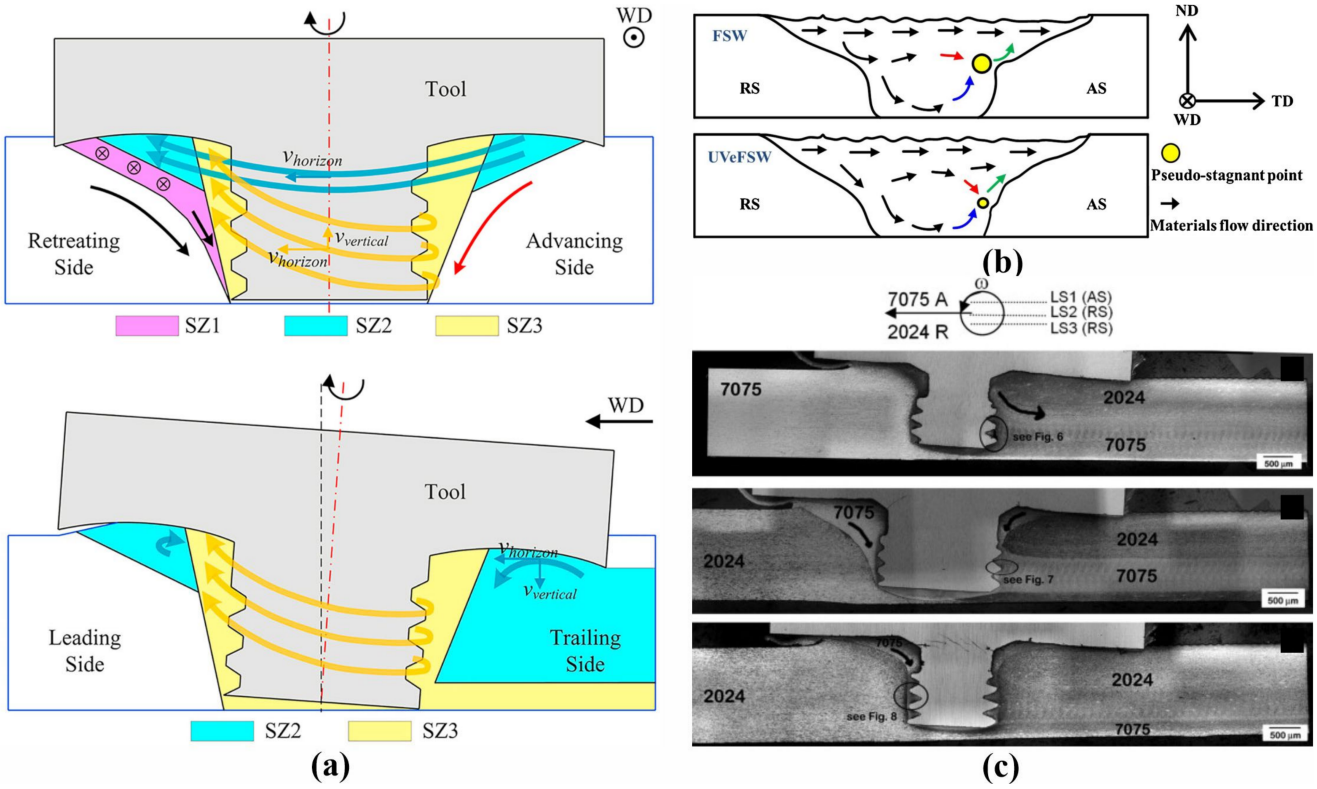

Figure 3. Metal flow during friction stir welding in transverse and longitudinal direction: heterogeneity of stir on the advancing and retreating sides. Reprinted with permission from [98] 2022, Elsevier (**a**), a formation of pseudo-statement point. Reprinted with permission from [99] 2017, Elsevier (**b**), and mixing of materials in the longitudinal section. Reprinted with permission from [100] 2011, Elsevier (**c**), see Figures 6–8.

In the plane perpendicular to the tool, an even more complex pattern of material flow along the tool contour is observed. In [196], it is shown that a single tool pass through the marker material arranged as a flat thin insert perpendicular to the processing line does not lead to its significant mixing. Behind the tool, the material forms a deformed and curved surface that conforms to the shape of the tool. The authors attributed this to the extrusive

nature of the material flow, which is due to the deformation of the machined material when it is constrained by the cold material, the substrate, and the shoulders of the tool.

In [102], using marker material introduced in the tool path, data were obtained on the transfer of material from the zone in front of the tool to the zone behind the tool (Figure 4a,b). It was shown that the material, which was originally on the advancing side, moved to the zone behind the tool also on the advancing side. Similarly, the material on the retreating side moved. Thus, movement of the marker material from the advancing side occurs with the overcoming of a longer way along the contour of the tool that causes a greater degree of deformation, mixing, and refinement (Figure 4a). At the same time, the material on the retreating side remains less deformed. Similar results were obtained in friction stir welding of alloy 6061 with the introduction of marker material in [101]. The formation of upward flows on the retreating side and downward flows on the advancing side was demonstrated. It was revealed that the mixing of the marker material at different sections along the height of the junction occurs in different ways. The authors of the paper concluded that the material extrusion process is determined by tool pressure on the material, and the material transfer process along the tool contour is determined by frictional forces.

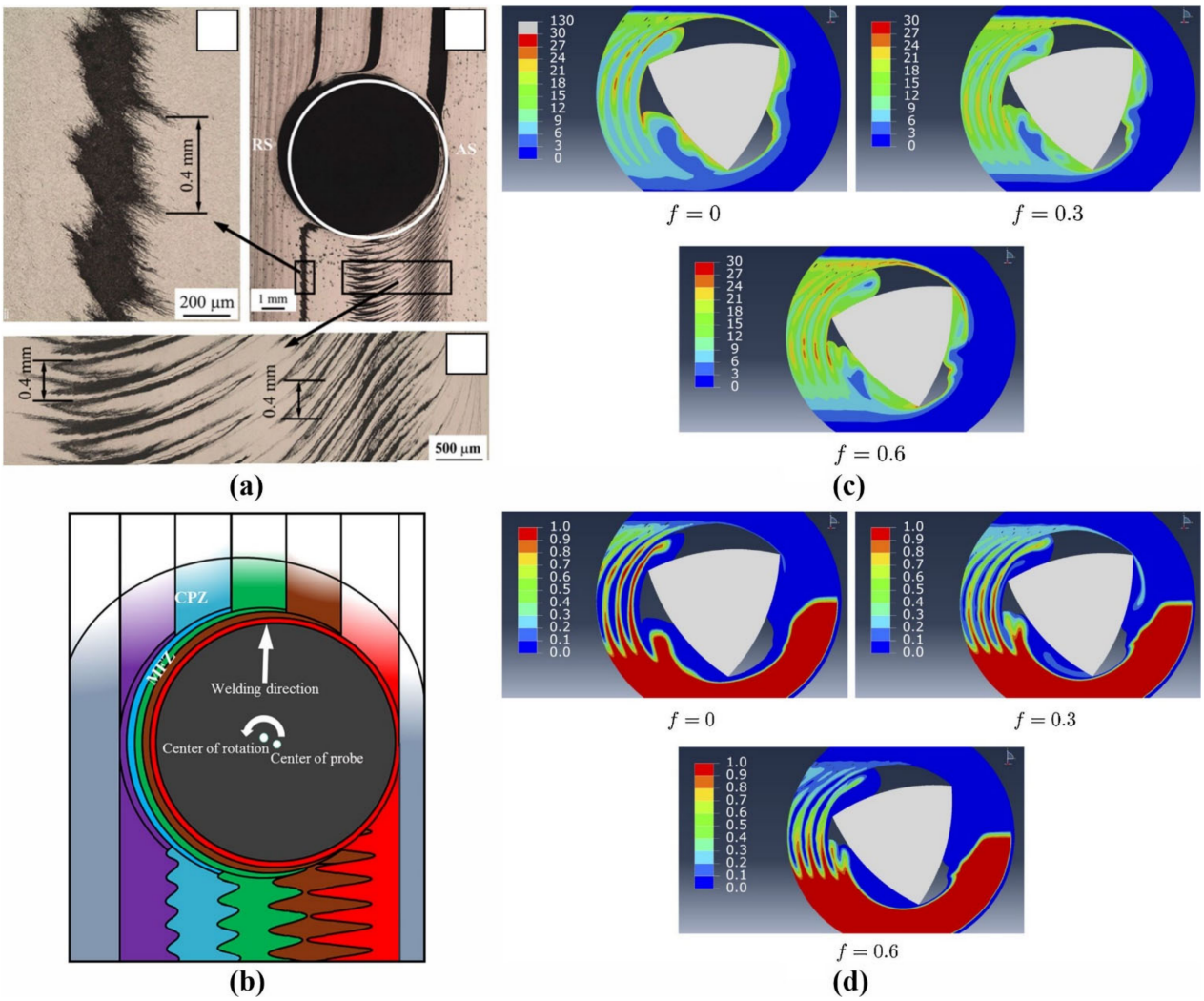

Figure 4. Features of metal transfer in friction stir welding, defined with the use of marker material: material structure after experiment (**a**) and schematic representation (**b**) (Reprinted with permission from [102] 2016, Elsevier) distribution of equivalent plastic strain (**c**), and mixing (**d**) of materials in friction stir welding with a triangular tool (Reprinted with permission from [191] 2017, Elsevier).

In [191], the peculiarities of material mixing and deformation during friction stir welding using a tool with a triangular profile were investigated in experiments and simulations (Figure 4c,d). Material transfer occurs when it is plastically displaced from the zone of contact with the tool. The greatest degree of material deformation is characteristic of that part of the transfer layer where there is direct contact between the tool edges and the material (Figure 4c). Mixing of the material on the advancing and retreating sides occurs non-uniformly, with the formation of a layered structure of the stir zone and alternation of the material of the adjacent plates (Figure 4d).

Material flow along the tool contour acquires a more complex character during friction stir processing of composite materials with the use of multipin tools [118]. In these conditions, due to a large number of small material flows, it is possible to obtain the most uniform distribution of fine-dispersed strengthening phases in the material volume. In turn, this leads to an increase in the operational characteristics of final products.

Understanding the peculiarities of the plastic flow of material under frictional mixing and their connection with the processes of extrusion, adhesion interaction, and structural-phase changes is important since the defectiveness of the processed material depends on them [197]. The formation of weld defects is related, for example, to the presence of a pseudo stagnation point region, or differences in material transfer from the advancing and retreating sides, etc. [99,102,198].

Such defects can be in the form of a tunnel or wormhole [199,200]. Joint lines or "lazy-S" can form at the junction of upward and downward metal flows [201]. Such features of material flow can also be applied, for example, to obtain cooling channels in aluminum plates by friction stir channeling [202]. Analysis of literature sources shows that such peculiarities of flow and material transfer during friction stirring are inherent to both aluminum and copper or titanium alloys, as well as steels, heterogeneous compounds, and composite materials [98–102,191]. However, when processing or welding metals and alloys of different types, material behavior may have features related to the material properties and phase composition, the stability of its structure at high temperatures, its melting temperature, the configuration of the tool used, etc. [16–19,203].

4. Friction Stir Welding and Processing of Various Alloys

Friction stir welding and processing have common features, which are inherent when affecting a wide class of metallic materials. These are heating the material to temperatures of the order of 0.6–0.8 of its melting temperature, formation of a transfer layer along a tool contour, metal flow into an area behind the tool through the retreating side, etc. The differences lie in the different nature of structural-phase transformations during heating and cooling, which causes changes in parameters of the friction stirring process, formation of a structure, and resulting mechanical properties. The treatment of different materials with different melting temperatures implies the use of different welding tools. Increasing the temperature of the frictional stirring process leads to the intensification of structural-phase interactions between a tool and a material, which complicates the process and reduces the durability of the tool.

For this reason, it is necessary to consider not only the general laws of frictional mixing influence but also the distinctive features caused by the properties of processed material and used tools. It is also necessary to compare processes occurring during the welding or processing of metals and alloys of different classes. In order to establish the main features of frictional mixing effects on titanium alloys, it is necessary to analyze data from similar studies of a wide range of materials. This section briefly presents an overview of friction stir welding and processing of various metals and alloys. The main areas of research are related to obtaining permanent joints of aluminum, magnesium, copper, titanium, nickel alloys, and steels. Additionally, in recent years, there is a fairly wide range of works on friction stir welding or processing of high-entropic alloys. A significant number of works are devoted to friction stir welding of dissimilar materials and obtaining composite materials by friction stir processing.

4.1. Friction Stir Welding and Processing of Aluminum and Magnesium Alloys

Some of the most easily friction-stirred alloys are deformable aluminum alloys of the Al-Mg, Al-Mg-Sc, Al-Mg-Sc-Zr, and other systems. [112,130,204–210]. These alloys are characterized by sufficiently high strength and ductility, as well as weldability by various methods. Friction stir welding of these alloys makes it possible to increase the productivity of the manufacturing process of metal parts or structures. Currently, friction stir welding and processing of aluminum–magnesium alloys are the most studied. The use of friction stir processing of Al-Mg-Sc alloys allows an increase in their plasticity at elevated temperatures with the realization of the effect of superplasticity and the formation of an ultrafine-dispersed structure of their surface layers [46,47,211]. For this reason, their processing can be used both for obtaining composite materials with metal matrices and for preparing blanks for subsequent molding using the effect of superplasticity. The typical structure of the thermomechanical affect zone, the stir zone, and the base metal of this type of alloy is shown in Figure 5 [212]. Grain refinement occurs gradually in the zone of thermo-mechanical affect, with small grains first appearing along the boundaries of large grains. The grains also extend along the direction of the metal flow, which is most pronounced near the stir zone. In the stir zone, a structure with equiaxed ultrafine grains measuring 3.0 microns is observed, with the initial grain size being 30 microns.

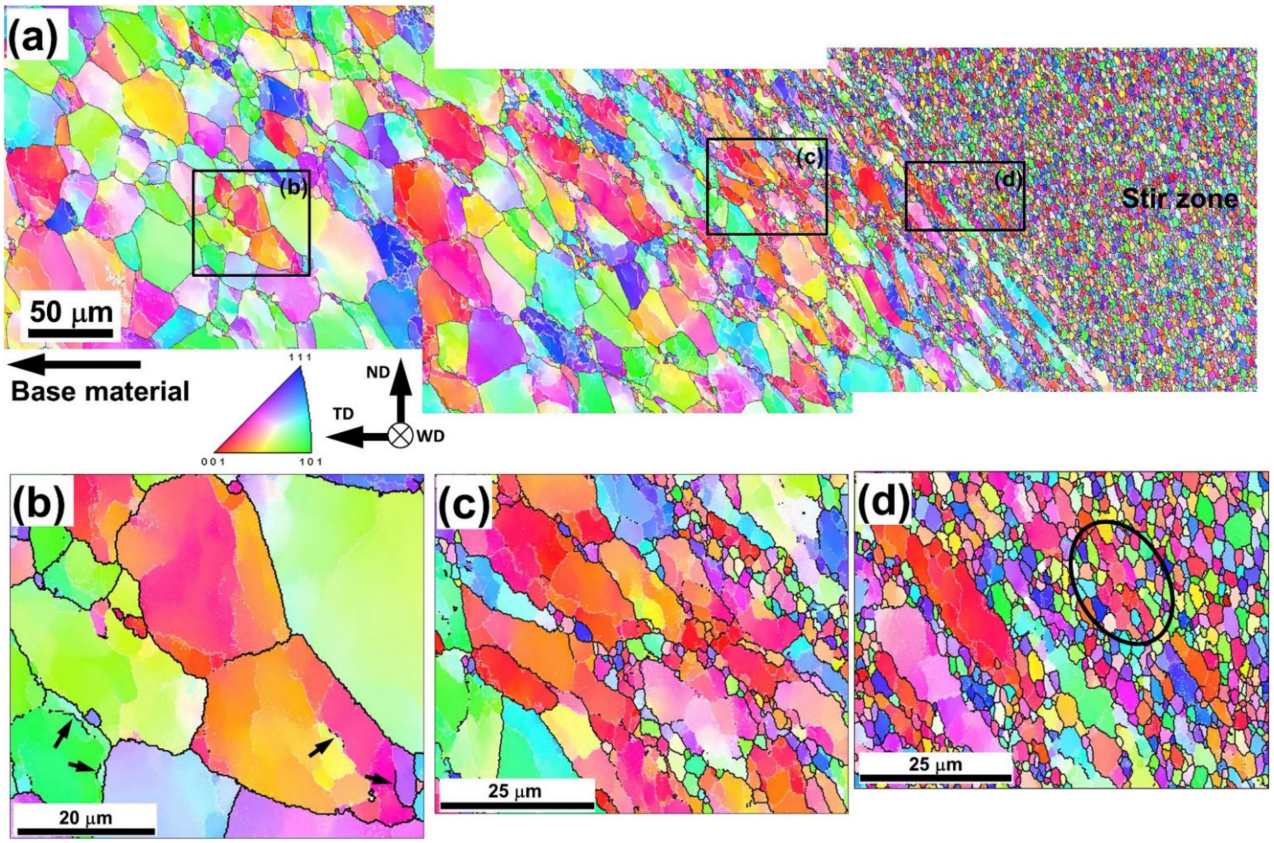

Figure 5. Grain refinement in friction stir welding of the aluminum alloy Al-Mg-Sc (**a**) Composite map from thermo-mechanically affected zone; (**b**) structure of TMAZ closer to the basic metall; (**c**) central part of TMAZ; (**d**) Structure of TMAZ closer to stir zone. Reprinted with permission from [212] 2019, Elsevier.

The effect of friction stirring on the mechanical properties of thermally unhardenable deformable aluminum alloys is due to a number of their structural features. The materials obtained in [212] are characterized by an increase in strength and ductility. For the materials obtained in [204], in spite of significant refinement of the solid solution grains, there is no

significant increase in the strength characteristics. This is due to the fact that the strength of these alloys is related not only to the grain size but also to the presence of iron-containing phases in the particle structure (also particles of intermetallic phases Al3 (Sc, Zr) in the Al-Mg-Sc-Zr alloy), as well as to the sticking of the initial material during its fabrication. During processing, there is no significant refinement of the particles of iron-containing phases, and the riveting of the material is removed, which explains the insignificant improvement of the material properties. Relatively low changes in tensile strength are also characteristic of aluminum–magnesium alloys without the introduction of scandium or zirconium. The yield strength of the alloy increases significantly after treatment. Multi-pass friction stir treatment allows for an increase in the effect of improving the strength properties of these alloys, but the greatest influence on the material properties is exerted by the first pass of the tool. It should be noted that the processing of aluminum–magnesium alloys could be applied to harden not only the surface layers but the entire volume of the material. A number of works indicate the positive effect of friction stir processing of hereditary fine-grained Al-Mg-Sc, Al-Mg-Sc-Zr alloys on the superplastic behavior when deformed at elevated temperatures. This makes the treatment potentially applicable to the preparation of workpieces for subsequent superplastic forming [47,122,213].

Friction stir processing is effective when applied to aluminum alloys produced by additive manufacturing techniques. For example, after multipass treatment of AA5056 alloy obtained by wire additive electron-beam technology [80], the strength limit of the material was increased by 1.7 times and the yield strength by 2.8 times. The main reason for such an increase in strength properties lies in their initially low values due to the additive method of material production. After four passes, the grain size and mechanical properties of the material in the stir zone are comparable to the properties of the processed rolled sheet of this alloy. The treatment eliminated pores and discontinuities in the material structure. This shows the effectiveness of processing to eliminate defects in materials obtained by additive methods and to form an equilibrium structure, only partially dependent on the initial structural-phase state of the material. The processing is also effective in enhancing the properties or joining of other types of aluminum alloy products [214–216].

Friction stir processing and welding of aluminum–silicon casting alloys allow for both permanent joints and hardened surface layers or composites [217–220]. These alloys are characterized by rather low mechanical properties, but they have good casting properties and can be easily 3D-printed using modern methods [221,222]. When manufactured by casting and electron-beam methods, these alloys are characterized by low values of mechanical properties, the presence of defects, and structural heterogeneities. For this reason, the strengthening of their surface layers is a rather urgent task and makes it possible to increase the strength properties of aluminum–silicon alloys [80].

Friction stir processing of heat-strengthened aluminum alloys such as Al-Cu-Mg [13], Al-Zn-Cu-Mg [21,24] and Al-Cu-Li-Mg [105] is a rather complex process and can lead to both positive and negative effects. The structure of the mixing zone of such alloys is represented by typical concentric rings [128]. Compared to non-thermal strengthening alloys, the average grain size of the solid solution can be [127] of the order of 1.0–1.1 μm. In most of the works, the authors fail to achieve high bond strength or treatment zone of complex hardenable alloys without the use of additional cooling [25,105,133]. There are also data on increasing the strength of welded joints with the use of subsequent heat treatment [223]. Alloys of the Al-Cu-Mg system lend themselves well to friction stir welding and processing [13]. The use of additional cooling during welding or processing makes it possible to achieve the high-strength characteristics of Al-Zn-Cu-Mg and other types of alloys, including when obtaining joints of dissimilar alloys [224–226].

Welding and processing of aluminum alloys may be performed with tools of various shapes and sizes, from 1–1.5 mm to 120 mm and more, including when obtaining metal matrix composites [130,227]. The formation of structures during friction stir processing of thick plates is associated with the division of the stir zone into separate flows formed by the flow of material along the contour of the tool [130].

Tool wear in friction stir welding of aluminum alloys is rather slow. This is due to the relatively low temperature of the welding process for heat-resistant or H13, high-carbon, and high-chromium HCHCr steels used for tool fabrication [43,228–232]. The WC-Co alloy tool showed high durability when welding aluminum alloys. Its pin was significantly worn when welding an Al-Si AC4A + 30% SiC-based composite [233]. WC is commonly used in the fabrication of tools for high tribological stresses. In its pure form, WC is brittle and prone to fracture under shock and vibration loads accompanying the friction stir impact. To increase its ductility, as a rule, the Co binder phase is added, obtaining a WC-Co composite material with a lower probability of tool fracture from it [234]. A study of the wear of the EN40 high-temperature steel tool during the welding of AA7075 and AA7039 aluminum alloys was also carried out. The effects of welded material strength and thickness and tool feed rate on torque, shear force, and resultant maximum shear stress determining tool wear resistance were evaluated [235].

Friction stir welding or processing of magnesium alloys is quite similar to aluminum alloys in its features [236–242]. For alloys such as WE43, the hardness of the material in the HAZ region has been shown to be less than 70% of the hardness of the parent alloy [243]. Although Mg-Nd-Y type alloys are more effectively hardened by grain refinement than aluminum alloys, the effect of grain refinement can compensate for any loss of strength due to the dissolution of hardening precipitates [244]. When welding magnesium alloys, tools made of H13 tool steel [245–247] or EN31 steel [248] are mostly used. There are also studies where D2 steel [249], AISI Type-302 [250], SKD 61 [251], and GH4169 [252,253] were used as tool materials.

The mechanism of tool wear has been determined in a number of works [108,254]. In friction stir welding, the diffusion interaction of the aluminum alloy and the tool with the formation of a tribological layer on the surface occurs (Figure 6). The phase composition of the tribological layer is presented by the aluminum alloy, oxides, silicides, and intermetallics of the Fe-Al system, and the intermetallide layer of FeAl3 composition is continuous and is located on the whole surface of the tool. In some areas of the layer, "spikes" are formed, which spread deep into the tool material (Figure 6b) and further lead to the formation of wear particles. Presumably, the intermetallic layer protects the tool material from intensive wear during the initial stages of the friction stir welding process. The formation and gradual destruction of such a layer is the main mechanism of tool wear during friction stir welding of aluminum alloys with steel tools [108].

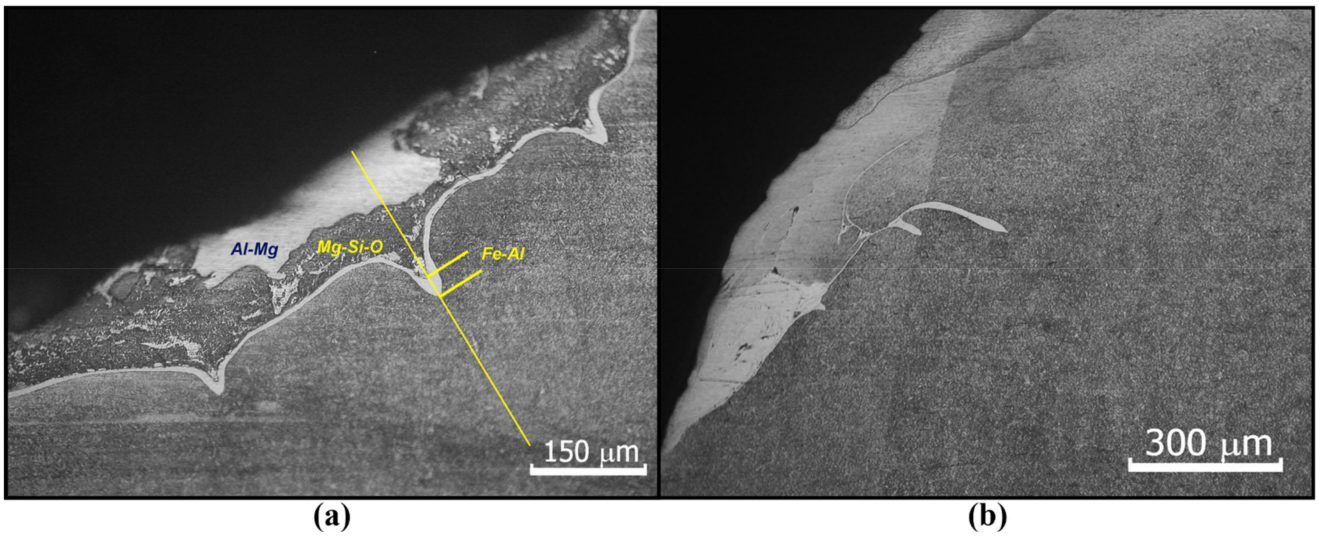

Figure 6. Wear of steel (1.2344 X40CrMoV5-1) tools during friction stir welding of aluminum alloys. (**a**) formation of intermetalic compounds layers on the surface of the tool; (**b**) formation of intermetallic interlayers spreading deep into the tool material. Optical images from the work [108] 2014, Elsevier.

4.2. Friction Stir Welding and Processing of Copper Alloys

Currently, friction stir welding and processing of copper and copper alloys is used both to obtain permanent joints [15,16,255] and to modify [51–53] or harden [256] the surface layer. Copper alloys are characterized by sufficient weldability, so the main application of welding or processing appears to be the joining of dissimilar metals [31,32] or processing to form tribologically resistant, hardened surface layers [257,258]. For the processing of copper and copper alloys, tools made of heat-resistant steels are mainly used [259–262]. However, they have low thermal stability at copper processing temperatures, so it seems more optimal to use tools made of hard alloys [263].

Copper alloys lend themselves quite well to friction stir processing. In the stir zone, mechanical properties increase and the grain size decreases, especially with the introduction of powders of different metals [259,264]. When pure copper is processed, a double increase in strength is possible [265] by reducing the grain size down to 400 nm. Processing of additive-produced copper samples reduces porosity and pore size by a factor of almost 10 [266]. At the same time, the yield strength of the material increases by 1.6 times compared to the base metal. This is due to grain refinement in the mixing zone down to 1–2.5 microns.

When welding copper alloys, steel tools are subjected to intense wear. In work [267], the phenomenon of self-optimization of the tool from steel H13 appeared during the wear process, and the greatest intensity of wear was in the first 300 mm of the welding path. The contact of tool and material does not lead to the formation of an intermetallide layer or tribological layer of variable composition (Figure 7a), which is characteristic of the Cu-Fe system. Only a thin diffusion layer is present on the surface of the tool and the adhered material (Figure 7b). This indicates that in copper welding, the wear mechanism of the steel tool may be related to the gradual thermal degradation of its structure due to a sufficiently high process temperature [267]. Additionally, a significant role can be played by the softening of the surface layer as a result of the formation of solid solutions on the surface of the tool.

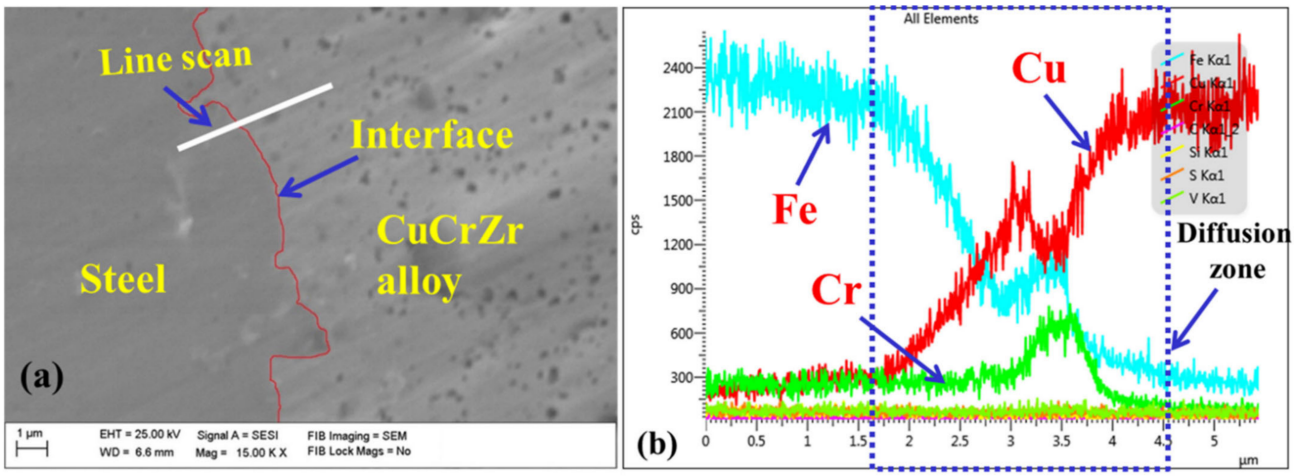

Figure 7. Wear of steel H13 tools during friction stir welding of copper alloy Cu-Cr-Zr SEM image (**a**) and the variation of the chemical element concentration at the boundary (**b**). Reprinted with permission from [267] 2019, Elsevier.

4.3. Friction Stir Welding and Processing of Steels and Nickel Alloys

The choice of welding tool material and tool wear play a key role in the friction stirring of heat-resistant nickel alloys [268–272]. In addition, the microstructure of nickel alloy joints can be affected by the interaction between the material being processed and the tool wear particles. Tools based on polycrystalline cubic boron nitride (pcBN) and tungsten (W) have high heat resistance, so they are often used in welding or processing high-strength alloys [267], such as carbon and stainless steel, titanium, and nickel-based alloys. Tool geometry also has a significant influence on several factors such as heat generated, torque,

shear force, and thermomechanical effects [268]. Important tool characteristics such as tool diameter, shoulder surface angle, pin geometry, and work surface quality of the tool [268,273–275] need to be considered when processing nickel alloys.

pcBN is the preferred tool material for friction stir treatment of nickel alloys because of its high strength and hardness as well as stability at elevated temperatures [276].

Tungsten carbide (WC)-based tools have excellent toughness, and their hardness is approximately 1650 HV [268].

The W-25 wt% Re alloy [276], which is the most common W-based tooling material, is more prone to wear than pcBN. The addition of rhenium lowers the ductile-to-brittle transition temperature, affecting the Peierls stress [277].

The thermal conductivity of a tool material determines the rate of heat dissipation and affects the microstructure of processed material. In terms of tool cost, W-Re or W-La alloys are cheaper than pcBN tools, but they wear more intensively because they have lower heat resistance and hardness [268].

A recently published study [278] on welding high-strength steels showed that a tool containing 70 wt% W, 20 wt% Re, and 10 wt% HfC had better wear resistance than a W-25 wt% Re tool. The alloy with the addition of 2 wt% HfC achieved 1.5 times better durability than the W-25 wt% Re material at 1926 °C. The addition of HfC particles to the alloy effectively prevents grain boundary separation as a result of plastic deformation at high temperatures. Dislocations are restrained by the HfC particles. In this study, it was demonstrated that the W-Re-HfC tool is most resistant to degradation mechanisms, especially strain. Since the approximate cost of a 1-inch diameter and 3-inch length rod for W-25 wt% Re material and W-20 wt% Re-10 wt% HfC material are almost identical, the WRe tool material with HfC addition is a promising tool material for welding high-strength alloys [278].

Another potential tool material was developed by Miyazawa et al., who added 1 at.% Zr to an iridium-based alloy also containing 10 at.% Re [279]. It was shown that when welding 2.2 m of 304 stainless steel, the Zr-stamping alloy tool showed only slight rounding of the pin boundaries, while the Ir-Re alloy tool showed significant wear. Nevertheless, the high cost of iridium makes it not economically feasible to produce such tools today.

Nickel alloys are highly heat-resistant. Therefore, their intense thermomechanical interaction with the tool surface during the frictional stirring action can be assumed. Under these conditions, the introduction of tool wear particles or diffusion of tool material elements into processed material is possible. For example, when welding Inconel 625 alloy, striped tool wear structures usually occur in the material. Research papers [280–282] presented an analysis of Inconel 625 and 718 alloy welds in which EDS analysis detected W in the joint material, presumably as a result of WC-Co tool wear. However, EDS analysis and SEM studies showed no cobalt in the processed material. Similarly, when alloy 600 was welded with a pcBN tool, a small grain size area containing small boron nitride wear particles was observed in the stir zone. It was concluded that grain growth during cooling was locally prevented by the presence of boron nitride particles at the grain boundaries [283].

Wearing hard-alloy tools in friction stir welding occurs in a rather complex way [284] (Figure 8). This paper suggests 3 basic mechanisms of wear with the realization of deformation and fatigue failure of binder, surface oxidation, and formation of complex W-Fe-O compounds, as evidenced by the formation of corresponding elements on the tool surface (Figure 8). The application of the tool modified by Ni and Cr3C2 allowed an increase in the wear resistance of titanium alloy due to the reduction in oxidative wear intensity (Figure 8a,b).

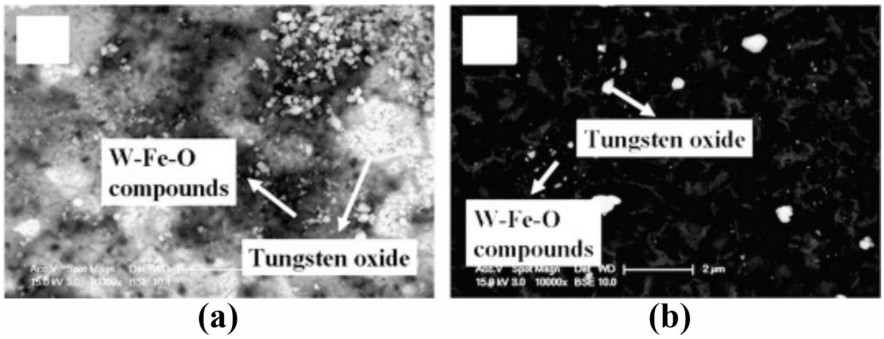

Figure 8. Structure of the tool surface after friction stir spot welding with a WC-Co carbide tool WC-13 weight% Co carbide tool (**a**) and tool of this alloy with 6 wt% Ni and 1.5 wt% Cr_3C_2 additions (**b**). Reprinted with permission from [284] 2021, Elsevier.

4.4. Friction Stir Welding and Processing of Dissimilar or Composite Materials

One of the significant advantages of friction stir welding or processing technologies is the possibility of obtaining inseparable joints from dissimilar metals, composites, and coatings [26,285,286]. It is possible to produce dissimilar weldments based on aluminum and titanium [27–29], magnesium and titanium [35–37], and aluminum and copper alloys [30–32], etc.

Under the conditions of friction stir processing or welding, a number of structural and phase changes of processed materials occur, caused by processes occurring in different areas along the contour of the tool [127,260,287]. Such processes may include mutual dissolution of system components with the formation of supersaturated solid solutions or intermetallic phases, occurring during intense plastic deformation under conditions of elevated temperature [105,127]. Another basic process is the decomposition of supersaturated solid solutions with the formation of particles of secondary intermetallic phases in the stir zone behind the tool at a gradual decrease in temperature [260,287].

The formation of a heterogeneous gradient structure during processing or welding depends significantly on the melting temperature of the components, their mutual solubility, the phases formed in the contact zone, the ratio of the components, as well as the rotational speed of the tool, the loading force, and the longitudinal speed [260,287]. These processes are further complicated by inhomogeneities of plastic deformation, grain refinement, and material flow, as well as by non-uniform temperature distribution at different distances from the tool [288,289]. Compounds from heterogeneous metals and alloys are usually obtained in a plasticized and fine-grained state [290–311]. If alloy components are capable of forming compounds, they can contact and exothermally react with each other to form intermetallic compounds and thus form a liquid phase, which was noted in [260,261]. Friction stir welding of dissimilar alloys with close melting temperatures is most effective, for example, when welding aluminum and magnesium alloys (Figure 9a) [302]. In this case, the formation of structure defects is possible, but by selecting the parameters, it is possible to minimize them without excessive formation of thick continuous interlayers of intermetallic compounds between the components.

The interaction of materials with limited solubility and significant differences in melting temperatures leads to the formation of intermetallic phases in the stir zone [298,300,301]. Intermetallide phases formed in welded joints of aluminum alloys and copper alloys, such as brasses, contain copper, aluminum, and zinc [292,293,299–301]. Various types of defects can form on the boundary of aluminum alloy and brass, which is associated with the formation of eutectics or large interlayers of intermetallides between the plates to be welded [292,293,301]. Brittle Al_2Cu, Al_4Cu_9, and CuZn intermetallides were found in the stir zone in the AA5083/CuZn34 weld joint [301]. The thickness of the intermetallide layer depended on the rotational speed of the tool and the welding speed.

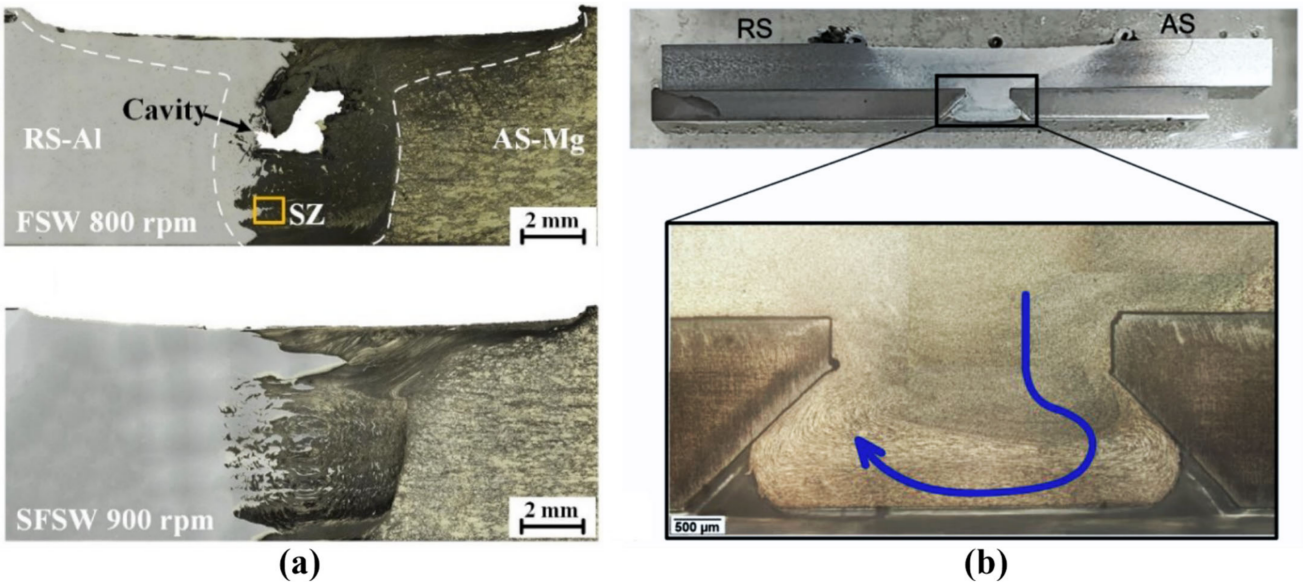

Figure 9. Structure formation in samples of dissimilar joints obtained by friction stir welding of aluminum and magnesium alloy (**a**). Reprinted with permission from [302] 2022, MDPI. Features of metal flow and structure formation when joining heterogeneous alloys based on titanium and aluminum (**b**). Reprinted with permission from [308] 2023, MDPI.

Intermetallides and their heterogeneous distribution are a major problem in dissimilar compounds because they reduce electrical and thermal conductivity and degrade the mechanical properties of the joint. Various methods are used to solve this problem, such as minimizing heat dissipation or using additional cooling in the process of joining materials [134–138]. When butt welding copper and aluminum, the formation of individual particles or interlayers of intermetallides is possible [303]. To reduce the thickness of intermetallic layers, a number of works use the introduction of ultrasonic impact during welding [304]. The effect of different tool configurations on heat release, metal flow, and formation of intermetallic layers in spot friction stir welding of dissimilar metals based on Cu and Al was studied in [305]. In butt welding of Cu and Al, cracks and intermetallic layers of $CuAl_2$ and Al_4Cu_9 have been found at material interfaces [306,307].

The method described in [308] can also be used to join dissimilar components without their structural-phase interaction associated with mutual diffusion. In this method, holes are drilled in the titanium plate to join aluminum and titanium alloys. Due to high pressure on the welding tool, plasticization, grinding, and superplastic material flow, the holes are filled with aluminum extruded into them, extruded out of the mixing zone (Figure 9b). A separate direction is friction stir brazing, also used to reduce the interaction between dissimilar metals during joining [299].

The processes of friction stir welding of titanium alloys with aluminum alloys are widely investigated. These groups of alloys are most commonly used in the aviation and space industries, so their welding is of great industrial interest [28,309]. Since titanium alloys are involved in the welding process, a welding tool is subjected to high thermomechanical stresses, due to which tools made of tool steel are very rarely used. Tungsten carbide tools with cobalt additives [310] as well as tungsten-rhenium tools [183] are mainly used in welding and processing titanium and aluminum alloys.

However, the use of tool steel [311] is acceptable in the case of a lap joint and only if the tool is introduced from the aluminum alloy side without deep plunging into the titanium alloy [312]. In studies on tool wear during the welding of titanium alloys, it has been shown that the greatest wear occurs at the pin-to-shoulder transition of the tool [313]. The use of tool steel is allowed if this place remains in the zone of the aluminum alloy during welding.

It should be noted that lap joints in welding titanium and aluminum alloys are preferable [314,315] since the thickness of the formed intermetallide layer is much smaller than in the case of butt welding [316].

In addition, research is being conducted on ways to reduce tool wear during the welding of titanium and aluminum alloys [317]. For example, in [29], it was proposed to use friction surfacing (FS) to increase tool life. The authors claim that the use of friction surfacing (FS) not only prevented tool wear but also ensured the strength characteristics of the joint at the level of 85.3% of the strength of the original aluminum alloy.

It is also worth mentioning heterogeneous joints of titanium alloy Ti6Al4V and titanium nickelide were obtained by the FSW method in the study [318]. Even though there were many defects in the resulting joint, the achieved mechanical properties of the joint were better than those of similar joints obtained by laser welding [319,320]. Such joints have great potential in medicine. Therefore, it is necessary to continue research work in the direction of titanium alloys and titanium nickelide joints.

HSS steel tools when welding aluminum alloy and copper [321] can experience both adhesion and abrasion wear due to the formation of intermetallic phases (Figure 10). The additional introduction of carbon nanotubes into the weld material led to the formation of carbides that increased the abrasive wear of the tool pins. In this case, such intensity of wear, as in the welding with a steel tool of copper or its alloys, does not occur in this case.

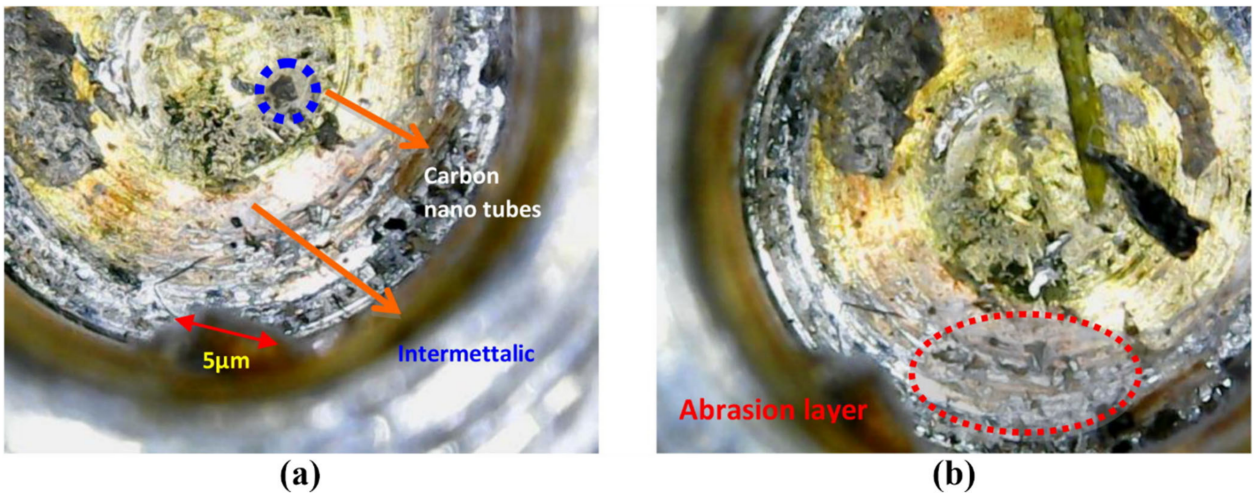

Figure 10. Pin surface morphology after friction stir welding of AA6061 aluminum alloy and pure copper. Formation of intermetallides (**a**) and abrasion marks (**b**) on the surface of the pin. Reprinted with permission from [321] 2020, Elsevier.

Metal-matrix composite materials obtained by friction stir processing on the surface of various objects have high strength and wear resistance of the surface layers with plasticity and fatigue resistance at the level of the base metal, for example, aluminum alloy [322]. When obtaining composite materials, not only structural-phase changes in the material occur, but also the plastic flow of the metal along the contour of the tool becomes more complicated [198].

Strengthening particles can either be introduced into the stirred material from outside [323–327] or formed in situ [328–330] due to solid-phase reactions between the components introduced into the volume and the base metal. Obtaining hybrid composites by the in situ method has several advantages. The first advantage is that in situ reactions allow the production of finer and more homogeneously distributed strengthening particles [331]. The second advantage is that either coherent or semi-coherent boundaries can be formed between these particles and the matrix [332–334], and hence the particle–matrix connection is strengthened [335].

A separate area of composite materials production is their production by a hybrid method that includes additive electron-beam printing and subsequent friction stir processing [79,336,337]. In this case, it is possible to solve several problems at once: homogenization of the structure, elimination of electron-beam defects, and improvement of mechanical and tribological properties of the finished material. In the mentioned works on obtaining composites on the basis of steel and copper, a nanocrystalline structure was formed in the mixing zone. Tools from nickel heat-resistant alloy and alloy on the basis of tungsten carbide were used for processing composites.

For friction stir processing of composite materials, tools that are used for the processing of basic metal can be applied. An increase in the wearability of tools in friction stir processing of composites is noted; this effect is due to the abrasive component being involved in the processes of wear and friction of the tool material [234,338]. The helical grooves on the surface of the tool pins are subject to the highest wear. The authors show that self-optimization of the tool pin shape occurs during welding. In [339], the mechanism of abrasive tool wear during the processing of composites on the basis of aluminum alloy and silicon carbide, based on micro plowing and micro cutting, is presented. The application of the additional hardening coating AlCrN allows for a significant reduction in tool wear. The authors offer an explanation of the tool wear process (Figure 11) in the form of sequential shearing of micro-incisions on the tool surface by silicon carbide particles. Accordingly, the wear of the tool surface is intensified by the abrasive effect of the hardening phase on the tool.

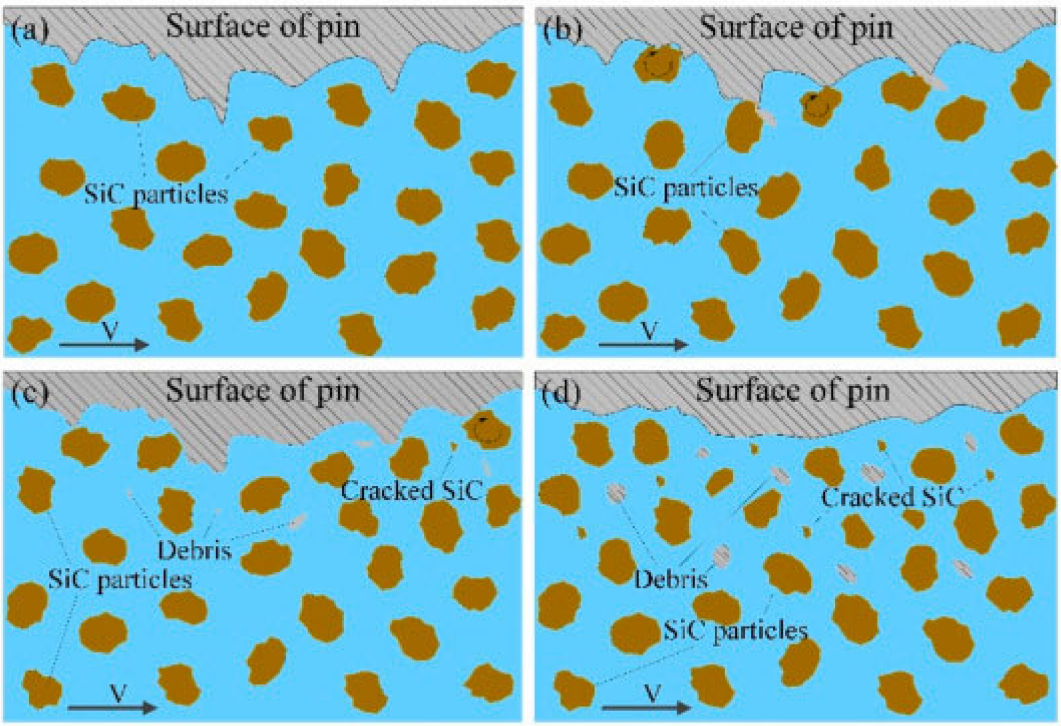

Figure 11. Schematic representation of the tool wear process during production of SiCp/Al composite material. Different stages of the tool pin wear process (**a**–**d**). Reprinted with permission from [339] 2022, Elsevier.

4.5. Friction Stir Welding and Processing of Titanium Alloys

Unlike weldable aluminum [108,340], magnesium [341], or copper alloys [336,342], titanium alloys are characterized by low thermal conductivity, high melting point, and high specific strength, and are subject to oxidation at high temperatures. Therefore, the welding of titanium alloys has a number of special features. Currently, friction stir welding of titanium alloys is intensively investigated, as evidenced by a rather large number of papers

in the literature [17,82–86,268,278,340,341,343–375]. In the field of friction stir welding of titanium alloys, the research is less intensive [81,106,287,313,357,376–382].

When welding titanium alloys, the weld is predominantly "pool-shaped" (Figure 12a–c [355,370,379]), although other weld shapes are available (Figure 12d [107]), unlike welds of aluminum and magnesium alloys, which have a predominantly elliptical weld shape [268,363,377,383–387].

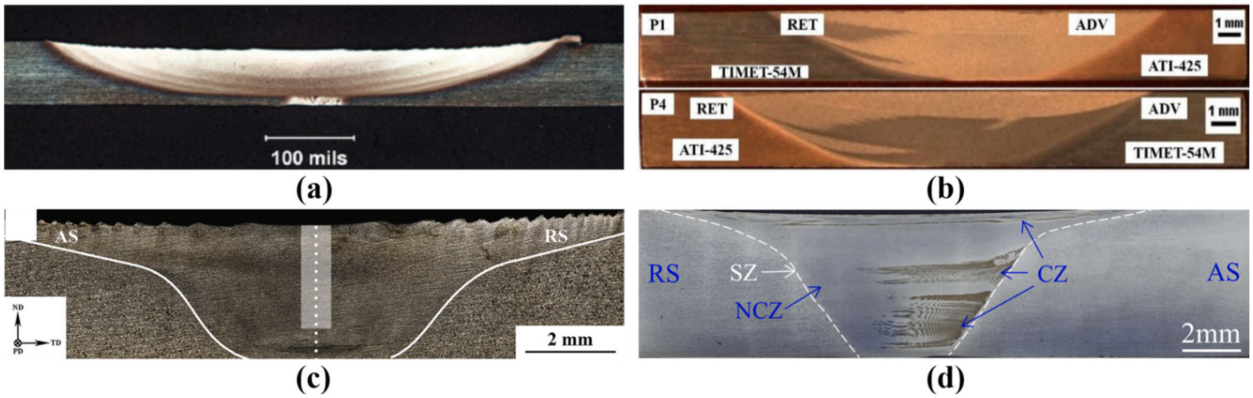

Figure 12. Cross-section structure after friction stir welding and processing of titanium alloys Ti-6Al-4V (**a**) (Reprinted with permission from [369]) 2010, Elsevier) ATTI-425 and TIMET-54M (**b**) (Reprinted with permission from [352] 2016, MDPI), pure titanium (**c**) (Reprinted with permission from [378] 2019, Elsevier) and TA5 (**d**) (Reprinted with permission from [107] 2022, Elsevier).

Since titanium alloys have low thermal conductivity, the thermomechanical and heat-affected zones in their weldings are extremely small [364,370,378,384–392]. Various authors note that there is no heat-affected zone in the welding of commercially pure titanium [343,392–394], and there is no thermomechanically-affected zone in the welding of Ti6Al4V alloy [385,386,389]. The method of friction stir processing makes it possible to significantly increase the mechanical properties of titanium alloys [395–397].

The alloys after treatment show high values of relative elongation at high temperatures and superplasticity due to dynamic grain globulation by dynamic recrystallization. Moreover, the superplastic behavior of the materials was realized in both high and low-temperature ranges. Friction stir processing from one to four passes with the tool leads to a gradual increase in the alpha phase volume fraction and a decrease in the beta phase volume fraction [398].

The first passage of the tool produces the most appreciable change in phase ratio with the formation of a relatively stable structure which is slightly affected by the subsequent passages. When welding or machining titanium alloys, the mechanical properties of the material in the stirred zone may exceed those of the base metal. In a number of works, friction stirring treatment was used to produce composites based on titanium alloys with the introduction of oxide powders Ti6Al4V/TiO2 [399], boron carbide Ti6Al4V/B4C [155], silver Ti-6Al-4V/Ag [400], and copper Ti-6Al-4V/Cu [287], etc. When obtaining composites, it is possible to form a material with increased hardness and wear resistance in the surface layer while maintaining the high strength and medium ductility of the titanium alloy in the main volume of the material.

According to data available in the literature, the welding and processing of titanium alloys with tools made of heat-resistant nickel or cobalt alloys allows for obtaining permanent joints or modified materials with high-strength properties and defect-free structures [106,343,368,392–394,401]. Despite this, tools based on refractory metals and carbide tools are more in demand [268,377,385–391].

Titanium alloys are characterized by the most obvious interaction with the tool material, which poses additional research challenges in the last section of this paper. In general, the welding and processing of titanium alloys is a difficult task due to their chemical activ-

ity, high melting point, low thermal conductivity, phase transformation during heating or cooling, etc. This necessitates a number of special welding process features, which include the use of a shielding gas atmosphere, tool cooling, and higher tool clamping forces, etc.

5. Peculiarities of Friction Stir Welding of Titanium Alloys

Due to the above-mentioned features of friction stir welding of titanium alloys, it is necessary to observe a number of requirements. In order to minimize oxidation during welding, protection in the form of inert gas should be used, for which mainly argon is used in the contact zone of the tool and material [83,85,107,343,352,353,355,358,359,362–368,372,373]. It is possible to use both an open system of shielding gas blowing during welding [353,368], as shown in Figure 13, and to use a tightly closed chamber in the welding area [363]. Since it is difficult to remove heat from the welding zone, most studies show that an active liquid cooling system is used in welding [353,359,368], which can be combined with the shielding gas supply system in one device (Figure 13) [353,368].

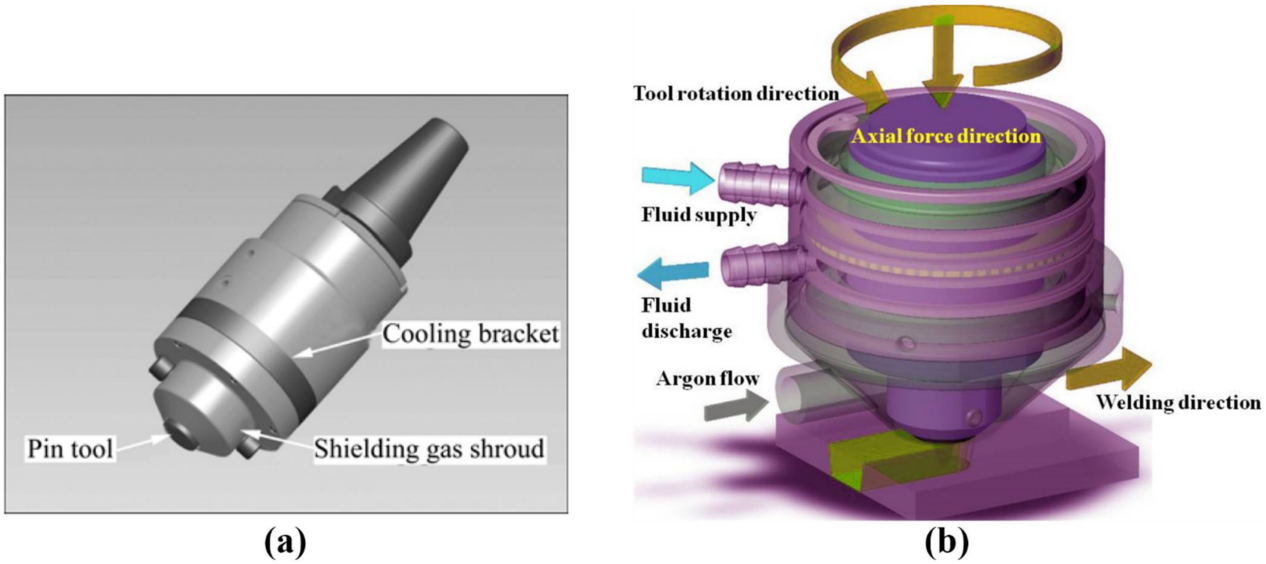

Figure 13. Schematic of friction stir welding process of titanium alloys with tool cooling system and argon blowing of the welding zone from paper (Reprinted with permission from [353] 2010, Elsevier) (**a**) and paper (Reprinted with permission from [368] 2023, MDPI) (**b**).

Friction stir welding or processing requires considerably higher axial loads than for welding aluminum alloys [85,368,402,403]. For this reason, tools for friction stir welding must have high values of strength properties at welding or processing temperatures, which can reach more than 1100 (in peak values, 1300), and when introducing powdered copper particles due to the exothermic formation of intermetallides, 1250 degrees Celsius [287]. Although processing subsequent passes over the same location will reduce the temperature to about 900 degrees Celsius, few materials remain capable of withstanding such high-temperature conditions. Because of the high sensitivity to temperature in the joint-forming zone during the FSW process, the parameters of the welding process must be chosen more precisely, since exceeding the axial load can lead to tool breakage. Additionally, the tool, especially the pin, is subject to cyclic alternating loads during welding or processing, so the tool must be made of a material that can operate for a long time under cyclic loading.

Despite the above requirements for tool strength at high temperatures, one of the most significant requirements for friction stir welding tools is related to their tribological friction resistance when friction is paired with titanium. Early experiments in friction stir welding of titanium alloys revealed a range of problems, including rapid tool wear and tool penetration into the joint [363,383]. In addition, little attention has been paid to the problem of tool wear in general. The highest degree of FSW tool wear occurs while the

tool is immersed in the welded workpieces. In the stir zone, the tool's remaining parts are most obvious near the top surface, as well as on the advancing side of the weld FSW [383]. Tool and titanium alloy contact necessarily lead to interaction at different levels. Mutual diffusion dissolution of the tool and material, formation of secondary phases on the tool surface, formation of the tribological layer, its destruction, and mixing of fragments into the material of the joint or processing zone take place [83,85,106,107,368,370,393,404].

A typical appearance of a tool before and after friction stir welding of titanium alloy Ti-6Al-4V with a tool from the heat-resistant nickel alloy JS6U is shown in Figure 14a,b [85]. A tribological layer of nickel and titanium alloy materials is formed on the tool surface, and the wear is mainly on the tool pin and the contact area of the tool pin and shoulders. On the periphery of the tool shoulders, the wear is minimal. Water cooling, according to the research in the work, allows for a significant reduction in the degree of tool wear after 2 m of welding. Friction stir welding with tools of different types leads to the mixing of tool fragments into the stir zone in addition to tool wear, which occurs in a number of experimental studies even with significant destruction of the instrument pin (Figure 14c) [343]. The insertion of large tool fragments leads to significant disturbances in the metal flow process and changes in the structure of the samples.

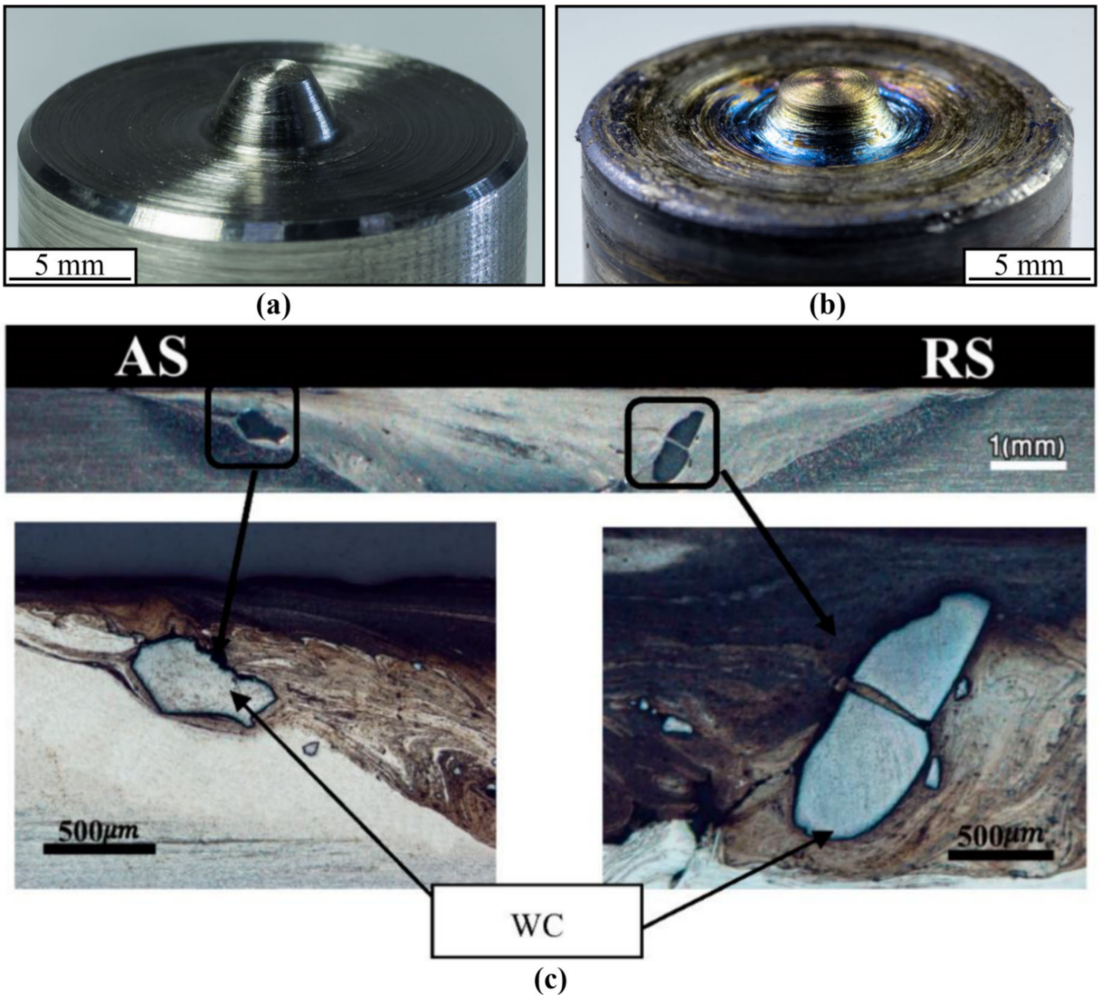

Figure 14. JS6U nickel superalloy tool before (**a**) and after (**b**) friction stir welding of 2 m of Ti-6Al-4V titanium alloy joint (Reprinted with permission from [85] 2021, MDPI), and macro- and microstructure of the stir zone after welding titanium alloy Ti-6Al-4V with a tungsten carbide tool (**c**) debris of WC welding tool in titanium joint (Reprinted with permission from [343] 2016, MDPI).

Given these requirements for friction stir welding tools, FSW tools are usually made of alloys based on refractory materials. These include tungsten or molybdenum-based alloys [268,371,377,385–391,405], cobalt-based alloys [304,392–394], polycrystalline cubic boron nitride [383,386,404], nickel alloys [85,106,368], hard alloys [268,343,357,377], etc. Although tools made of zirconium di-boride ZrB2, sintered titanium carbide, or Ni_3Al-Ni_3V intermetallic alloy were used for friction stir welding [367,406], the five types mentioned above are the main classes of friction stir welding tools currently investigated. Even among the rarely used materials for friction stir welding, some are quite suitable, forming an equally strong base metal joint and having no significant influence on the structure of the stir zone [354], though information about the wear of these tools in welding is not found in the literature. The process of welding with tools of different types is characterized by different regularities of the process of interaction between the tool and material, the structure formed in the material, and mechanical and operational properties.

6. Friction Stir Welding of Titanium Alloys with Working Tools of Various Materials, Tool Wear Mechanism and Change in Structure in Friction Stir Welding and Processing

There are relatively few studies on the structural degradation, wear, and failure of tools made of different materials during friction stir welding or processing [83,85,106,107,343,368–370]. As mentioned earlier, the most studied processes in this field are friction stir welding processes using tools made of tungsten or molybdenum-based alloys, hard alloys, polycrystalline boron nitride, and heat-resistant nickel or cobalt alloys. Each of these alloys in contact with the titanium alloy being processed or welded has its own characteristics of tribological behavior, mechanism, and wear intensity. At the same time, most of them in general wear in a similar way to each other, with a step-by-step formation of a tribological reaction of a mechanically mixed layer on the tool surface, its destruction, and mixing into the welded or processed material. In addition, it should be noted that rapid tool wear in the FSW/FSP process is a key problem preventing the use of this technology on an industrial scale [357], so a review of its wear has been subjected to more detailed analysis.

6.1. Tungsten and Molybdenum Based Alloys

There is quite a lot of information about the welding and processing of titanium alloys in the literature. The least investigated in this area is the application of tools based on various molybdenum-based alloys. For example, a tool made of molybdenum-based alloy was used in the works [371,405,407]. However, the wear process of the tool is not described in the works, and there is no information about how the use of the tool made of this alloy affected the joint.

Technically, pure tungsten has good strength characteristics at elevated temperatures but has low impact toughness and wears out quickly during FSW of materials such as steel or titanium alloys [268]. Although, when rhenium is added to the tungsten alloy, the heat resistance of the tool increases, so that the degree of tool wear decreases. The reserves of rhenium in the earth's crust are limited and adding it to the tool material significantly increases the cost of the tool. There are also reports about obtaining W-25%Re-HfC alloy with AlCrN coating for welding titanium alloy [408]. The obtained samples had high tribological resistance and adhesion of the coating to the base metal. Tungsten tools with the addition of lanthanum are used much less frequently. The authors [355] obtained joints of titanium alloy Ti-6Al-4V using a tungsten-based alloy (W-1%La_2O_3). The structure of welded joints using tools of this type is the least changed due to the interaction of titanium and the tool in comparison with tools of other types (Figure 15). Tool wear during friction stir welding using tungsten and lanthanum oxide tools was performed in [83]. The authors revealed that the deformation and wear of tungsten alloy tools are associated with high shear stresses and low strength of the alloy at high temperatures. The authors also revealed the presence of tool particles in joints.

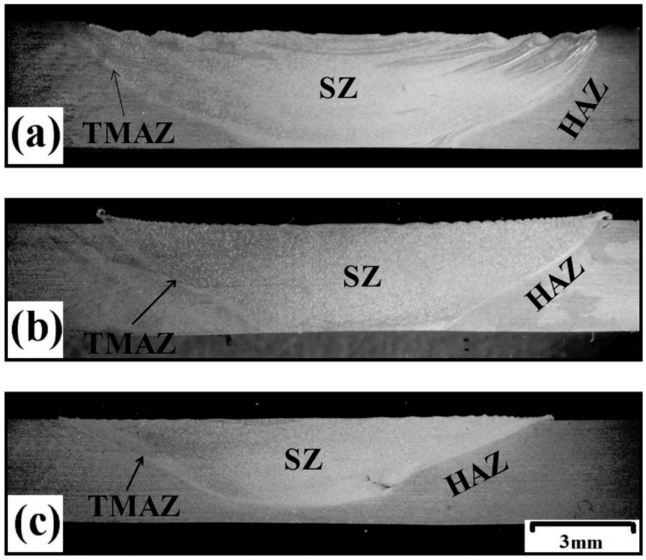

Figure 15. Structure of Ti-6Al-4V alloy welded joints obtained by friction stir welding with tungsten and lanthanum oxide (W-1%La_2O_3) tools (Reprinted with permission from [355] 2018, Elsevier). Traverse speed: (**a**) 40 mm/min, (**b**) 120 mm/min and (**c**) 200 mm/min.

6.2. Hard Alloys

Tools made of tungsten carbide are very popular for FSW of titanium alloys. This material has a high hardness of up to 1650 HV and is insensitive to sudden temperature changes [268]. However, other research demonstrates that during FSW, there is an adhesion layer of titanium carbide on the surface of the FSW joint because of the tendency of titanium and carbon to join together [357]. In addition, carbon monoxide (CO) can be produced during the FSW process due to high temperatures and high pressures [268]. However, if the FSW process is carried out in a protective atmosphere of argon, this observation is insignificant. Friction stir welding with tungsten carbide-based tools produces almost defect-free joints of titanium alloys [379]. However, in this case, the tool gradually wears out and microscopic particles of material enter the stir zone (Figure 16), although they are much smaller than those found in the work [343]. This can be caused by various processes, presumably associated with non-uniform and high contact stresses in the welding zone, leading to fatigue scraping of tool particles from the surface.

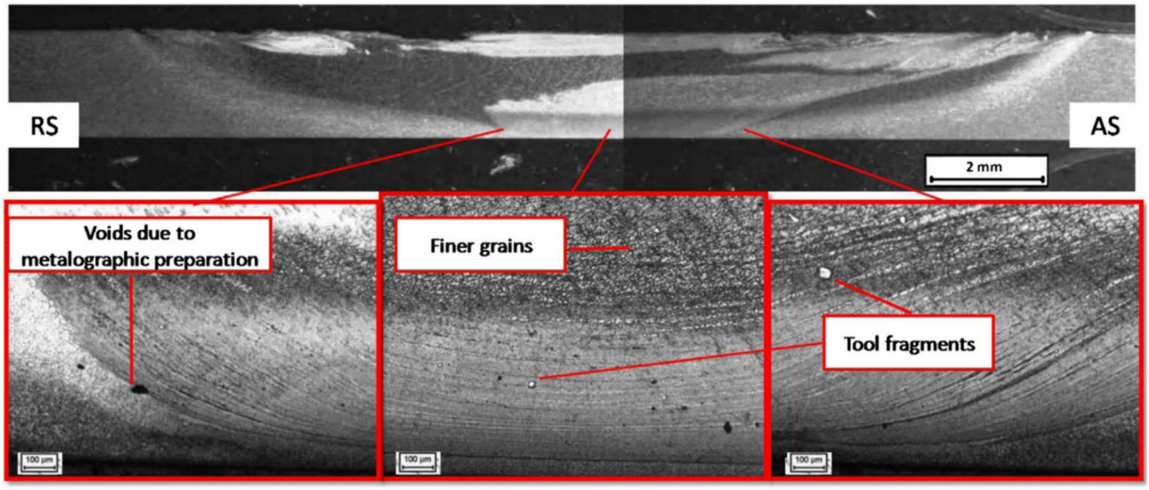

Figure 16. Structure of titanium alloy Ti-6Al-4V after friction stir welding with a tungsten carbide tool. Reprinted with permission from [377] 2013, Elsevier.

In the paper [85], the investigations carried out show that when welding the titanium alloy Ti-6Al-4V by the tool due to the high affinity of titanium and carbon at high temperatures, the formation of a reaction layer occurred on the surface of the tool (Figure 17). This layer consists of fragments of the tool, material, and elements formed because of their interaction.

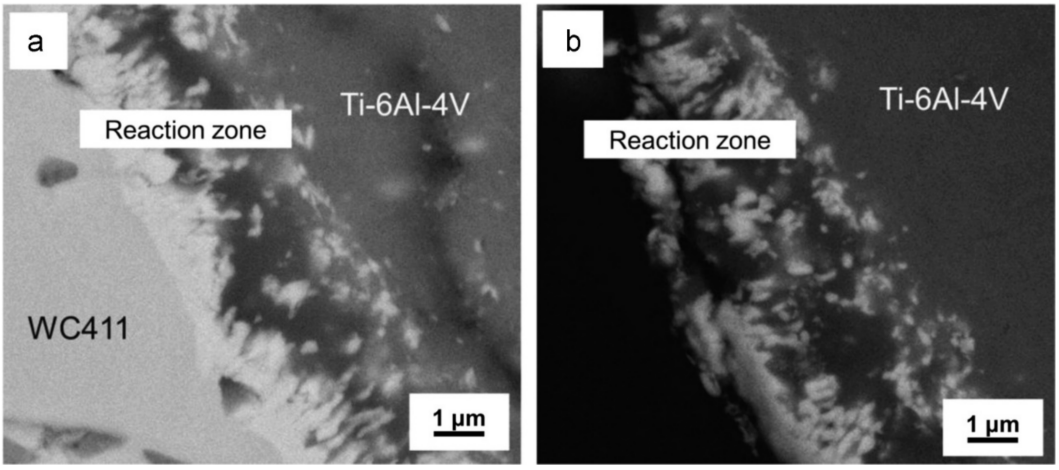

Figure 17. Formation of reaction zone at WC-Co pin surface (**a**) and the product layer was "sheared off" from WC411 tool (**b**). in friction stir welding Ti-6Al-4V Reprinted with permission from [85]. 2022, Elsevier.

Based on the investigations carried out and the analysis of literature information, the authors connect this phenomenon with WC + Ti = TiC + W and 2TiC + Ti + W2C + TiC reactions, which can take place in the tool and material contact zone. The alloy based on tungsten, titanium, and tantalum carbides studied by the authors also showed a tendency to mechanical destruction due to its low impact toughness [85].

6.3. Polycrystalline Cubic Boron Nitride

One of the most heat-resistant materials for welding tools is polycrystalline cubic boron nitride. This material has sufficiently high mechanical properties and is widely used for friction stir welding of materials with high melting points. However, for friction stir welding of titanium alloys, its use is also associated with a number of negative aspects. First of all, this is associated with changes in the structure when obtaining joints. During FSW of titanium alloys with a polycrystalline cubic nitride tool, tool remnants in the form of titanium boride, nitrogen, and oxygen were found in the weld [383]. The wear mechanism of tools made of this material was studied in [404]. Chemical analysis of tool remnants in the stirred zone demonstrates the complex nature of the wear process. The high-temperature conditions in the FSW process facilitate a chemical reaction between titanium and boron nitride, due to which the TiB2 and free nitrogen phase appears (Figure 18). Because of the high solubility of nitrogen in the α phase of titanium, the released nitrogen remains in the titanium matrix. In addition, for these reasons, the Ti2N phase may appear, which also has a negative effect on the strength of the joint.

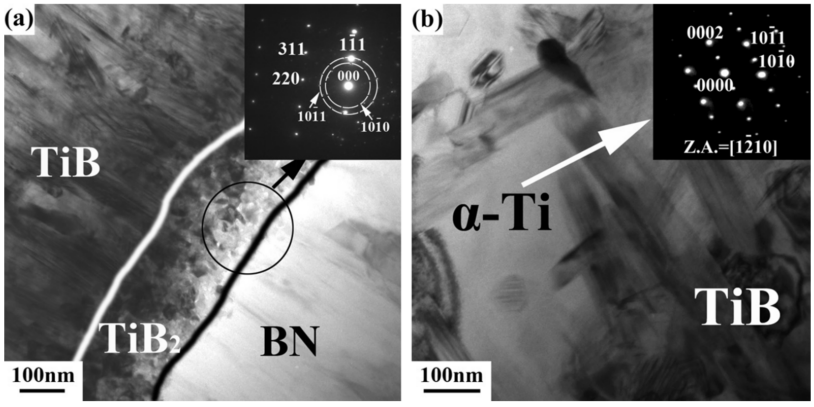

Figure 18. (**a**) Remnants of the boron nitride and titanium boride tool in the FSW joint; (**b**) titanium boride layer transitioning to α-titanium. Reprinted with permission from [404] 2014, Elsevier.

6.4. Cobalt-Based Alloys

Tools made of cobalt heat-resistant alloys have been used for friction stir welding for quite a long time [107,343,357,392–394,401]. When using a cobalt-based tool, a number of studies have revealed that a portion of the titanium alloy plates to be welded adhered to the tool during the FSW process. Although this was found to increase the high-temperature strength of the tool and, consequently, to reduce tool wear, this result could not be considered acceptable. [357]. Further research in this area has shown that the friction and wear processes of cobalt alloy tools during friction stir welding of titanium alloys occur in a more complex and heterogeneous manner [107,370] (Figure 19).

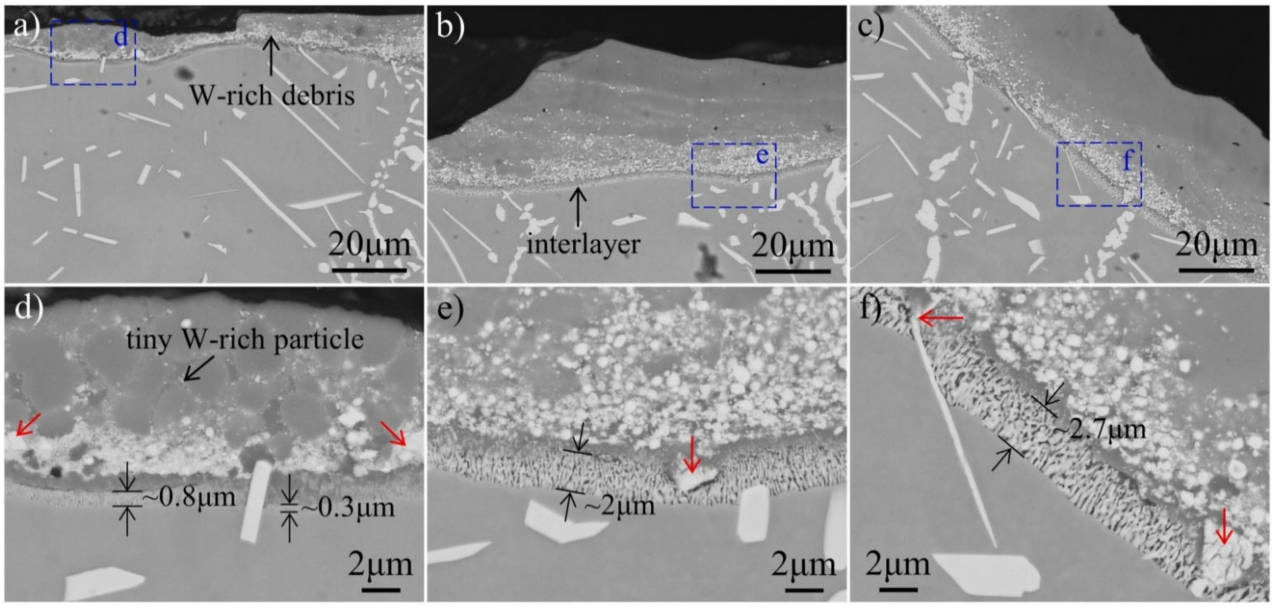

Figure 19. Tribological layer on the tool surface made of cobalt heat-resistant alloy (Co35W26.8Ni26Cr7.4Al4.8) after welding of titanium alloy TA5. Reprinted with permission from [107] 2022, Elsevier. Structure of areas differently spaced from the contact zone of the pin and shoulders of the tool (**a**–**c**) and their increased images (**d**–**f**) 6.5. Nickel-Based Alloys.

Friction stir welding results in the formation of a mechanically mixed tribological layer on the tool surface consisting of fragmented tungsten-enriched particles, tool fragments, and a grid of fine tungsten-enriched particles. This indicates a primarily mechanical or adhesive nature of this layer formation and tool wear. However, the formation of the transition zone with titanium diffusing into it is also noted on the surface, which also

indicates the diffusive nature of the friction process and wear of the tool material. Tool fragments are mixed in the stir zone and partially distributed in the titanium alloy structure along the grain boundaries. The material in the stir zone has mechanical properties that are higher than those of the base metal.

The work [379] used nickel-based polycrystalline heat-resistant alloys as the tool material in FSW of steel. This work showed quite successful results, despite the fact that there were minor defects in the resulting joint. In further studies, the wear mechanism of tools made of nickel heat-resistant alloys was found to be quite similar to that realized in the welding of cobalt alloys but also showed differences in the structures formed on the surface [85,106]. During the interaction of the processed or welded titanium alloy Ti-6Al-4V with the tool material, the formation of a tribological layer occurs under the influence of mutual diffusion of the components (Figure 20). In the surface layer, a mechanically mixed layer of intermetallic Ti_2Ni and Ni_3Ti_4 is formed. A zone of intermetallides is formed along the boundary of this layer with the presence of a carbide network of small particles along the grain boundaries. In some areas, this layer breaks down and tool fragments are present. The gradual formation and breakout of this layer is the main mechanism of friction and wear of titanium alloy tools during welding or friction-stirred machining. The resulting intermetallide particles are mixed into the joint material and clearly identified in the structure. Their formation does not embrittle the weld and they have rather high static tensile strength. However, under cyclic loading, the presence of a stir zone on the boundary can lead to a decrease in the fatigue life of the joint [368].

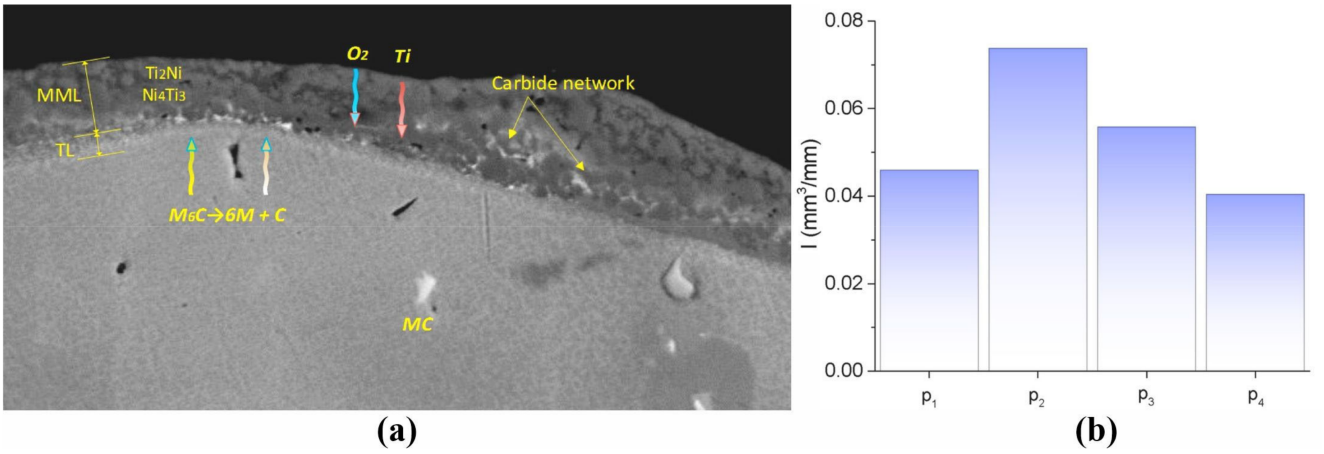

Figure 20. Formation of mechanically mixed layer on the surface of a nickel heat-resistant alloy tool during friction stir processing of titanium alloy Ti-6Al-4V with the introduction of copper powder (**a**) and tool wear rate (**b**). Reprinted with permission from [106] 2022, Elsevier.

This nickel alloy tool wear mechanism is typical for both friction stir welding [85] and processing [106] with the formation of composite materials. However, a higher intensity of wear is observed during processing due to additional heat generation caused by the exothermic formation of inthermetallides. The wear intensity (Figure 19) is maximal on the second pass of the tool and decreases further, which is caused by the reduction in the volume fraction of mixed powders that have not reacted with the base metal and, as a consequence, the reduction in the intensity of exothermic reactions of formation of TixCuy inter-thermetallides.

This is similar to the wear behavior of heat-resisting steel tools during friction stir welding of aluminum alloys. [108]. However, due to the higher processing temperature for titanium alloy, the mutual dissolution of material and tool is more intensive. The thermal expansion of the tool and contact stresses increase due to the higher pressing force of the tool. As a result, the formation of the tribological layer with intermetallic structure occurs faster, and the rate of its destruction increases, which determines the time

before the tool fails. However, there is a significant difference in the FSW/FSP of titanium α-alloys and FSW/FSP of titanium (α + β)-alloys. So, in the case of titanium α-alloys, the TixNiy intermetallides are much fewer, and they can be detected only during scanning tests [311,313,367,373,376], while in the case of titanium (α + β)-alloys, these intermetallides are detected at the macrolevel [81,85,365,366,368].

The tool wear process is identical in welding [85] and in friction stir processing with the incorporation of copper powder [106]. However, the intensity of the wear process is much higher when processing with the incorporation of powder due to exothermic reactions of the formation of intermetallic phases of various types. This determines a higher tool resistance in welding than in obtaining composite material.

In addition, the authors pay more attention to intermetallics, tool debris, and wear characteristics. Yet, there are extremely rare works that establish the relationship between tool wear and the strength characteristics of the resulting material and, consequently, the length of the allowable tool pass during FSW/FSP of titanium alloys. Such studies are quite time-consuming and have little scientific value, but in practice would identify which tool gives the longest machining length, which could help to bring FSW/FSP titanium alloys to large-scale industry.

7. Conclusions

Friction stir welding and processing of titanium alloys is a rather complex and dynamically developing area of research, relevant from both fundamental and applied points of view. This method allows the investigation of such complex and heterogeneous processes as deformation and fragmentation under high-loaded friction and accompanying structural-phase changes. Friction stir welding and processing allow a wide range of materials to be joined or modified, including those that cannot be welded or processed using traditional methods. Among other things, these technologies make it possible to form permanent joints or complex coatings of heterogeneous metals and alloys.

Friction stir welding and processing are realized through tribological contact between tool and material, associated with the implementation of a series of processes. As a material interacts with a tool, plastic deformation and fragmentation take place, which results in an ultrafine-grained or nanocrystalline structure with a simultaneous increase in temperature. Through refinement of grains and high temperature, transfer of material from the area in front of the tool behind the tool is possible, involving one of two mechanisms: adhesion or extrusion. The adhesion mechanism is related to metal flow caused by tribological interaction between material and tool, whereas the extrusion mechanism is related to the pressure exerted by the tool on a material as it is moved along a welding or processing line. Both mechanisms can only be realized through grain size reduction and are related to the phenomenon of superplastic flow. The material, which is transported from the zone in front of a tool to behind a tool, forms a stirred zone with an ultrafine particle structure. The grain size and phase-structure of the stirred zone may significantly vary if different welding conditions, tools, and material types as well as additional external influences (ultrasonic, cooling etc.) are applied. In friction stir welding and processing, the material is subject to thermal or thermo-mechanical impact along the contour of the stirred zone. These impacts may cause changes in the structural-phase state of a material and create thermally and thermomechanically affected zones, and their size may vary significantly during the processing or welding of different metals and alloys. In the heat-affected zone, after processing or welding, recrystallization and formation of equiaxed grains and structure-phase transformations caused by supersaturated solid solutions produced by deformation along a tool contour in various heat-hardening alloys or hardening phenomena in steels are the result. The introduction of additional powder particles, tool interaction, or obtaining heterogeneous compounds considerably complicate the process of organizing the structural-phase state of the stirred zone due to the realization of mutual dissolution of components, increasing the stirred zone temperature, and the realization of the contact melting phenomenon, etc. The realization of these processes depends on alloys being

welded or processed, their melting point, chemical activity, interaction with the material of the tools being used, and application of additional controlling actions, etc. The higher the material's melting point, the more intensively it interacts with the tool. This is additionally affected by the intensity of interaction between the workpiece and tool materials. For this reason, the more active the material and the higher its melting point, the more difficult it is to select a tool material for welding or processing.

One of the most difficult applications of friction stir welding or processing is the joining or modification of titanium alloys. This is due to the high temperatures required to realize the process, requiring the use of not only tribologically resistant but also heat-resistant materials. Titanium oxidizes quite intensively at high temperatures and reacts with various metals or alloys.

Additional influence is exerted by the necessity of cooling the working tool and the inert gas supply to the welding zone. Structure formation during friction stir welding has a common physical nature with structure formation during the welding of aluminum, copper, magnesium alloys, steels, and others. It is based on the formation of an ultrafine-dispersed material structure with subsequent formation of complexly organized metal flows along the tool contour with the realization of the flow of an adhesive and extrusive nature.

There are no materials that are used for friction stir welding of titanium alloys; almost all have an effect on the structure and material properties of the stirred zone. The introduction of small particles of silicon carbide or nickel- or cobalt-based intermetallides into the stirred zone does not lead to a significant decrease in the properties of the joints. Stirring large fragments can lead to a decrease in mechanical properties and structure disturbance with the formation of defects in the form of discontinuities. The formation of boride or nitride particles during friction stir welding of titanium with a boron nitride tool can have a negative effect on the mechanical properties of the resulting parts. Such features of structural changes and effects on mechanical properties are associated with the process of friction and wear of the tool and material during welding, and the mixing of wear particles by metal flows into the welded area. The mechanism of tool wear in friction stir welding is based on the formation of a reactive tribological layer consisting of elements formed by the interaction between the material and the tool. During processing or welding with tools made of nickel superalloy, intermetallic Ti_2Ni and Ni_3Ti_4 are formed in the surface tribological layer and a carbide network at its boundary with the tool material.

Welding with a cobalt heat-resistant alloy tool is associated with the formation of an adhesive layer, cracked tool layer, and tool debris zone, and no formation of intermetallides is observed. Welding titanium alloys with a polycrystalline boron nitride cBNp tool results in the formation of TiB2 borides and Ti2N nitrides of titanium in the tool–material contact. The processing or welding of titanium alloys with WC tungsten carbide tools occurs with the formation of a reaction tribological layer and tool particles breaking out and mixing in the material, including the possible shearing of rather large fragments. The wear mechanism of most nickel tools in friction stir welding of titanium alloys is similar to that in welding aluminum alloys with steel tools, but it is considerably more intensive. Various wolfram and rhenium or lanthanum oxide alloys have a relatively high applicability for welding titanium alloys, but they are expensive and also subject to wear during friction stir welding.

The literature review in the field of friction stir welding or processing of titanium alloys shows that during these processes, a number of material–tool interaction processes can be realized which have different influences on the structure and properties of the stirred zone (Figure 21). These processes depend on the tool material and can be either single or complex. For polycrystalline boron nitride tools, diffusion interactions and chemical reactions of tool and titanium are typical, presumably with the formation of a reaction zone along the tool contour. This results in a mixing of chemical compounds of titanium, boron, and nitrogen in the material and a reduction in its mechanical properties. According to the literature data, there are no data concerning the formation of the reaction zone along the contour of tools made of tungsten and molybdenum alloys, which is indirectly

confirmed by the fact that in some works, the stirred zone is almost absent. However, there is some evidence of tool softening at high temperatures and its plastic deformation in operation conditions, which makes mixing of tool fragments into the material of the stirred zone possible. Nickel and cobalt alloys are characterized by the formation of a mechanically mixed reactive layer on the tool surface composed of its fragments, titanium alloy, and intermetallides, as well as a transition layer to the main metal of a tool. This results in the introduction of tool fragments and resulting intermetallic compounds into the material of the stirred zone. It is notable that in the case of a static tensile test, this does not decrease the strength of the weld, but in the case of a cyclic test, intermetallic ingresses act as stress concentrators and reduce the number of cycles before fracture. Additionally, when welding titanium alloys with tools made of nickel alloys, softening and plastic deformation may occur.

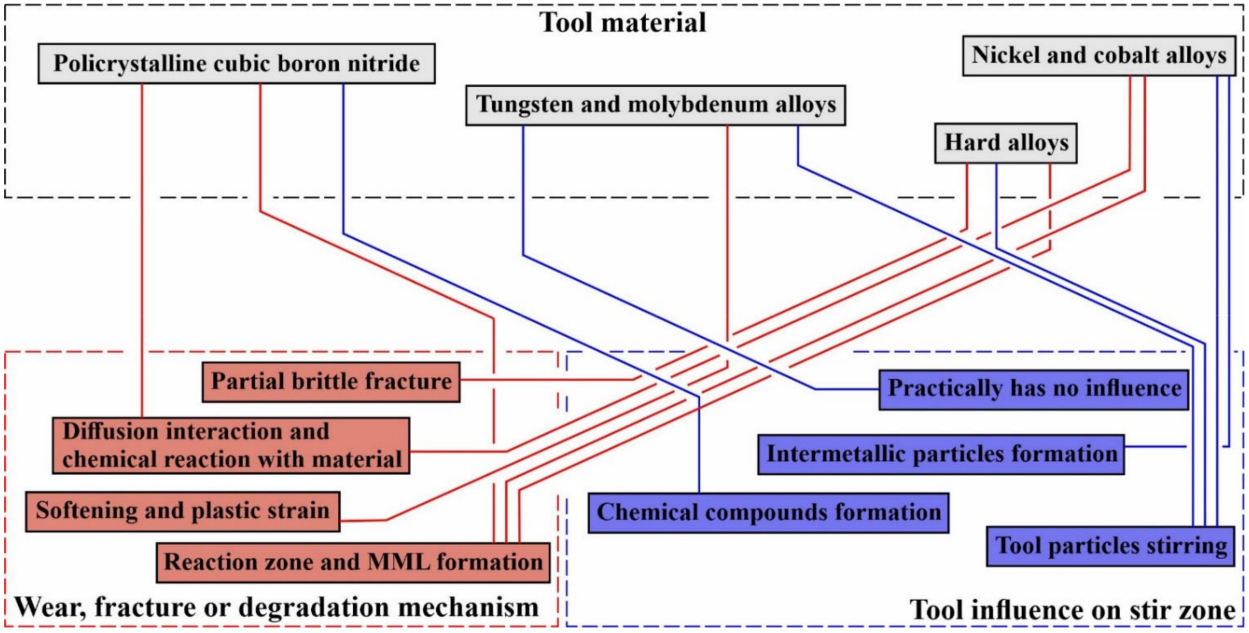

Figure 21. Schematic representation of the influence of the tool material on its wear, structural degradation, and fracture processes as well as on the structure of the stirred zone after welding or processing titanium alloys.

Hard-alloy tools, despite their high mechanical properties under static loading and thermal resistance, do not show significant resistance under friction stir welding or processing conditions with titanium alloys. They tend to develop a reaction layer in the same way as cobalt alloys. This is due to the binder in the hard alloys, which is primarily cobalt. The most severe wear occurs in this type of tool due to the brittle cleavage of the fragments from the surface and their mixing into the material. Exactly this phenomenon, based on the low resistance of hard alloys to operation in a complex stressed state, leads to a rather low service life of these tools.

Thus, in spite of high mechanical properties and high-temperature stability, tools of cubic boron nitride and hard alloys are not effective enough for friction stir welding of titanium alloys. Tungsten-based tools offer relatively high welding resistance and low or no stirring zone contamination but are very expensive. Tools of nickel or cobalt alloys have comparatively low cost and medium resistance to welding and allow obtaining joints with high mechanical properties. However, contamination of the stirring zone with particles of formed intermetallic compounds may result in low cyclic loading characteristics of these alloys. Thus, friction stir welding or processing with almost any tool has significant limitations due to high process temperatures, alternating cyclic complex-tensioned loading of the tool, and the high chemical activity of titanium.

In this regard, it can be assumed that the main possible task in the field of friction stir welding of titanium alloys can be to reduce the degree of interaction between the material and the tool while maintaining high heat resistance and resistance to cyclic loads. This can be achieved by applying diffusion or other coatings on the surfaces of tungsten, molybdenum, nickel, or cobalt heat-resistant alloys while maintaining a strong and resistant-to-fatigue-failure of the main volume of the tool. Such a direction may be an actual task for further research in this field.

This literature review leads to the following conclusions:

1. Friction stir welding or processing of most metals and alloys occurs by plastic deformation, fragmentation, and formation of ultrafine or nanocrystalline structure, implementation of adhesion or extrusion material transfer, and changing its phase composition through thermal, thermomechanical effect or interaction with a tool. Flow and transport behavior may differ for different metals and alloys but the physical nature of the process remains the same.
2. When welding and friction stir welding of aluminum and magnesium alloys, the problem of tool wear exists but is rather weak due to a low process temperature for the heat-resisting stamp steels used. In friction stir welding and processing of titanium alloys and steels, the process temperature is much higher so that tools resistant to thermal and thermomechanical effects as well as to mutual diffusion with the processed material (polycrystalline cubic boron nitride, hard alloys, heat-proof nickel and cobalt alloys, tungsten alloys) must be used. Processing and friction stir welding of copper and copper alloys have an intermediate position, which makes tools of stamped or high-speed steels of limited applicability, and results in good applicability of carbide tools and heat-resistant alloys.
3. Friction stir welding and processing results in an intensive interaction of titanium alloy and tools, in nearly all application materials. The mechanism of wear, structure degradation, or fracture depends on the material of which the tool is made, and the wear rate can be determined by welding or processing conditions.
4. The use of tungsten alloy tools enables the production of permanent joints of titanium alloys with the least changed chemical and phase composition of the stirred zone, but these tools are prone to thermal unstrengthening and deformation.
5. Polycrystalline boron nitride tools are less likely to wear or break when welding titanium alloys, but they have a tendency to be contaminated by borides and titanium nitrides.
6. Carbide tools based on tungsten carbides and cobalt binder are prone to severe brittle fracture by shearing off large fragments from the surface and mixing them into the stirred zone material when welding or processing titanium.
7. Tools of nickel and cobalt heat-resistant alloys have a similar nature of interaction with titanium alloys. The basic mechanism of their wear is connected with the formation of a mechanically mixed reaction layer containing fragments of the tool, forming intermetallides and titanium alloy, and also a transition layer enriched with high-melting phases based on tungsten.
8. During friction stir welding or processing of dissimilar alloys or composite materials, it is possible to intensify the process of mutual diffusion and tool wear due to an increase in temperature and also due to the formation of solid intermetallic phases and the realization of abrasive wear.
9. Mechanical properties of the stir zone can be reduced by the formation of borides or titanium nitrides when welding with pcBN tools. With most other types of tools, welds have properties of the stir zone at least as good as those of the base metal. When welding with tools made of nickel alloys, static loading strength properties of the stir zone of titanium alloys may improve, but introductions of intermetallic phases have a negative effect on the number of cycles to failure in fatigue tests.

Author Contributions: Conceptualization, A.A. and A.C.; resources, A.C. and E.K.; writing—original draft preparation, A.A., A.C., and V.R.; translation, A.I.; guidance and corrections to the article, A.C. and A.I. All authors have read and agreed to the published version of the manuscript.

Funding: The work was performed under State Assignment for ISPMS SB RAS (project No. FWRW-2022-0004).

Data Availability Statement: Not applicable.

Conflicts of Interest: The authors declare no conflict of interest.

References

1. Rathee, S.; Maheshwari, S.; Siddiquee, A.N.; Srivastava, M. A Review of Recent Progress in Solid State Fabrication of Composites and Functionally Graded Systems Via Friction Stir Processing. *Crit. Rev. Solid State Mater. Sci.* **2018**, *43*, 334–366. [CrossRef]
2. Mishra, R.S.; Ma, Z.Y. Friction stir welding and processing. *Mater. Sci. Eng. R Rep.* **2005**, *50*, 1–78. [CrossRef]
3. Weglowski, M.S. Friction stir processing. *State Art Arch. Civ. Mech. Eng.* **2018**, *18*, 114–129. [CrossRef]
4. Feng, I.-M. Metal transfer and wear. *J. Appl. Phys.* **1952**, *23*, 1011–1019. [CrossRef]
5. Kuznetsov, V.P.; Tarasov, S.Y.; Dmitriev, A.I. Nanostructuring burnishing and subsurface shear instability. *J. Mater. Process. Technol.* **2015**, *217*, 327–335. [CrossRef]
6. Bowden, F.P.; Moore, A.J.W.; Tabor, D. The ploughing and adhesion of sliding metals. *J. Appl. Phys.* **1943**, *14*, 80–91. [CrossRef]
7. Alphonse, M.; Raja, V.K.B.; Palanikumar, K. Effect of friction drilling on metallurgical and mechanical properties of composite materials: A review. *Curr. Mater. Sci.* **2021**, *14*, 53–69. [CrossRef]
8. Khodabakhshi, F.; Gerlich, A.P. Potentials and strategies of solid-state additive friction-stir manufacturing technology: A critical review. *J. Manuf. Process.* **2018**, *36*, 77–92. [CrossRef]
9. Mehta, K.P.; Vilaça, P. A review on friction stir-based channeling. *Crit. Rev. Solid State Mater. Sci.* **2022**, *47*, 1–45. [CrossRef]
10. Abbasi, M.; Baghei, B. New attempt to improve friction stir brazing. *Mater. Lett.* **2021**, *304*, 130688. [CrossRef]
11. Nicholas, E.D. Friction welding: A State-of-the-art report. *Weld. Des. Fabr.* **1977**, *50*, 56–62.
12. Ouyang, J.; Yarrapareddy, E.; Kovacevic, R. Microstructural evolution in the friction stir welded 6061 aluminum alloy (T6-temper condition) to copper. *J. Mater. Process. Technol.* **2006**, *172*, 110–122. [CrossRef]
13. Schmidt, H.N.B.; Dickerson, T.L.; Hattel, J.H. Material flow in butt friction stir welds in AA2024-T3. *Acta Mater.* **2006**, *54*, 1199–1209. [CrossRef]
14. Lakshminarayanan, A.K.; Balasubramanian, V. Comparison of RSM with ANN in predicting tensile strength of friction stir welded AA7039 aluminium alloy joints. *Trans. Nonferrous Met. Soc. China* **2009**, *19*, 9–18. [CrossRef]
15. Park, H.S.; Kimura, T.; Murakami, T.; Nagano, Y.; Nakata, K.; Ushio, M. Microstructures and mechanical properties of friction stir welds of 60% Cu-40% Zn copper alloy. *Mater. Sci. Eng. A* **2004**, *371*, 160–169. [CrossRef]
16. Xie, G.M.; Ma, Z.Y.; Geng, L. Development of a fine-grained microstructure and the properties of a nugget zone in friction stir welded pure copper. *Scr. Mater.* **2007**, *57*, 73–76. [CrossRef]
17. Gangwar, K.; Ramulu, M. Friction stir welding of titanium alloys: A review. *Mater. Des.* **2018**, *141*, 230–255. [CrossRef]
18. Singh, K.; Singh, G.; Singh, H. Review on friction stir welding of magnesium alloys. *J. Magnes. Alloy.* **2018**, *6*, 399–416. [CrossRef]
19. Ishikawa, T.; Fujii, H.; Genchi, K.; Cui, L.; Matsuoka, S.; Nogi, K. Joint properties of friction stir welded austenitic stainless steels. *Yosetsu Gakkai Ronbunshu/Q. J. Jpn. Weld. Soc.* **2006**, *24*, 174–180.
20. Cui, L.; Zhang, C.; Liu, Y.-C.; Liu, X.-G.; Wang, D.-P.; Li, H.-J. Recent progress in friction stir welding tools used for steels. *J. Iron Steel Res. Int.* **2018**, *25*, 477–486. [CrossRef]
21. Mahoney, M.W.; Rhodes, C.G.; Flintoff, J.G.; Spurling, R.A.; Bingel, W.H. Properties of friction-stir-welded 7075 T651 aluminum. *Metall. Mater. Trans. A Phys. Metall. Mater. Sci.* **1998**, *29*, 1955–1964. [CrossRef]
22. Shen, Z.; Yang, X.; Zhang, Z.; Cui, L.; Li, T. Microstructure and failure mechanisms of refill friction stir spot welded 7075-T6 aluminum alloy joints. *Mater. Des.* **2013**, *44*, 476–486. [CrossRef]
23. Niu, P.; Li, W.; Yang, C.; Chen, Y.; Chen, D. Low cycle fatigue properties of friction stir welded dissimilar 2024-to-7075 aluminum alloy joints. *Mater. Sci. Eng. A* **2022**, *832*, 142423. [CrossRef]
24. Zhang, L.; Hou, Y.F.; Liu, C.Y.; Huang, H.F.; Sun, H.M. Effects of Short-Time Heat Treatment on Microstructure and Mechanical Properties of 7075 Friction Stir Welded Joint. *J. Mater. Eng. Perform.* **2021**, *30*, 7826–7834. [CrossRef]
25. Deng, C.; Wang, C.; Wang, F.; Song, B.; Zhang, H. Effect of microstructure evolution on corrosion behavior of 2195 Al-Li alloy friction stir welding joint. *Mater. Charact.* **2022**, *184*, 111652. [CrossRef]
26. Mehta, K.P. A review on friction-based joining of dissimilar aluminum-steel joints. *J. Mater. Res.* **2019**, *34*, 78–96. [CrossRef]
27. Bang, H.; Bang, H.; Song, H.; Joo, S. Joint properties of dissimilar Al6061-T6 aluminum alloy/Ti-6%Al-4%V titanium alloy by gas tungsten arc welding assisted hybrid friction stir welding. *Mater. Des.* **2013**, *51*, 544–551. [CrossRef]
28. Song, Z.; Nakata, K.; Wu, A.; Liao, J.; Zhou, L. Influence of probe offset distance on interfacial microstructure and mechanical properties of friction stir butt welded joint of Ti6Al4V and A6061 dissimilar alloys. *Mater. Des.* **2014**, *57*, 269–278. [CrossRef]
29. Huang, Y.; Lv, Z.; Wan, L.; Shen, J.; Santos, J.F.D. A new method of hybrid friction stir welding assisted by friction surfacing for joining dissimilar Ti/Al alloy. *Mater. Lett.* **2017**, *207*, 172–175. [CrossRef]

30. Tan, C.W.; Jiang, Z.G.; Li, L.Q.; Chen, Y.B.; Chen, X.Y. Microstructural evolution and mechanical properties of dissimilar Al-Cu joints produced by friction stir welding. *Mater. Des.* **2013**, *51*, 466–473. [CrossRef]
31. Abdollah-Zadeh, A.; Saeid, T.; Sazgari, B. Microstructural and mechanical properties of friction stir welded aluminum/copper lap joints. *J. Alloys Compd.* **2008**, *460*, 535–538. [CrossRef]
32. Saeid, T.; Abdollah-zadeh, A.; Sazgari, B. Weldability and mechanical properties of dissimilar aluminum-copper lap joints made by friction stir welding. *J. Alloys Compd.* **2010**, *490*, 652–655. [CrossRef]
33. Eyvazian, A.; Hamouda, A.; Tarlochan, F.; Derazkola, H.A.; Khodabakhshi, F. Simulation and experimental study of underwater dissimilar friction-stir welding between aluminium and steel. *J. Mater. Res. Technol.* **2020**, *9*, 3767–3781. [CrossRef]
34. Shah, L.H.; Othman, N.H.; Gerlich, A. Review of research progress on aluminium–magnesium dissimilar friction stir welding. *Sci. Technol. Weld. Join.* **2018**, *23*, 256–270. [CrossRef]
35. Aonuma, M.; Nakata, K. Effect of alloying elements on interface microstructure of Mg-Al-Zn magnesium alloys and titanium joint by friction stir welding. *Mater. Sci. Eng. B Solid-State Mater. Adv. Technol.* **2009**, *161*, 46–49. [CrossRef]
36. Li, Q.; Ma, Z.; Ji, S.; Song, Q.; Gong, P.; Li, R. Effective joining of Mg/Ti dissimilar alloys by friction stir lap welding. *J. Mater. Process. Technol.* **2020**, *278*, 116483. [CrossRef]
37. Ji, S.; Hu, W.; Ma, Z.; Li, Q.; Gong, X. Friction Stir Lap Welding of Mg/Ti Dissimilar Alloys Using a Slight Penetration Depth. *JOM* **2020**, *72*, 1589–1596. [CrossRef]
38. Singh, V.P.; Patel, S.K.; Kumar, N.; Kuriachen, B. Parametric effect on dissimilar friction stir welded steel-magnesium alloys joints: A review. *Sci. Technol. Weld. Join.* **2019**, *24*, 653–684. [CrossRef]
39. Lu, X.; Zhou, Y.; Sun, S.; Luan, Y.; Qiao, J.; Qian, J. Temperature Field Measurement and Analyses of Friction Stir Welding of 18mm Thick 2219 Aluminum Alloy. *Exp. Tech.* **2022**, 1–12. [CrossRef]
40. Xu, X.; Yu, H.; Lin, Z. Study of residual stress variation with depth of friction stir welded aluminium plates with different thicknesses. *Sci. Technol. Weld. Join.* **2020**, *25*, 297–302. [CrossRef]
41. Sun, Y.; Fujii, H.; Morisada, Y. Double-sided friction stir welding of 40 mm thick low carbon steel plates using a pcBN rotating tool. *J. Manuf. Process.* **2020**, *50*, 319–328. [CrossRef]
42. Liu, D.Q.; Ke, L.M.; Xu, W.P.; Xing, L.; Mao, Y.Q. Intergranular corrosion behavior of friction-stir welding joint for 20 mm thick plate of 7075 al-alloy. *J. Chin. Soc. Corros. Prot.* **2017**, *37*, 293–299.
43. Ivanov, A.N.; Rubtsov, V.E.; Chumaevskii, A.V.; Osipovich, K.S.; Kolubaev, E.A.; Bakshaev, V.A.; Ivashkin, I.N. Features of structure formation processes in AA2024 alloy joints formed by the friction stir welding with bobbin tool. *Obrab. Met. (Tekhnologiya Oborud. Instrum.) = Met. Work. Mater. Sci.* **2021**, *23*, 98–115. [CrossRef]
44. Kalashnikov, K.N.; Chumaevskii, A.V.; Kalashnikova, T.A.; Ivanov, A.N.; Rubtsov, V.E.; Kolubaev, E.A.; Bakshaev, V.A. On the problem of tool destruction when obtaining fixed joints of thick-walled aluminum alloy blanks by friction welding with mixing. *Obrab. Met. (Tekhnologiya Oborud. Instrum.) = Met. Work. Mater. Sci.* **2021**, *23*, 72–83. [CrossRef]
45. Ma, Z.Y. Friction Stir Processing Technology: A Review. *Metall. Mater. Trans. A* **2008**, *39*, 642–658. [CrossRef]
46. ZMa, Y.; Mishra, R.S.; Mahoney, M.W. Superplastic deformation behaviour of friction stir processed 7075 Al alloy. *Acta Mater.* **2002**, *50*, 4419–4430.
47. Patel, V.V.; Badheka, V.; Kumar, A. Influence of Friction Stir Processed Parameters on Superplasticity of Al-Zn-Mg-Cu Alloy. *Mater. Manuf. Process.* **2016**, *31*, 1573–1582. [CrossRef]
48. Song, L.; Zhang, Y.; Wang, J.; Lu, Y. Microstructure and tensile properties of friction-stir-processed Al-Li-Cu-Zr-Sc alloy. *Mater. Tehnol.* **2020**, *54*, 589–593. [CrossRef]
49. Gangil, N.; Noor, A.; Maheshwari, S. Aluminium based in-situ composite fabrication through friction stir processing: A review. *J. Alloys Compd.* **2017**, *715*, 91–104. [CrossRef]
50. Barmouz, M.; Asadi, P.; Givi, M.K.B.; Taherishargh, M. Investigation of mechanical properties of Cu/SiC composite fabricated by FSP: Effect of SiC particles' size and volume fraction. *Mater. Sci. Eng. A* **2011**, *528*, 1740–1749. [CrossRef]
51. Sarmadi, H.; Kokabi, A.H.; Reihani, S.M.S. Friction and wear performance of copper-graphite surface composites fabricated by friction stir processing (FSP). *Wear* **2013**, *304*, 1–12. [CrossRef]
52. Sun, Y.F.; Fujii, H. The effect of SiC particles on the microstructure and mechanical properties of friction stir welded pure copper joints. *Mater. Sci. Eng. A* **2011**, *528*, 5470–5475. [CrossRef]
53. Sathiskumar, R.; Murugan, N.; Dinaharan, I.; Vijay, S.J. Characterization of boron carbide particulate reinforced in situ copper surface composites synthesized using friction stir processing. *Mater. Charact.* **2013**, *84*, 16–27. [CrossRef]
54. Zhang, W.; Liu, H.; Ding, H.; Fujii, H. The optimal temperature for enhanced low-temperature superplasticity in fine-grained Ti–15V–3Cr–3Sn–3Al alloy fabricated by friction stir processing. *J. Alloys Compd.* **2020**, *832*, 154917. [CrossRef]
55. Mironov, S.; Sato, Y.S.; Kokawa, H.; Hirano, S.; Pilchak, A.L.; Semiatin, S.L. Microstructural characterization of friction-stir processed Ti-6Al-4V. *Metals* **2020**, *10*, 976. [CrossRef]
56. Wang, L.; Wang, Y.; Huang, W.; Liu, J.; Tang, Y.; Zhang, L.; Fu, Y.; Zhang, L.-C.; Lu, W. Tensile and superelastic behaviors of Ti-35Nb-2Ta-3Zr with gradient structure. *Mater. Des.* **2020**, *194*, 108961. [CrossRef]
57. Manroo, S.A.; Khan, N.Z.; Ahmad, B. Study on surface modification and fabrication of surface composites of magnesium alloys by friction stir processing: A review. *J. Eng. Appl. Sci.* **2022**, *69*, 25. [CrossRef]

58. Mohankumar, A.; Duraisamy, T.; Chidambaramseshadri, R.; Pattabi, T.; Ranganathan, S.; Kaliyamoorthy, M.; Balachandran, G.; Sampathkumar, D.; Rajendran, P.R. Enhancing the Corrosion Resistance of Low Pressure Cold Sprayed Metal Matrix Composite Coatings on AZ31B Mg Alloy through Friction Stir Processing. *Coatings* **2022**, *12*, 135. [CrossRef]
59. Wang, H.; Zhang, D.T.; Cao, G.H.; Qiu, C. Improving room-temperature ductility of a Mg–Zn–Ca alloy through friction stir processing. *J. Mater. Res. Technol.* **2022**, *17*, 1176–1186. [CrossRef]
60. Merah, N.; Azeem, M.A.; Abubaker, H.M.; Al-Badour, F.; Albinmousa, J.; Sorour, A.A. Friction stir processing influence on microstructure, mechanical, and corrosion behavior of steels: A review. *Materials* **2021**, *14*, 5023. [CrossRef]
61. Mironov, Y.P.; Barmina, E.G.; Beloborodov, V.A. Microhardness of TiNi alloy after friction stir processing. *AIP Conf. Proc.* **2020**, *2310*, 020203.
62. Ardalanniya, A.; Nourouzi, S.; Aval, H.J. Effects of Multipass Additive Friction Stir Processing on Microstructure and Mechanical Properties of Al-Zn-Cup/Al-Zn Laminated Composites. *JOM* **2021**, *73*, 2844–2858. [CrossRef]
63. Papantoniou, I.G.; Markopoulos, A.P.; Manolakos, D.E. A new approach in surface modification and surface hardening of aluminum alloys using friction stir process: Cu-Reinforced AA5083. *Materials* **2020**, *13*, 1278. [CrossRef] [PubMed]
64. Seenivasan, S.; Prakash, K.S.; Nandhakumar, S.; Gopal, P.M. Influence of AlCoCrCuFe High Entropy Alloy particles on the microstructural, mechanical and tribological properties of copper surface composite made through friction stir processing. *Proc. Inst. Mech. Eng. Part C J. Mech. Eng. Sci.* **2021**, *235*, 5555–5566. [CrossRef]
65. Gupta, A.K.; Puram, M.M. Fabrication of the Composites (AA6082-T6/SiC) by Using Friction Stir Processing. In *Recent Advances in Mechanical Engineering*; Springer: Singapore, 2021; pp. 435–440.
66. Kumar, H.; Prasad, R.; Kumar, P. Effect of multi-groove reinforcement strategy on Cu/SiC surface composite fabricated by friction stir processing. *Mater. Chem. Phys.* **2020**, *256*, 123720. [CrossRef]
67. Iwaszko, J.; Kudła, K. Characterization of Cu/SiC surface composite produced by friction stir processing. *Bull. Pol. Acad. Sci. Tech. Sci.* **2020**, *68*, 555–564.
68. Biradar, A.; Rijesh, M. Feasibility of Stir Casting Method for Processing Al-6063/Graphite Composite with Desired Microstructure, Mechanical, Flow, and Frictional Properties. *Trans. Indian Inst. Met.* **2022**, *75*, 407–416. [CrossRef]
69. You, G.L.; Ho, N.J.; Kao, P.W. The microstructure and mechanical properties of an Al-CuO in-situ composite produced using friction stir processing. *Mater. Lett.* **2013**, *90*, 26–29. [CrossRef]
70. Heidarpour, A.; Mousavi, Z.S.; Karimi, S.; Hosseini, S.M. On the corrosion behavior and microstructural characterization of Al2024 and Al2024/Ti2SC MAX phase surface composite through friction stir processings. *J. Appl. Electrochem.* **2021**, *51*, 1123–1136. [CrossRef]
71. Kurt, H.I. Influence of hybrid ratio and friction stir processing parameters on ultimate tensile strength of 5083 aluminum matrix hybrid composites. *Compos. Part B Eng.* **2016**, *93*, 26–34. [CrossRef]
72. Devaraju, A.; Kumar, A.; Kotiveerachari, B. Influence of addition of Grp/Al2O3p with SiCp on wear properties of aluminum alloy 6061-T6 hybrid composites via friction stir processing. *Trans. Nonferrous Met. Soc. China* **2013**, *23*, 1275–1280. [CrossRef]
73. Aruri, D.; Adepu, K.; Adepu, K.; Bazavada, K. Wear and mechanical properties of 6061-T6 aluminum alloy surface hybrid composites [(SiC + Gr) and (SiC + Al2O3)] fabricated by friction stir processing. *J. Mater. Res. Technol.* **2013**, *2*, 362–369. [CrossRef]
74. Sharma, D.K.; Patel, V.; Badheka, V.; Mehta, K.; Upadhyay, G. Different reinforcement strategies of hybrid surface composite AA6061/(B4C+MoS2) produced by friction stir processing. *Mater. Und Werkst.* **2020**, *51*, 1493–1506. [CrossRef]
75. Sharma, D.K.; Patel, V.; Badheka, V.; Mehta, K.; Upadhyay, G. Fabrication of Hybrid Surface Composites AA6061/(B4C + MoS2) via Friction Stir Processing. *J. Tribol.* **2019**, *141*, 052201. [CrossRef]
76. Srinivasu, R.; Rao, A.S.; Reddy, G.M.; Rao, K.S. Friction stir surfacing of cast A356 aluminium–silicon alloy with boron carbide and molybdenum disulphide powders. *Def. Technol.* **2015**, *11*, 140–146. [CrossRef]
77. Dieguez, T.; Burgueño, A.; Svoboda, H. Superplasticity of a Friction Stir Processed 7075-T651 aluminum alloy. *Procedia Mater. Sci.* **2012**, *1*, 110–117. [CrossRef]
78. Kolubaev, E.A.; Rubtsov, V.E.; Chumaevsky, A.V.; Astafurova, E.G. Micro-, Meso- and Macrostructural Design of Bulk Metallic and Polymetallic Materials by Wire-Feed Electron-Beam Additive Manufacturing. *Phys. Mesomech.* **2022**, *25*, 479. [CrossRef]
79. Zykova, A.; Chumaevskii, A.; Vorontsov, A.; Kalashnikov, K.; Gurianov, D.; Gusarova, A.; Kolubaev, E. Evolution of Microstructure and Properties of Fe-Cu, Manufactured by Electron Beam Additive Manufacturing with Subsequent Friction Stir Processing. *Mater. Lett.* **2022**, *307*, 131023. [CrossRef]
80. Kalashnikova, T.; Chumaevskii, A.; Kalashnikov, K.; Knyazhev, E.; Gurianov, D.; Panfilov, A.; Nikonov, S.; Rubtsov, V.; Kolubaev, E. Regularities of Friction Stir Processing Hardening of Aluminum Alloy Products Made by Wire-Feed Electron Beam Additive Manufacturing. *Metals* **2022**, *12*, 183. [CrossRef]
81. Kalashnikov, K.; Chumaevskii, A.; Kalashnikova, T.; Cheremnov, A.; Moskvichev, E.; Amirov, A.; Krasnoveikin, V.; Kolubaev, E. Friction Stir Processing of Additively Manufactured Ti-6al-4v Alloy: Structure Modification and Mechanical Properties. *Metals* **2022**, *12*, 55. [CrossRef]
82. Liu, H.; Nakata, K.; Yamamoto, N.; Liao, J. Friction Stir Welding of Pure Titanium Lap Joint. *Sci. Technol. Weld. Join.* **2010**, *15*, 428–432. [CrossRef]
83. Wang, J.; Su, J.; Mishra, R.S.; Xu, R.; Baumann, J.A. Tool Wear Mechanisms in Friction Stir Welding of Ti-6Al-4V Alloy. *Wear* **2014**, *321*, 25–32. [CrossRef]

84. Edwards, P.D.; Ramulu, M. Material Flow during Friction Stir Welding of Ti-6Al-4V. *J. Mater. Process. Technol.* **2015**, *218*, 107–115. [CrossRef]
85. Tarasov, S.; Amirov, A.; Chumaevskiy, A.; Savchenko, N.; Rubtsov, V.E.; Ivanov, A.; Moskvichev, E.; Kolubaev, E. Friction Stir Welding of Ti-6Al-4V Using a Liquid-Cooled Nickel Superalloy Tool. *Technologies* **2022**, *10*, 118. [CrossRef]
86. Ramulu, M.; Edwards, P.D.; Sanders, D.G.; Reynolds, A.P.; Trapp, T. Tensile Properties of Friction Stir Welded and Friction Stir Welded-Superplastically Formed Ti-6Al-4V Butt Joints. *Mater. Des.* **2010**, *31*, 3056–3061. [CrossRef]
87. Paranthaman, V.; Dhinakaran, V.; Sai, M.S.; Devaraju, A. A systematic review of fatigue behaviour of laser welding titanium alloys. *Mater. Today Proc.* **2021**, *19 Pt 1*, 520–523. [CrossRef]
88. Peters, M.; Leyens, C. Fabrication of Titanium Alloys. In *Titanium and Titanium Alloys: Fundamentals and Applications*; Leyens, C., Peters, M., Eds.; Wiley-VCH Verlag GmbH & Co. KGaA: Weinheim, Germany, 2005; pp. 245–261. [CrossRef]
89. Peters, M.; Kumpfert, J.; Ward, C.H.; Leyens, C. Titanium alloys for aerospace applications. *Adv. Eng. Mater.* **2003**, *5*, 419–427. [CrossRef]
90. Zhao, Q.; Sun, Q.; Xin, S.; Chen, Y.; Wu, C.; Wang, H.; Xu, J.; Wan, M.; Zeng, W.; Zhao, Y. High-Strength Titanium Alloys for Aerospace Engineering Applications: A Review on Melting-Forging Process. *Mater. Sci. Eng. A* **2022**, *845*, 143260. [CrossRef]
91. Yu, W.; Hou, S.; Lv, Y.; Cao, J.; Su, C.; Gao, F.; Zhang, J. Evolution of Microstructure and Mechanical Properties of Vacuum Electron Beam Welded Joints in a near Beta Titanium Alloy: Influence of Heat Treatment. *Vacuum* **2022**, *204*, 111362. [CrossRef]
92. Chattopadhyay, A.; Muvvala, G.; Sarkar, S.; Racherla, V.; Nath, A.K. Effect of Laser Shock Peening on Microstructural, Mechanical and Corrosion Properties of Laser Beam Welded Commercially Pure Titanium. *Opt. Laser Technol.* **2021**, *133*, 106527. [CrossRef]
93. Chen, J.; Pan, C. Welding of Ti-6Al-4V Alloy Using Dynamically Controlled Plasma Arc Welding Process. *Trans. Nonferrous Met. Soc. China* **2011**, *21*, 1506–1512. [CrossRef]
94. Feng, X.; Pan, X.; He, W.; Liu, P.; An, Z.; Zhou, L. Improving High Cycle Fatigue Performance of Gas Tungsten Arc Welded Ti6Al4V Titanium Alloy by Warm Laser Shock Peening. *Int. J. Fatigue* **2021**, *149*, 106270. [CrossRef]
95. Balasubramanian, M.; Jayabalan, V.; Balasubramanian, V. Modeling Corrosion Behavior of Gas Tungsten Arc Welded Titanium Alloy. *Trans. Nonferrous Met. Soc. China* **2007**, *17*, 676–680. [CrossRef]
96. Shapovalov, V.; Protokovilov, I.; Porokhonko, V. Structure and Mechanical Properties of Thick-Walled Joints of Ti-6-4 Titanium Alloy Made by Electroslag Welding. *Procedia Struct. Integr.* **2022**, *36*, 262–268. [CrossRef]
97. Hu, M.; Liu, J. Effects of Zonal Heat Treatment on Residual Stresses and Mechanical Properties of Electron Beam Welded TC4 Alloy Plates. *Trans. Nonferrous Met. Soc. China* **2009**, *19*, 324–329. [CrossRef]
98. Xie, L.; Zhu, X.; Sun, W.; Jiang, C.; Wang, P.; Yang, S.; Fan, Y.; Song, Y. Investigations on the material flow and the influence of the resulting texture on the tensile properties of dissimilar friction stir welded ZK60/Mg–Al–Sn–Zn joints. *J. Mater. Res. Technol.* **2022**, *17*, 1716–1730. [CrossRef]
99. Gao, S.; Wu, C.S.; Padhy, G.K. Material flow, microstructure and mechanical properties of friction stir welded AA 2024-T3 enhanced by ultrasonic vibrations. *J. Manuf. Process.* **2017**, *30*, 385–395. [CrossRef]
100. da Silva, A.A.M.; Arruti, E.; Janeiro, G.; Aldanondo, E.; Alvarez, P.; Echeverria, A. Material flow and mechanical behaviour of dissimilar AA2024-T3 and AA7075-T6 aluminium alloys friction stir welds. *Mater. Des.* **2011**, *32*, 2021–2027.
101. Chen, S.; Han, Y.; Jiang, X.; Li, X.; Yuan, T.; Jiang, W.; Wang, X. Study on in-situ material flow behaviour during friction stir welding via a novel material tracing technology. *J. Mater. Process. Technol.* **2021**, *297*, 117205. [CrossRef]
102. Liu, F.C.; Nelson, T.W. In-situ material flow pattern around probe during friction stir welding of austenitic stainless steel. *Mater. Des.* **2016**, *110*, 354–364. [CrossRef]
103. Bayazid, S.M.; Farhangi, H.; Asgharzadeh, H.; Radan, L.; Ghahramani, A.; Mirhaji, A. Effect of Cyclic Solution Treatment on Microstructure and Mechanical Properties of Friction Stir Welded 7075 Al Alloy. *Mater. Sci. Eng. A* **2016**, *649*, 293–300. [CrossRef]
104. Lee, H.-S.; Yoon, J.-H.; Yoo, J.-T.; No, K. Friction Stir Welding Process of Aluminum-Lithium Alloy 2195. *Procedia Eng.* **2016**, *149*, 62–66. [CrossRef]
105. Tarasov, S.Y.; Rubtsov, V.E.; Fortuna, S.V.; Eliseev, A.A.; Chumaevsky, A.V.; Kalashnikova, T.A.; Kolubaev, E.A. Ultrasonic-Assisted Aging in Friction Stir Welding on Al-Cu-Li-Mg Aluminum Alloy. *Weld. World* **2017**, *61*, 679–690. [CrossRef]
106. Zykova, A.; Vorontsov, A.; Chumaevskii, A.; Gurianov, D.; Gusarova, A.; Kolubaev, E.; Tarasov, S. Structural Evolution of Contact Parts of the Friction Stir Processing Heat-Resistant Nickel Alloy Tool Used for Multi-Pass Processing of Ti6Al4V/(Cu+Al) System. *Wear* **2022**, *488–489*, 204138. [CrossRef]
107. Du, S.; Liu, H.; Jiang, M.; Zhou, L.; Gao, F. The Performance of a Co-Based Alloy Tool in the Friction Stir Welding of TA5 Alloy. *Wear* **2022**, *488–489*, 204180. [CrossRef]
108. Tarasov, S.Y.; Rubtsov, V.E.; Kolubaev, E.A. A Proposed Diffusion-Controlled Wear Mechanism of Alloy Steel Friction Stir Welding (FSW) Tools Used on an Aluminum Alloy. *Wear* **2014**, *318*, 130–134. [CrossRef]
109. Feistauer, E.E.; Bergmann, L.A.; dos Santos, J.F. Effect of Reverse Material Flow on the Microstructure and Performance of Friction Stir Welded T-Joints of an Al-Mg Alloy. *Mater. Sci. Eng. A* **2018**, *731*, 454–464. [CrossRef]
110. Su, Y.; Li, W.; Liu, X.; Gao, F.; Yu, Y.; Vairis, A. Evolution of Microstructure, Texture and Mechanical Properties of Special Friction Stir Welded T-Joints for an α Titanium Alloy. *Mater. Charact.* **2021**, *177*, 111152. [CrossRef]
111. Shankar, S.; Saw, K.; Chattopadhyaya, S.; Hloch, S. Investigation on Different Type of Defects, Temperature Variation and Mechanical Properties of Friction Stir Welded Lap Joint of Aluminum Alloy 6101-T6. *Mater. Today Proc.* **2018**, *5*, 24378–24386. [CrossRef]

112. Chu, Q.; Yang, X.W.; Li, W.Y.; Zhang, Y.; Lu, T.; Vairis, A.; Wang, W.B. On Visualizing Material Flow and Precipitate Evolution during Probeless Friction Stir Spot Welding of an Al-Li Alloy. *Mater. Charact.* **2018**, *144*, 336–344. [CrossRef]
113. Kashaev, N.; Ventzke, V.; Çam, G. Prospects of Laser Beam Welding and Friction Stir Welding Processes for Aluminum Airframe Structural Applications. *J. Manuf. Process.* **2018**, *36*, 571–600. [CrossRef]
114. Keshavarz, H.; Kokabi, A.; Movahedi, M. Microstructure and Mechanical Properties of Al/Graphite- Zirconium Oxide Hybrid Composite Fabricated by Friction Stir Processing. *Mater. Sci. Eng. A* **2023**, *862*, 144470. [CrossRef]
115. Wang, Z.L.; Zhang, Z.; Xue, P.; Ni, D.R.; Ma, Z.Y.; Hao, Y.F.; Zhao, Y.H.; Wang, G.Q. Defect Formation, Microstructure Evolution, and Mechanical Properties of Bobbin Tool Friction–Stir Welded 2219-T8 Alloy. *Mater. Sci. Eng. A* **2022**, *832*, 142414. [CrossRef]
116. Yang, C.; Wang, Z.L.; Zhang, M.; Xue, P.; Liu, F.C.; Ni, D.R.; Xiao, B.L.; Ma, Z.Y. Enhancing Joint Strength of Bobbin Tool Friction Stir Welded Al–Mg–Si Alloy via Post-Weld Aging Process. *J. Mater. Res. Technol.* **2022**, *21*, 4688–4698. [CrossRef]
117. Liu, Z.; Guan, W.; Li, H.; Wang, D.; Cui, L. Study on the Relationship between Welding Force and Defects in Bobbin Tool Friction Stir Welding. *J. Manuf. Process.* **2022**, *84*, 1122–1132. [CrossRef]
118. Tang, J.; Shen, Y.; Li, J. Influences of Friction Stir Processing Parameters on Microstructure and Mechanical Properties of SiC/Al Composites Fabricated by Multi-Pin Tool. *J. Manuf. Process.* **2019**, *38*, 279–289. [CrossRef]
119. Elangovan, K.; Balasubramanian, V. Influences of Pin Profile and Rotational Speed of the Tool on the Formation of Friction Stir Processing Zone in AA2219 Aluminium Alloy. *Mater. Sci. Eng. A* **2007**, *459*, 7–18. [CrossRef]
120. Liu, F.C.; Ma, Z.Y. Achieving Exceptionally High Superplasticity at High Strain Rates in a Micrograined Al–Mg–Sc Alloy Produced by Friction Stir Processing. *Scr. Mater.* **2008**, *59*, 882–885. [CrossRef]
121. Liu, F.C.; Ma, Z.Y. Contribution of Grain Boundary Sliding in Low-Temperature Superplasticity of Ultrafine-Grained Aluminum Alloys. *Scr. Mater.* **2010**, *62*, 125–128. [CrossRef]
122. Malopheyev, S.; Mironov, S.; Vysotskiy, I.; Kaibyshev, R. Superplasticity of Friction-Stir Welded Al–Mg–Sc Sheets with Ultrafine-Grained Microstructure. *Mater. Sci. Eng. A* **2016**, *649*, 85–92. [CrossRef]
123. Pashazadeh, H.; Teimournezhad, J.; Masoumi, A. Numerical Investigation on the Mechanical, Thermal, Metallurgical and Material Flow Characteristics in Friction Stir Welding of Copper Sheets with Experimental Verification. *Mater. Des.* **2014**, *55*, 619–632. [CrossRef]
124. Vilaça, P.; Quintino, L.; dos Santos, J.F. ISTIR—Analytical Thermal Model for Friction Stir Welding. *J. Mater. Process. Technol.* **2005**, *169*, 452–465. [CrossRef]
125. Hwang, Y.-M.; Kang, Z.-W.; Chiou, Y.-C.; Hsu, H.-H. Experimental Study on Temperature Distributions within the Workpiece during Friction Stir Welding of Aluminum Alloys. *Int. J. Mach. Tools Manuf.* **2008**, *48*, 778–787. [CrossRef]
126. Upadhyay, P.; Reynolds, A.P. Effects of Thermal Boundary Conditions in Friction Stir Welded AA7050-T7 Sheets. *Mater. Sci. Eng. A* **2010**, *527*, 1537–1543. [CrossRef]
127. Kalashnikov, K.N.; Tarasov, S.Y.; Chumaevskii, A.V.; Fortuna, S.V.; Eliseev, A.A.; Ivanov, A.N. Towards Aging in a Multipass Friction Stir–Processed AA2024. *Int. J. Adv. Manuf. Technol.* **2019**, *103*, 2121–2132. [CrossRef]
128. Krishnan, K.N. On the formation of onion rings in friction stir welds. *Mater. Sci. Eng. A* **2002**, *327*, 246–251. [CrossRef]
129. Hofmann, D.C.; Vecchio, K.S. Submerged Friction Stir Processing (SFSP): An Improved Method for Creating Ultra-Fine-Grained Bulk Materials. *Mater. Sci. Eng. A* **2005**, *402*, 234–241. [CrossRef]
130. Kalashnikova, T.; Chumaevskii, A.; Kalashnikov, K.; Fortuna, S.; Kolubaev, E.; Tarasov, S. Microstructural Analysis of Friction Stir Butt Welded Al-Mg-Sc-Zr Alloy Heavy Gauge Sheets. *Metals* **2020**, *10*, 806. [CrossRef]
131. Cheng, C.; Kadoi, K.; Fujii, H.; Ushioda, K.; Inoue, H. Improved Strength and Ductility Balance of Medium-Carbon Steel with Chromium and Titanium Fabricated by Friction Stir Welding Process. *Mater. Sci. Eng. A* **2021**, *803*, 140689. [CrossRef]
132. Duan, R.H.; Wang, Y.Q.; Luo, Z.A.; Wang, G.D.; Xie, G.M. Achievement of Excellent Strength and Plasticity in the Nugget Zone of Friction Stir Welded Bainitic Steel and Its Deformation Behavior. *J. Mater. Res. Technol.* **2022**, *20*, 3381–3390. [CrossRef]
133. Wang, Q.; Zhao, Z.; Zhao, Y.; Yan, K.; Liu, C.; Zhang, H. The Strengthening Mechanism of Spray Forming Al-Zn-Mg-Cu Alloy by Underwater Friction Stir Welding. *Mater. Des.* **2016**, *102*, 91–99. [CrossRef]
134. Tao, Y.; Zhang, Z.; Xue, P.; Ni, D.R.; Xiao, B.L.; Ma, Z.Y. Effect of Post Weld Artificial Aging and Water Cooling on Microstructure and Mechanical Properties of Friction Stir Welded 2198-T8 Al-Li Joints. *J. Mater. Sci. Technol.* **2022**, *123*, 92–112. [CrossRef]
135. Kumar, K.K.; Kumar, A.; Satyanarayana, M.V.N.V.; Nagu, K. Microstructure and Strain Hardening Behaviour at the Inter-Mixing Zone of Water-Cooled Friction Stir Welded Dissimilar Aluminum Alloys. *Mater. Lett.* **2022**, *326*, 132991. [CrossRef]
136. Shi, L.; Dai, X.; Tian, C.; Wu, C. Effect of Splat Cooling on Microstructures and Mechanical Properties of Friction Stir Welded 2195 Al–Li Alloy. *Mater. Sci. Eng. A* **2022**, *858*, 144169. [CrossRef]
137. Snyder, B.; Strauss, A.M. In-Process Cooling of Friction Stir Extruded Joints for Increased Weld Performance via Compressed Air, Water, Granulated Dry Ice, and Liquid Nitrogen. *J. Manuf. Process.* **2021**, *68*, 1004–1017. [CrossRef]
138. Xu, N.; Qiu, Z.; Ren, Z.; Shen, J.; Wang, D.; Song, Q.; Zhao, J.; Jiang, Y.; Bao, Y. Enhanced Strength and Ductility of Rapid Cooling Friction Stir Welded Ultralight Mg-14Li-1Al Alloy Joint. *J. Mater. Res. Technol.* **2023**, *23*, 4444–4453. [CrossRef]
139. Baradarani, F.; Mostafapour, A.; Shalvandi, M. Effect of Ultrasonic Assisted Friction Stir Welding on Microstructure and Mechanical Properties of AZ91−C Magnesium Alloy. *Trans. Nonferrous Met. Soc. China* **2019**, *29*, 2514–2522. [CrossRef]
140. Zhang, Z.; He, C.; Li, Y.; Yu, L.; Zhao, S.; Zhao, X. Effects of Ultrasonic Assisted Friction Stir Welding on Flow Behavior, Microstructure and Mechanical Properties of 7N01-T4 Aluminum Alloy Joints. *J. Mater. Sci. Technol.* **2020**, *43*, 1–13. [CrossRef]

141. Hu, Y.; Liu, H.; Fujii, H. Improving the Mechanical Properties of 2219-T6 Aluminum Alloy Joints by Ultrasonic Vibrations during Friction Stir Welding. *J. Mater. Process. Technol.* **2019**, *271*, 75–84. [CrossRef]
142. Mehdi, H.; Mishra, R.S. Effect of Multi-Pass Friction Stir Processing and SiC Nanoparticles on Microstructure and Mechanical Properties of AA6082-T6. *Adv. Ind. Manuf. Eng.* **2021**, *3*, 100062. [CrossRef]
143. Mohammadzadeh Jamalian, H.; Ramezani, H.; Ghobadi, H.; Ansari, M.; Yari, S.; Besharati Givi, M.K. Processing–Structure–Property Correlation in Nano-SiC-Reinforced Friction Stir Welded Aluminum Joints. *J. Manuf. Process.* **2016**, *21*, 180–189. [CrossRef]
144. Qiao, Q.; Su, Y.; Cao, H.; Zhang, D.; Ouyang, Q. Effect of Post-Weld Heat Treatment on Double-Sided Friction Stir Welded Joint of 120 Mm Ultra-Thick SiCp/Al Composite Plates. *Mater. Charact.* **2020**, *169*, 110668. [CrossRef]
145. Furkon, W.M.; Kim, D.; Song, M.; Mun, S.; Kim, J.; Lee, K. Effect of Post–Weld Heat Treatment on Multi-Scale Microstructures and Mechanical Properties of Friction Stir Welded T-Joints of Al–Mg–Si Alloys. *J. Mater. Res. Technol.* **2022**, *18*, 496–507. [CrossRef]
146. Moradi, M.M.; Jamshidi Aval, H.; Jamaati, R. Effect of Pre and Post Welding Heat Treatment in SiC-Fortified Dissimilar AA6061-AA2024 FSW Butt Joint. *J. Manuf. Process.* **2017**, *30*, 97–105. [CrossRef]
147. Pradeep, S.; Jain, V.K.S.; Muthukumaran, S.; Kumar, R. Microstructure and Texture Evolution during Multi-Pass Friction Stir Processed AA5083. *Mater. Lett.* **2021**, *288*, 129382. [CrossRef]
148. Wang, Y.; Tsutsumi, S.; Kawakubo, T.; Fujii, H. Microstructure and Mechanical Properties of Weathering Mild Steel Joined by Friction Stir Welding. *Mater. Sci. Eng. A* **2021**, *823*, 141715. [CrossRef]
149. Ma, Z.Y.; Sharma, S.R.; Mishra, R.S. Effect of Friction Stir Processing on the Microstructure of Cast A356 Aluminum. *Mater. Sci. Eng. A* **2006**, *433*, 269–278. [CrossRef]
150. Zhou, C.; Yang, X.; Luan, G. Effect of Root Flaws on the Fatigue Property of Friction Stir Welds in 2024-T3 Aluminum Alloys. *Mater. Sci. Eng. A* **2006**, *418*, 155–160. [CrossRef]
151. Zhang, H.; Zhang, B.; Gao, Q.; Song, J.; Han, G. A Review on Microstructures and Properties of Graphene-Reinforced Aluminum Matrix Composites Fabricated by Friction Stir Processing. *J. Manuf. Process.* **2021**, *68*, 126–135. [CrossRef]
152. Patel, K.; Ghetiya, N.D.; Bharti, S. Effect of Single and Double Pass Friction Stir Processing on Microhardness and Wear Properties of AA5083/Al2O3 Surface Composites. *Mater. Today Proc.* **2022**, *57*, 38–43. [CrossRef]
153. Maji, P.; Nath, R.K.; Karmakar, R.; Paul, P.; Meitei, R.K.B.; Ghosh, S.K. Effect of Post Processing Heat Treatment on Friction Stir Welded/Processed Aluminum Based Alloys and Composites. *CIRP J. Manuf. Sci. Technol.* **2021**, *35*, 96–105. [CrossRef]
154. Reihanian, M.; Bavi, M.A.; Ranjbar, K. CNT-Reinforced Al-XZr (x = 0.25, 0.5 and 1 Wt.%) Surface Composites Fabricated by Friction Stir Processing: Microstructural, Mechanical and Wear Characterisation. *Philos. Mag.* **2022**, *102*, 1011–1041. [CrossRef]
155. Wang, T.; Gwalani, B.; Shukla, S.; Frank, M.; Mishra, R.S. Development of in Situ Composites via Reactive Friction Stir Processing of Ti–B4C System. *Compos. Part B* **2019**, *172*, 54–60. [CrossRef]
156. Barmouz, M.; Givi, M.K.B. Fabrication of in Situ Cu/SiC Composites Using Multi-Pass Friction Stir Processing: Evaluation of Microstructural, Porosity, Mechanical and Electrical Behavior. *Compos. Part A Appl. Sci. Manuf.* **2011**, *42*, 1445–1453. [CrossRef]
157. Pragada, V.; Soni, V.; Ghetiya, N.D.; Bharti, S. Influence of Tool Travel Direction on Microhardness and Tribological Properties of AA2014/SiC-CNT Hybrid Surface Composites Produced by Multi-Pass Friction Stir Processing. *Mater. Today Proc.* **2022**, *56*, 150–156. [CrossRef]
158. Yang, K.; Li, W.; Niu, P.; Yang, X.; Xu, Y. Cold Sprayed AA2024/Al2O3 Metal Matrix Composites Improved by Friction Stir Processing: Microstructure Characterization, Mechanical Performance and Strengthening Mechanisms. *J. Alloys Compd.* **2018**, *736*, 115–123. [CrossRef]
159. Radisavljevic, I.; Zivkovic, A.; Radovic, N.; Grabulov, V. Influence of FSW Parameters on Formation Quality and Mechanical Properties of Al 2024-T351 Butt Welded Joints. *Trans. Nonferrous Met. Soc. China* **2013**, *23*, 3525–3539. [CrossRef]
160. Liu, H.J.; Zhang, H.J.; Yu, L. Effect of Welding Speed on Microstructures and Mechanical Properties of Underwater Friction Stir Welded 2219 Aluminum Alloy. *Mater. Des.* **2011**, *32*, 1548–1553. [CrossRef]
161. Zhao, Y.; Wang, Q.; Chen, H.; Yan, K. Microstructure and Mechanical Properties of Spray Formed 7055 Aluminum Alloy by Underwater Friction Stir Welding. *Mater. Des.* **2014**, *56*, 725–730. [CrossRef]
162. Hasui, A. Friction Welding. *J. Jpn. Weld. Soc.* **1963**, *32*, 763–769. [CrossRef]
163. Fukushima, S.; Hasui, A. Some contributions to the heating phase in friction welding. *J. Jpn. Weld. Soc.* **1972**, *41*, 1074–1084. [CrossRef]
164. Machlin, E.S.; Yankee, W.R. Friction of clean metals and oxides with special reference to titanium. *J. Appl. Phys.* **1954**, *25*, 576–581. [CrossRef]
165. Milner, D.R.; Rowe, G.R. Fundamentals of solid-phase welding. *Metall. Rev.* **1962**, *7*, 433–480. [CrossRef]
166. Mcandrew, A.R.; Colegrove, P.A.; Bühr, C.; Flipo, B.C.D. Progress in Materials Science A Literature Review of Ti-6Al-4V Linear Friction Welding. *Prog. Mater. Sci.* **2018**, *92*, 225–257. [CrossRef]
167. Thomas, W.M.; Nicholas, E.D.; Needham, J.C.; Murch, M.G.; Temple-Smith, P.; Dawes, C.J. Friction Stir Butt. Welding. Patent Application No. PCT/GB92/02203, 6 December 1991.
168. Ohno, Y.; Inotani, J.; Kaneko, Y.; Hashimoto, S. Orientation Dependence of High-Angle Grain Boundary Formation during Sliding Wear in Copper Single Crystall. *J. Jpn. Inst. Met. Mater.* **2010**, *74*, 384–391. [CrossRef]
169. Ohno, Y.; Inotani, J.; Kaneko, Y.; Hashimoto, S. Lattice Rotation and For-mation of Low-Angle Boundary in a (001) Copper Single Crystal Subjected to Sliding. *J. Jpn. Inst. Met. Mater.* **2012**, *72*, 625–630. [CrossRef]

170. Lychagin, D.V.; Filippov, A.V.; Novitskaia, O.S.; Chumlyakov, Y.I.; Kolubaev, E.A.; Sizova, O.V. Friction-induced slip band relief of -Hadfield steel single crystal oriented for multiple slip deformation. *Wear* **2017**, *374–375*, 5–14. [CrossRef]
171. Tarasov, S.Y.; Chumaevskii, A.V.; Lychagin, D.V.; Nikonov, A.Y.; Dmitriev, A.I. Subsurface structural evolution and wear lip formation on copper single crystals under unlubricated sliding conditions. *Wear* **2018**, *410–411*, 210–221. [CrossRef]
172. Rigney, D.A. Transfer, mixing and associated chemical and mechanical pro-cesses during the sliding of ductile materials. *Wear* **2000**, *245*, 1–9. [CrossRef]
173. Emge, A.; Karthikeyan, S.; Rigney, D.A. The effects of sliding velocity and sliding time on nanocrystalline tribolayer development and properties in copper. *Wear* **2009**, *267*, 562–567. [CrossRef]
174. Tarasov, S.Y.; Kolubaev, A.V. Formation of surface layer with nanosize grain-subgrain structure due to friction of a copper—Tool steel pair. *Met. Sci. Heat Treat.* **2010**, *52*, 183–188. [CrossRef]
175. Tarasov, S.; Rubtsov, V.; Kolubaev, A. Subsurface shear instability and nanostructuring of metals in sliding. *Wear* **2010**, *268*, 59–66. [CrossRef]
176. So, H.; Chen, H.M.; Chen, L.W. Extrusion wear and transition of wear mechanisms of steel. *Wear* **2008**, *265*, 1142–1148. [CrossRef]
177. Arbegast, W.J.; Jin, Z.; Beaudoin, A.; Bieler, T.A.; Radhakrishnan, B. Hot Deformation of Aluminum Alloys III. In Proceedings of the 2003 TMS Annual Meeting, San Diego, CA, USA, 2–6 March 2003; 313p.
178. Venkatesh, K.M.; Arivarsu, M.; Manikandan, M.; Arivazhagan, N. Review on friction stir welding of steels. *Mater. Today Proc.* **2018**, *5*, 13227–13235. [CrossRef]
179. bin Ariffin, M.A.; bin Muhamad, M.R.; Raja, S.; Jamaludin, M.F.; Yusof, F.; Suga, T.; Liu, H.; Morisada, Y.; Fujii, H. Friction Stir Alloying of AZ61 and Mild Steel with Cu-CNT Additive. *J. Mater. Res. Technol.* **2022**, *21*, 2400–2415. [CrossRef]
180. Tavassolimanesh, A.; Alavi Nia, A. A New Approach for Manufacturing Copper-Clad Aluminum Bimetallic Tubes by Friction Stir Welding (FSW). *J. Manuf. Process.* **2017**, *30*, 374–384. [CrossRef]
181. Muhammad, N.A.; Wu, C.; Su, H. Concurrent Influences of Tool Offset and Ultrasonic Vibration on the Joint Quality and Performance of Dissimilar Al/Cu Friction Stir Welds. *J. Mater. Res. Technol.* **2021**, *14*, 1035–1051. [CrossRef]
182. Zhang, M.; Wang, Y.D.; Xue, P.; Zhang, H.; Ni, D.R.; Wang, K.S.; Ma, Z.Y. High-Quality Dissimilar Friction Stir Welding of Al to Steel with No Contacting between Tool and Steel Plate. *Mater. Charact.* **2022**, *191*, 112128. [CrossRef]
183. Yu, M.; Zhao, H.; Jiang, Z.; Zhang, Z.; Xu, F.; Zhou, L.; Song, X. Influence of Welding Parameters on Interface Evolution and Mechanical Properties of FSW Al/Ti Lap Joints. *J. Mater. Sci. Technol.* **2019**, *35*, 1543–1554. [CrossRef]
184. Azimi-Roeen, G.; Kashani-Bozorg, S.F.; Nosko, M.; Švec, P. Reactive Mechanism and Mechanical Properties of In-Situ Hybrid Nano-Composites Fabricated from an Al–Fe2O3 System by Friction Stir Processing. *Mater. Charact.* **2017**, *127*, 279–287. [CrossRef]
185. Rigney, D.A.; Hammerberg, J.E. Mechanical mixing and the development of nanocrystalline material during the sliding of metals. In Proceedings of the TMS Fall Meeting, Boston, MA, USA, 29 November–3 December 1999; pp. 465–474.
186. Zhang, Y.S.; Han, Z.; Wang, K.; Lu, K. Friction and wear behaviors of nanocrystalline surface layer of pure copper. *Wear* **2006**, *260*, 942–948. [CrossRef]
187. Venkataraman, B.; Sundararajan, G. Correlation between the characteristics of the mechanically mixed layer and wear behaviour of aluminium, Al-7075 alloy and Al-MMCs. *Wear* **2000**, *245*, 22–38. [CrossRef]
188. Hassan, A.M.; Alrashdan, A.; Hayajneh, M.T.; Mayyas, A.T. Wear behavior of Al-Mg-Cu-based composites containing SiC particles. *Tribol. Int.* **2009**, *42*, 1230–1238. [CrossRef]
189. Li, Y.; Murr, L.E.; McClure, J.C. Solid-state flow visualization in the friction-stir welding of 2024 Al to 6061 Al. *Scr. Mater.* **1999**, *40*, 1041–1046. [CrossRef]
190. Kumar, R.; Pancholi, V. Three-dimensional material flow during friction stir welding of AA5083. *J. Manuf. Process.* **2021**, *68*, 1214–1223. [CrossRef]
191. Tongne, A.; Desrayaud, C.; Jahazi, M.; Feulvarch, E. On material flow in Friction Stir Welded Al alloys. *J. Mater. Process. Technol.* **2017**, *239*, 284–296. [CrossRef]
192. Morisada, Y.; Fujii, H.; Kawahito, Y.; Nakata, K.; Tanaka, M. Three-dimensional visualization of material flow during friction stir welding by two pairs of X-ray transmission systems. *Scripta Materialia* **2011**, *65*, 1085–1088. [CrossRef]
193. Nandan, R.; Lienert, T.; DebRoy, T. Toward reliable calculations of heat and plastic flow during friction stir welding of Ti-6Al-4V alloy. *Int. J. Mater. Res.* **2008**, *99*, 434–444. [CrossRef]
194. Smolin, A.Y.; Shilko, E.V.; Astafurov, S.V.; Kolubaev, E.A.; Eremina, G.M.; Psakhie, S.G. Understanding the mechanisms of friction stir welding based on computer simulation using particles. *Def. Technol.* **2018**, *14*, 643–656. [CrossRef]
195. Long, L.; Chen, G.; Zhang, S.; Liu, T.; Shi, Q. Finite-Element Analysis of the Tool Tilt Angle Effect on the Formation of Friction Stir Welds. *J. Manuf. Process.* **2017**, *30*, 562–569. [CrossRef]
196. Reynolds, A.P.; Reynolds, A.P. Visualisation of material flow in autogenous friction stir welds. *Sci. Technol. Weld. Join.* **2013**, *1718*, 120–124. [CrossRef]
197. Zeng, X.H.; Xue, P.; Wang, D.; Ni, D.R.; Xiao, B.L.; Wang, K.S.; Ma, Z.Y. Material Flow and Void Defect Formation in Friction Stir Welding of Aluminium Alloys. *Sci. Technol. Weld. Join.* **2018**, *23*, 677–686. [CrossRef]
198. Rubtsov, V.; Chumaevskii, A.; Gusarova, A.; Knyazhev, E.; Gurianov, D.; Zykova, A.; Kalashnikova, T.; Cheremnov, A.; Savchenko, N.; Vorontsov, A.; et al. Macro- and Microstructure of In Situ Composites Prepared by Friction Stir Processing of AA5056 Admixed with Copper Powders. *Materials* **2023**, *16*, 1070. [CrossRef] [PubMed]

199. Dialami, N.; Cervera, M.; Chiumenti, M. Defect Formation and Material Flow in Friction Stir Welding. *Eur. J. Mech. A/Solids* **2020**, *80*, 103912. [CrossRef]
200. Rasti, J. Study of the Welding Parameters Effect on the Tunnel Void Area during Friction Stir Welding of 1060 Aluminum Alloy. *Int. J. Adv. Manuf. Technol.* **2018**, *97*, 2221–2230. [CrossRef]
201. Zhang, H.; Sun, Y.; Gong, W.; Cui, H. Growth Mechanism and Motion Trajectory of Lazy "S" in Friction Stir Welding Joint of 6082-T6 Aluminum Alloy. *SN Appl. Sci.* **2021**, *3*, 278. [CrossRef]
202. Pandya, S.; Mishra, R.S.; Arora, A. Channel Formation during Friction Stir Channeling Process—A Material Flow Study Using X-Ray Micro-Computed Tomography and Optical Microscopy. *J. Manuf. Process.* **2019**, *41*, 48–55. [CrossRef]
203. Simar, A.; Bréchet, Y.; de Meester, B.; Denquin, A.; Gallais, C.; Pardoen, T. Integrated Modeling of Friction Stir Welding of 6xxx Series Al Alloys: Process, Microstructure and Properties. *Prog. Mater. Sci.* **2012**, *57*, 95–183. [CrossRef]
204. Kalashnikova, T.; Knyazhev, E.; Gurianov, D.; Chumaevskii, A.; Vorontsov, A.; Kalashnikov, K.; Teryukalova, N.; Kolubaev, E. Structure, Mechanical Properties and Friction Characteristics of the Al-Mg-Sc Alloy Modified by Friction Stir Processing with the Mo Powder Addition. *Metals* **2022**, *12*, 1015. [CrossRef]
205. Sun, Y.B.; Chen, X.P.; Xie, J.; Wang, C.; An, Y.F.; Liu, Q. High Strain Rate Superplasticity and Secondary Strain Hardening of Al-Mg-Sc-Zr Alloy Produced by Friction Stir Processing. *Mater. Today Commun.* **2022**, *33*, 104217. [CrossRef]
206. Czechowski, M. Low-Cycle Fatigue of Friction Stir Welded Al-Mg Alloys. *J. Mater. Process. Technol.* **2005**, *164–165*, 1001–1006. [CrossRef]
207. Zha, M.; Tian, T.; Jia, H.-L.; Zhang, H.-M.; Wang, H.-Y. Sc/Zr Ratio-Dependent Mechanisms of Strength Evolution and Microstructural Thermal Stability of Multi-Scale Hetero-Structured Al–Mg–Sc–Zr Alloys. *J. Mater. Sci. Technol.* **2023**, *140*, 67–78. [CrossRef]
208. Zhemchuzhnikova, D.; Malopheyev, S.; Mironov, S.; Kaibyshev, R. Cryogenic Properties of Al–Mg–Sc–Zr Friction-Stir Welds. *Mater. Sci. Eng. A* **2014**, *598*, 387–395. [CrossRef]
209. Malopheyev, S.; Mironov, S.; Kulitskiy, V.; Kaibyshev, R. Friction-Stir Welding of Ultra-Fine Grained Sheets of Al–Mg–Sc–Zr Alloy. *Mater. Sci. Eng. A* **2015**, *624*, 132–139. [CrossRef]
210. Ma, Z.Y.; Mishra, R.S. Development of Ultrafine-Grained Microstructure and Low Temperature (0.48 Tm) Superplasticity in Friction Stir Processed Al–Mg–Zr. *Scr. Mater.* **2005**, *53*, 75–80. [CrossRef]
211. Mironov, S.; Malopheyev, S.; Vysotskiy, I.; Kaibyshev, R. Superplasticity of friction-stir welds of Zr-modified 5083 aluminum alloy with ultrafine-grained structure. *Defect Diffus. Forum* **2018**, *385*, 15–20. [CrossRef]
212. Vysotskiy, I.; Zhemchuzhnikova, D.; Malopheyev, S.; Mironov, S.; Kaibyshev, R. Microstructure Evolution and Strengthening Mechanisms in Friction-Stir Welded Al–Mg–Sc Alloy. *Mater. Sci. Eng. A* **2020**, *770*, 138540. [CrossRef]
213. Pereira, P.H.R.; Huang, Y.; Kawasaki, M.; Langdon, T.G. Achieving superplasticity in fine-grained Al-Mg-Sc alloys. *Mater. Sci. Forum* **2021**, *1016*, 11–17. [CrossRef]
214. He, P.; Bai, X.; Zhang, H. Microstructure Refinement and Mechanical Properties Enhancement of Wire and Arc Additively Manufactured 6061 Aluminum Alloy Using Friction Stir Processing Post-Treatment. *Mater. Lett.* **2023**, *330*, 133365. [CrossRef]
215. Rafieazad, M.; Mohammadi, M.; Gerlich, A.; Nasiri, A. Enhancing the Corrosion Properties of Additively Manufactured AlSi10Mg Using Friction Stir Processing. *Corros. Sci.* **2021**, *178*, 109073. [CrossRef]
216. Mondal, M.; Das, H.; Hong, S.-T.; Jeong, B.-S.; Han, H.N. Local Enhancement of the Material Properties of Aluminium Sheets by a Combination of Additive Manufacturing and Friction Stir Processing. *CIRP Ann.* **2019**, *68*, 289–292. [CrossRef]
217. Alidokht, S.A.; Abdollah-zadeh, A.; Soleymani, S.; Saeid, T.; Assadi, H. Evaluation of Microstructure and Wear Behavior of Friction Stir Processed Cast Aluminum Alloy. *Mater. Charact.* **2012**, *63*, 90–97. [CrossRef]
218. Cheng, W.; Liu, C.Y.; Ge, Z.J. Optimizing the Mechanical Properties of Al–Si Alloys through Friction Stir Processing and Rolling. *Mater. Sci. Eng. A* **2021**, *804*, 140786. [CrossRef]
219. Rao, A.G.; Ravi, K.R.; Ramakrishnarao, B.; Deshmukh, V.P.; Sharma, A.; Prabhu, N.; Kashyap, B.P. Recrystallization Phenomena During Friction Stir Processing of Hypereutectic Aluminum-Silicon Alloy. *Metall. Mater. Trans. A* **2013**, *44*, 1519–1529. [CrossRef]
220. Chumaevskii, V.; Indoitu, D.V.; Sudarikov, V.; Zykova, P.; Dobrovolsky, R.; Kalashnikova, T.A.; Rubtsov, V.E.; Kolubaev, E.A. Mechanical Properties and Structure Formation of Aluminum-Silicon Alloys after Friction Stir Processing. *Diagn. Resour. Mech. Mater. Struct.* **2021**, 44–59. [CrossRef]
221. Li, X.P.; Ji, G.; Chen, Z.; Addad, A.; Wu, Y.; Wang, H.W.; Vleugels, J.; Van Humbeeck, J.; Kruth, J.P. Selective laser melting of nano-TiB2decorated AlSi10Mg alloy with high fracture strength and ductility. *Acta Mater.* **2017**, *129*, 183–193. [CrossRef]
222. Kempen, K.; Thijs, L.; Humbeeck, J.V.; Kruth, J.-P. Processing AlSi10Mg by selective laser melting: Parameter optimisation and material characterisation. *Mater. Sci. Technol. (UK)* **2015**, *31*, 917–923. [CrossRef]
223. Kumar, K.S.A.; Yogesha, K.B. Experimental investigations to find the effect of post weld heat treatment (PWHT) on the microstructure and mechanical properties of FSW dissimilar joints of AA2024-T351 and AA7075-T651. *Mater. Today Proc.* **2021**, *49*, 243–249. [CrossRef]
224. Derazkola, H.A.; García, E.; Eyvazian, A.; Aberoumand, M. Effects of rapid cooling on properties of aluminum-steel friction stir welded joint. *Materials* **2021**, *14*, 908. [CrossRef]
225. Patel, P.; Rana, H.; Badheka, V.; Patel, V.; Li, W. Effect of active heating and cooling on microstructure and mechanical properties of friction stir–welded dissimilar aluminium alloy and titanium butt joints. *Weld. World* **2020**, *64*, 365–378. [CrossRef]

226. Mehta, K.P.; Badheka, V.J. Hybrid approaches of assisted heating and cooling for friction stir welding of copper to aluminum joints. *J. Mater. Process. Technol.* **2017**, *239*, 336–345. [CrossRef]
227. Qiao, Q.; Su, Y.; Li, Z.; Cui, Q.; Yu, H.; Ouyang, Q.; Zhang, D. Effect of Overlapping Region on Double-Sided Friction Stir Welded Joint of 120 mm Ultra-Thick SiCp/Al Composite Plates. *Mater. Sci. Eng. A* **2020**, *782*, 139238. [CrossRef]
228. Bakavos, D.; Prangnell, P.B. Effect of Reduced or Zero Pin Length and Anvil Insulation on Friction Stir Spot Welding Thin Gauge 6111 Automotive Sheet. *Sci. Technol. Weld. Join.* **2009**, *14*, 443–456. [CrossRef]
229. Prado, R.A.; Murr, L.E.; Soto, K.F.; McClure, J.C. Self-optimization in tool wear for friction-stir welding of Al 6061+20% Al2O3 MMC. *Mater. Sci. Eng. A* **2003**, *349*, 156–165. [CrossRef]
230. Colegrove, P.A.; Shercliff, H.R. Development of Trivex Friction Stir Welding Tool Part 1—Two-Dimensional Flow Modelling and Experimental Validation. *Sci. Technol. Weld. Join.* **2004**, *9*, 345–351. [CrossRef]
231. Scialpi, A.; De Filippis, L.A.C.; Cavaliere, P. Influence of Shoulder Geometry on Microstructure and Mechanical Properties of Friction Stir Welded 6082 Aluminium Alloy. *Mater. Des.* **2007**, *28*, 1124–1129. [CrossRef]
232. Colegrove, P.A.; Shercliff, H.R. Experimental and Numerical Analysis of Aluminium Alloy 7075-T7351 Friction Stir Welds. *Sci. Technol. Weld. Join.* **2003**, *8*, 360–368. [CrossRef]
233. Liu, H.J.; Feng, J.C.; Fujii, H.; Nogi, K. Wear characteristics of a WC–Co tool in friction stir welding of AC4A+ 30 vol% SiCp composite. *Int. J. Mach. Tools Manuf.* **2005**, *45*, 1635–1639. [CrossRef]
234. Prado, R.A.; Murr, L.E.; Shindo, D.J.; Soto, K.F. Tool wear in the friction-stir welding of aluminum alloy 6061 + 20% Al2O3: A preliminary study. *Scr. Mater.* **2001**, *45*, 75–80. [CrossRef]
235. Buchibabu, V.; Reddy, G.M.; De, A. Probing torque, traverse force and tool durability in friction stir welding of aluminum alloys. *J. Mater. Process. Technol.* **2017**, *241*, 86–92. [CrossRef]
236. Mironov, S.; Onuma, T.; Sato, Y.S.; Kokawa, H. Microstructure evolution during friction-stir welding of AZ31 magnesium alloy. *Acta Mater.* **2015**, *100*, 301–312. [CrossRef]
237. Feng, A.H.; Ma, Z.Y. Microstructural evolution of cast Mg–Al–Zn during friction stir processing and subsequent aging. *Acta Mater.* **2009**, *57*, 4248–4260. [CrossRef]
238. Woo, W.; Choo, H.; Prime, M.B.; Feng, Z.; Clausen, B. Microstructure, texture and residual stress in a friction-stir-processed AZ31B magnesium alloy. *Acta Mater.* **2008**, *56*, 1701–1711. [CrossRef]
239. Park, S.H.C.; Sato, Y.S.; Kokawa, H. Basal plane texture and flow pattern in friction stir weld of a magnesium alloy. *Metall. Mater. Trans. A* **2003**, *34*, 987–994. [CrossRef]
240. Liu, D.; Tang, Y.; Shen, M.; Hu, Y.; Zhao, L. Analysis of Weak Zones in Friction Stir Welded Magnesium Alloys from the Viewpoint of Local Texture: A Short Review. *Metals* **2018**, *8*, 970. [CrossRef]
241. Woo, W.; Choo, H.; Brown, D.W.; Liaw, P.K.; Feng, Z. Texture variation and its influence on the tensile behavior of a friction-stir processed magnesium alloy. *Scr. Mater.* **2006**, *54*, 1859–1864. [CrossRef]
242. Yuan, W.; Panigrahi, S.K.; Su, J.-Q.; Mishra, R.S. Influence of grain size and texture on Hall-Petch relationship for a magnesium alloy. *Scr Mater* **2011**, *65*, 994–997. [CrossRef]
243. Palanivel, S.; Mishra, R.S.; Davis, B.; DeLorme, R.; Doherty, K.J.; Cho, K.C. Effect of initial microstructure on the microstructural evolution and joint efficiency of a WE43 alloy during friction stir welding. In *Friction Stir Welding and Processing VII*; Springer: Berlin, Germany, 2013; pp. 253–261.
244. Cao, G.; Zhang, D.; Zhang, W.; Qiu, C. Microstructure evolution and mechanical properties of Mg–Nd–Y alloy in different friction stir processing conditions. *J. Alloys Compd.* **2015**, *636*, 12–19. [CrossRef]
245. Wang, W.; Han, P.; Qiao, K.; Li, T.; Wang, K.; Cai, J.; Wang, L. Liqiang Effect of the rotation rate on the low-cycle fatigue behavior of friction-stir welded AZ31 magnesium alloy. *Eng. Fract. Mech.* **2020**, *228*, 106925. [CrossRef]
246. Sahu, P.K.; Vasudevan, N.P.; Das, B.; Pal, S. Assessment of self-reacting bobbin tool friction stir welding for joining AZ31 magnesium alloy at inert gas environment. *J. Magnes. Alloy.* **2019**, *7*, 661–671. [CrossRef]
247. Mohamed, N.S.; Alias, J. The influence of friction stir welding of dissimilar AZ31 and AZ91 magnesium alloys on the microstructure and tensile properties. *Int. J. Automot. Mech. Eng.* **2019**, *16*, 6675–6683. [CrossRef]
248. Chauhan, A.; Kumar, S. Effect of friction stir welding parameters on impact strength of the AZ31 magnesium alloy joints. *Int. J. Mech. Prod. Eng. Res. Dev.* **2018**, *8*, 615–622.
249. Dorbane, A.; Ayoub, G.; Mansoor, B.; Hamade, R.F.; Kridli, G.; Shabadi, R.; Imad, A. Microstructural observations and tensile fracture behavior of FSW twin roll cast AZ31 Mg sheets. *Mater. Sci. Eng. A* **2016**, *649*, 190–200. [CrossRef]
250. Ugender, S.; Jayakrishna, S.; Francis, E.D. Influence of welding speed, axial force and rotational speed on the formation of friction stir welding zone in AZ31 magnesium alloy. *Int. J. Mech. Eng. Technol.* **2018**, *9*, 845–857.
251. Zhang, B.; Yuan, S.; Wang, X. Friction stir welding of AZ31 magnesium alloys processed by equal channel angular pressing. *Rare Met.* **2008**, *27*, 393–399. [CrossRef]
252. Zhang, H.; Ge, H.; Yang, J. Improved Gaussian Mixture PHD for close multi-target tracking. In Proceedings of the 2014 IEEE 7th Joint International Information Technology and Artificial Intelligence Conference, Chongqing, China, 20–21 December 2014; pp. 311–315. [CrossRef]
253. Wang, S.L.; Zhang, H.Y.; Li, X. Characteristics of Microstructure and Microhardness of Friction Stir Welded Joints for AZ31 Magnesium Alloy. *Appl. Mech. Mater.* **2014**, *472*, 612–616. [CrossRef]

254. Chowdhury, I.; Sengupta, K.; Kumar Maji, K.; Roy, S.; Ghosal, S. Experimental Study of Tool Wears to Join Al6026 Aluminium Alloy by Ultrasonic Assisted Friction Stir Welding. *Mater. Today Proc.* **2022**, *50*, 1221–1225. [CrossRef]
255. Meran, C. The Joint Properties of Brass Plates by Friction Stir Welding. *Mater. Des.* **2006**, *27*, 719–726. [CrossRef]
256. Cartigueyen, S.; Mahadevan, K. Study of friction stir processed zone under different tool pin profiles in pure copper. *IOSR J. Mech. Civ. Eng.* **2014**, *11*, 06–12. [CrossRef]
257. Thankachan, T.; Prakash, K.S.; Kavimani, V. Investigating the effects of hybrid reinforcement particles on the microstructural, mechanical and tribological properties of friction stir processed copper surface composites. *Compos. Part B Eng.* **2019**, *174*, 107057. [CrossRef]
258. Dinaharan, I.; Sathiskumar, R.; Murugan, N. Effect of ceramic particulate type on microstructure and properties of copper matrix composites synthesized by friction stir processing. *J. Mater. Res. Technol.* **2016**, *5*, 302–316. [CrossRef]
259. Ebrahimi, M.; Par, M.A. Twenty-year uninterrupted endeavor of friction stir processing by focusing on copper and its alloys. *J. Alloys Compd.* **2019**, *781*, 1074–1090. [CrossRef]
260. Zykova, A.; Chumaevskii, A.; Gusarova, A.; Gurianov, D.; Savchenko, N.; Kolubaev, E.; Tarasov, S.; Kalashnikova, T. Evolution of microstructure in friction stir processed dissimilar CuZn37/AA5056 stir zone. *Materials* **2021**, *14*, 5208. [CrossRef]
261. Zykova, A.; Chumaevskii, A.; Gusarova, A.; Kalashnikova, T.; Fortuna, S.; Savchenko, N.; Kolubaev, E.; Tarasov, S. Microstructure of in-situ friction stir processed Al-Cu transition zone. *Metals* **2020**, *10*, 818. [CrossRef]
262. Gusarova, A.V.; Chumaevskii, A.V.; Zykova, A.P.; Gur'yanov, D.A.; Kalashnikov, K.N.; Kalashnikova, T.A. Features of Forming a Structure of the Copper-Zinc Alloy Coating on the Aluminum Alloy Surface by Friction Stir Processing. *Russ. Phys. J.* **2020**, *63*, 1179–1185. [CrossRef]
263. Sathiskumar, R.; Dinaharan, I.; Murugan, N.; Vijay, S.J. Metallurgy of friction stir–processed Cu/B4C surface composite. *Emerg. Mater. Res.* **2013**, *2*, 27–31. [CrossRef]
264. Cheremnov, A.M.; Kalashnikova, T.A.; Chumaevskii, A.V.; Kalashnikov, K.N.; Teryukalova, N.V.; Beloborodov, V.A.; Kolubaev, E.A. Regularities of Structure Formation During Friction Stir Processing of CuAl9Mn2 Copper Alloy with Addition of Tungsten Powder to the Surface Layer. *Russ. Phys. J.* **2022**, *65*, 1224–1230. [CrossRef]
265. Xue, P.; Xiao, B.L.; Ma, Z.Y. High Tensile Ductility via Enhanced Strain Hardening in Ultrafine-Grained Cu. *Mater. Sci. Eng. A* **2012**, *532*, 106–110. [CrossRef]
266. Mukherjee, S.; Ghosh, A.K. Friction Stir Processing of Direct Metal Deposited Copper–Nickel 70/30. *Mater. Sci. Eng. A* **2011**, *528*, 3289–3294. [CrossRef]
267. Sahlot, P.; Jha, K.; Dey, G.K.; Arora, A. Quantitative Wear Analysis of H13 Steel Tool during Friction Stir Welding of Cu-0.8%Cr-0.1%Zr Alloy. *Wear* **2017**, *378–379*, 82–89. [CrossRef]
268. Rai, R.; De, A.; Bhadeshia, H.K.D.H.; DebRoy, T. Review: Friction stir welding tools. *Sci. Technol. Weld. Join.* **2011**, *16*, 325–342. [CrossRef]
269. Dawes, C.J.; Thomas, W.M. Friction stir process welds aluminum alloys. *Weld. J.* **1996**, *75*, 41–45.
270. Nicholas, E.D.; Thomas, W.M. A review of friction processes for aerospace applications. *Int. J. Mater. Prod. Technol.* **1998**, *13*, 45–55.
271. Thomas, W.M.; Threadgill, P.L.; Nicholas, E.D. Feasibility of friction stir welding steel. *Sci. Technol. Weld. Join.* **1999**, *4*, 365–372. [CrossRef]
272. Thomas, W.M. Friction stir welding—Recent developments. *Mater. Sci. Forum.* **2003**, *426–432*, 229–236. [CrossRef]
273. Kumar, K.; Kailas, S.V.; Srivatsan, T.S. Influence of tool geometry in friction stir welding. *Mater. Manuf. Process.* **2008**, *23*, 189–195. [CrossRef]
274. Hattingh, D.G.; Blignault, C.; Van Niekerk, T.I.; James, M.N. Characterization of the influences of FSW tool geometry on welding forces and weld tensile strength using an instrumented tool. *J. Mater. Process. Technol.* **2008**, *203*, 46–57. [CrossRef]
275. Nandan, R.; DebRoy, T.; Bhadeshia, H. Recent advances in friction-stir welding–process, weldment structure and properties. *Prog. Mater. Sci.* **2008**, *53*, 980–1023. [CrossRef]
276. Mishra, R.S.; Mahoney, M.W. *Friction Stir Welding and Processing*; ASM International: Materials Park, OH, USA, 2007; p. 360.
277. Raffo, P.L. Yielding and fracture in tungsten and tungsten-rhenium alloys. *J. Less-Common. Met.* **1969**, *7*, 133–149. [CrossRef]
278. Thompson, B.; Babu, S.S. Tool degradation characterization in the friction stir welding of hard metals. *Weld. J.* **2010**, *89*, 256s–261s.
279. Miyazawa, T.; Iwamoto, Y.; Maruko, T.; Fujii, H. Development of high strength Ir based alloy tool for friction stir welding. *Sci. Technol. Weld. Join.* **2012**, *17*, 213–218. [CrossRef]
280. Song, K.H.; Nakata, K. Effect of precipitation on postheat-treated Inconel 625 alloy after friction stir welding. *Mater. Design.* **2010**, *31*, 2942–2947. [CrossRef]
281. Song, K.H.; Nakata, K. Microstructural and mechanical properties of friction-stir-welded and post-heattreated inconel 718 alloy. *J. Alloy Compd.* **2010**, *505*, 144–150. [CrossRef]
282. Song, K.H.; Nakata, K. Mechanical properties of frictionstir-welded Inconel 625 alloy. *Mater. Trans.* **2009**, *50*, 2498–2501. [CrossRef]
283. Sato, Y.S.; Arkom, P.; Kokawa, H.; Nelson, T.W.; Steel, R.J. Effect of microstructure on properties of friction stir welded Inconel alloy 600. *Mat. Sci. Eng. A-Struct.* **2008**, *477*, 250–258. [CrossRef]
284. Choi, D.H.; Lee, C.Y.; Ahn, B.W.; Choi, J.H.; Yeon, Y.M.; Song, K.; Park, H.S.; Kim, Y.J.; Yoo, C.D.; Jung, S.B. Frictional Wear Evaluation of WC–Co Alloy Tool in Friction Stir Spot Welding of Low Carbon Steel Plates. *Int. J. Refract. Met. Hard Mater.* **2009**, *27*, 931–936. [CrossRef]

285. Isa, M.S.M.; Moghadasi, K.; Ariffin, M.A.; Raja, S.; Muhamad, M.R.B.; Yusof, F.; Jamaludin, M.F.; Yusoff, N.B.; Karim, M.S.B.A. Recent research progress in friction stir welding of aluminium and copper dissimilar joint: A review. *J. Mater. Res. Technol.* **2021**, *15*, 2735–2780. [CrossRef]
286. Bhattacharjee, R.; Biswas, P. Review on thermo-mechanical and material flow analysis of dissimilar friction stir welding. *Weld. Int.* **2021**, *35*, 295–332. [CrossRef]
287. Zykova, A.; Vorontsov, A.; Chumaevskii, A.; Gurianov, D.; Savchenko, N.; Gusarova, A.; Kolubaev, E.; Tarasov, S. In Situ Intermetallics-Reinforced Composite Prepared Using Multi-Pass Friction Stir Processing of Copper Powder on a Ti6Al4V Alloy. *Materials* **2022**, *15*, 2428. [CrossRef]
288. Kumar, M.; Kumar, R.; Kore, S.D. Modeling and analysis of effect of tool geometry on temperature distribution and material flow in friction stir welding of AA6061-T6. *J. Braz. Soc. Mech. Sci. Eng.* **2022**, *44*, 153. [CrossRef]
289. Lu, X.; Luan, Y.; Meng, X.; Zhou, Y.; Zhao, N.; Liang, S.Y. Temperature distribution and mechanical properties of FSW medium thickness aluminum alloy 2219. *Int. J. Adv. Manuf. Technol.* **2022**, *119*, 7229–7241. [CrossRef]
290. Yu, M.; Zhao, H.; Xu, F.; Chen, T.; Zhou, L.; Song, X.; Ma, N. Influence of ultrasonic vibrations on the microstructure and mechanical properties of Al/Ti friction stir lap welds. *J. Mater. Process. Technol.* **2020**, *282*, 116676. [CrossRef]
291. Dorbane, A.; Mansoor, B.; Ayoub, G.; Shunmugasamy, V.C.; Imad, A. Mechanical, microstructural and fracture properties of dissimilar welds produced by friction stir welding of AZ31B and Al6061. *Mater. Sci. Eng. A* **2016**, *651*, 720–733. [CrossRef]
292. Esmaeili, A.; Rajani, H.R.Z.; Sharbati, M.; Givi, M.K.B.; Shamanian, M. The role of rotation speed on intermetallic compounds formation and mechanical behavior of friction stir welded brass/aluminum 1050 couple. *Intermetallics* **2011**, *19*, 1711–1719. [CrossRef]
293. Esmaeili, A.; Givi, M.K.B.; Rajani, H.R.Z. A metallurgical and mechanical study on dissimilar Friction Stir welding of aluminum 1050 to brass (CuZn30). *Mater. Sci. Eng. A* **2011**, *528*, 7093–7102. [CrossRef]
294. Boucherit, A.; Avettand-Fènoël, M.-N.; Taillard, R. Effect of a Zn interlayer on dissimilar FSSW of Al and Cu. *Mater. Des.* **2017**, *124*, 87–99. [CrossRef]
295. Patel, N.P.; Parlikar, P.; Dhari, R.S.; Mehta, K.; Pandya, M. Numerical modelling on cooling assisted friction stir welding of dissimilar Al-Cu joint. *J. Manuf. Process.* **2019**, *47*, 98–109. [CrossRef]
296. Mabuwa, S.; Msom, V.I. The effect of friction stir processing on the friction stir welded AA1050-H14 and AA6082-T6 joints. *Mater. Today Proc.* **2020**, *26*, 193–199. [CrossRef]
297. Das, U.; Das, R.; Toppo, V. Dry sliding wear behavior study on friction stir weld joints of dissimilar aluminum alloys. *Mater. Today Proc.* **2020**, *26*, 1815–1821. [CrossRef]
298. Shunmugasundaram, M.; Kumar, A.P.; Sankar, L.P.; Sivasankar, S. Optimization of process parameters of friction stir welded dissimilar AA6063 and AA5052 aluminum alloys by Taguchi technique. *Mater. Today Proc.* **2020**, *27*, 871–876. [CrossRef]
299. Huang, G.; Feng, X.; Shen, Y.; Zheng, Q.; Zhao, P. Friction stir brazing of 6061 aluminum alloy and H62 brass: Evaluation of microstructure, mechanical and fracture behavior. *Mater. Des.* **2016**, *99*, 403–411. [CrossRef]
300. Shojaeefard, M.H.; Khalkhali, A.; Akbari, M.; Tahani, M. Application of Taguchi optimization technique in determining aluminum to brass friction stir welding parameters. *Mater. Des.* **2013**, *52*, 587–592. [CrossRef]
301. Akbari, M.; Behnagh, R.A. Dissimilar Friction-Stir Lap Joining of 5083 Aluminum Alloy to CuZn34 Brass. *Metall. Mater. Trans. B* **2012**, *43*, 1177–1186. [CrossRef]
302. Huang, T.; Zhang, Z.; Liu, J.; Chen, S.; Xie, Y.; Meng, X.; Huang, Y.; Wan, L. Interface Formation of Medium-Thick AA6061 Al/AZ31B Mg Dissimilar Submerged Friction Stir Welding Joints. *Materials* **2022**, *15*, 5520. [CrossRef]
303. Xue, P.; Xiao, B.L.; Ni, D.R.; Ma, Z.Y. Enhanced mechanical properties of friction stir welded dissimilar Al–Cu joint by intermetallic compounds. *Mater. Sci. Eng. A* **2010**, *527*, 5723–5727. [CrossRef]
304. Muhammad, N.A.; Wu, C.S.; Tian, W. Effect of ultrasonic vibration on the intermetallic compound layer formation in Al/Cu friction stir weld joints. *J. Alloys Compd.* **2019**, *785*, 512–522. [CrossRef]
305. Zhou, L.; Zhang, R.X.; Li, G.H.; Zhou, W.L.; Huang, Y.X.; Song, X.G. Effect of pin profile on microstructure and mechanical properties of friction stir spot welded Al-Cu dissimilar metals. *J. Manuf. Process.* **2018**, *36*, 1–9. [CrossRef]
306. Shankar, S.; Vilaça, P.; Dash, P.; Chattopadhyaya, S.; Hloch, S. Joint strength evaluation of friction stir welded Al-Cu dissimilar alloys. *Measurement* **2019**, *146*, 892–902. [CrossRef]
307. Khojastehnezhad, V.M.; Pourasl, H.H. Microstructural characterization and mechanical properties of aluminum 6061-T6 plates welded with copper insert plate (Al/Cu/Al) using friction stir welding. *Trans. Nonferrous Met. Soc. China* **2018**, *28*, 415–426. [CrossRef]
308. Dias, F.; Cipriano, G.; Correia, A.N.; Braga, D.F.O.; Moreira, P.; Infante, V. Joining of Aluminum Alloy AA7075 and Titanium Alloy Ti-6Al-4V through a Friction Stir Welding-Based Process. *Metals* **2023**, *13*, 249. [CrossRef]
309. MKar, A.; Choudhury, S.K.; Suwas, S.; Kailas, S.V. Effect of niobium interlayer in dissimilar friction stir welding of aluminum to titanium. *Mater. Charact.* **2018**, *145*, 402–412. [CrossRef]
310. Wu, A.; Song, Z.; Nakata, K.; Liao, J.; Zhou, L. Interface and properties of the friction stir welded joints of titanium alloy Ti6Al4V with aluminum alloy 6061. *Mater. Des.* **2015**, *71*, 85–92. [CrossRef]
311. Amirov, A.I.; Beloborodov, V.A.; Ivanov, A.N.; Zhukov, L.L. Lap welded joint of aluminum and titanium alloy by friction stir welding. *Proc. Int. Conf. Adv. Mater. Hierarchical Struct. New Technol. Reliab. Struct.* **2018**, *2051*, 020013. [CrossRef]

312. Kalinenko, A.; Dolzhenko, P.; Borisova, Y.; Malopheyev, S.; Mironov, S.; Kaibyshev, R. Tailoring of Dissimilar Friction Stir Lap Welding of Aluminum and Titanium. *Metals* **2022**, *10*, 8418. [CrossRef] [PubMed]
313. Amirov, A.; Eliseev, A.; Kolubaev, E.; Filippov, A.; Rubtsov, V. Wear of ZhS6U Nickel Superalloy Tool in Friction Stir Processing on Commercially Pure Titanium. *Metals* **2020**, *10*, 799. [CrossRef]
314. Chen, Z.W.; Yazdanian, S. Microstructures in interface region and mechanical behaviours of friction stir lap Al6060 to Ti–6Al–4V welds. *Mater. Sci. Eng. A* **2015**, *634*, 37–45. [CrossRef]
315. Simar, A.; Avettand-Fenoel, M.-N. State of the art about dissimilar metal friction stir welding. Sci. Technol. *Weld. Join.* **2017**, *22*, 389–403. [CrossRef]
316. Jain, S.; Bhuva, K.; Patel, P.; Badheka, V.J. A Review on Dissimilar Friction Stir Welding of Aluminum Alloys to Titanium Alloys. In *Innovations in Infrastructure. Advances in Intelligent Systems and Computing*; Springer: Singapore, 2019. [CrossRef]
317. Dressler, U.; Biallas, G.; Mercado, U.A. Friction stir welding of titanium alloy TiAl6V4 to aluminium alloy AA2024-T3. *Mater. Sci. Eng. A* **2009**, *526*, 113–117. [CrossRef]
318. Deng, H.; Chen, Y.; Jia, Y.; Pang, Y.; Zhang, T.; Wang, S.; Yin, L. Microstructure and mechanical properties of dissimilar NiTi/Ti6Al4V joints via back-heating assisted friction stir welding. *J. Manuf. Process.* **2021**, *64*, 379–391. [CrossRef]
319. Yuhua, C.; Yuqing, M.; Weiwei, L.; Peng, H. Investigation of welding crack in micro laser welded NiTiNb shape memory alloy and Ti6Al4V alloy dissimilar metals joints. *Opt. Laser Technol.* **2017**, *91*, 197–202. [CrossRef]
320. Chen, Y.; Sun, S.; Zhang, T.; Zhou, X.; Li, S. Effects of post-weld heat treatment on the microstructure and mechanical properties of laser-welded NiTi/304SS joint with Ni filler. *Mater. Sci. Eng. A* **2020**, *771*, 138545. [CrossRef]
321. Prabhu, L.; Satish Kumar, S. Tribological Characteristics of FSW Tool Subjected to Joining of Dissimilar AA6061-T6 and Cu Alloys. *Mater. Today Proc.* **2020**, *33*, 741–745. [CrossRef]
322. Sudhakar, M.; Rao, C.H.S.; Saheb, K.M. Production of Surface Composites by Friction Stir Processing-A Review. *Mater. Today Proc.* **2018**, *5*, 929–935. [CrossRef]
323. Barati, M.; Abbasi, M.; Abedini, M. The effects of friction stir processing and friction stir vibration processing on mechanical, wear and corrosion characteristics of Al6061/SiO2 surface composite. *J. Manuf. Process.* **2019**, *45*, 491–497. [CrossRef]
324. Bourkhani, R.D.; Eivani, A.R.; Nateghi, H.R. Through-thickness inhomogeneity in microstructure and tensile properties and tribological performance of friction stir processed AA1050-Al2O3 nanocomposite. *Compos. Part B Eng.* **2019**, *174*, 107061. [CrossRef]
325. Abraham, S.J.; Dinaharan, I.; Selvam, J.D.R.; Akinlabi, E.T. Microstructural characterization of vanadium particles reinforced AA6063 aluminum matrix composites via friction stir processing with improved tensile strength and appreciable ductility. *Compos. Commun.* **2019**, *12*, 54–58. [CrossRef]
326. Jain, V.K.S.; Varghese, J.; Muthukumaran, S. Effect of First and Second Passes on Microstructure and Wear Properties of Titanium Dioxide-Reinforced Aluminum Surface Composite via Friction Stir Processing. *Arab. J. Sci. Eng.* **2019**, *44*, 949–957. [CrossRef]
327. Nazari, M.; Eskandari, H.; Khodabakhshi, F. Production and characterization of an advanced AA6061-Graphene-TiB2 hybrid surface nanocomposite by multi-pass friction stir processing. *Surf. Coat. Technol.* **2019**, *377*, 124914. [CrossRef]
328. Mahmoud, E.R.I.; Al-qozaim, A.M.A. Fabrication of In-Situ Al–Cu Intermetallics on Aluminum Surface by Friction Stir Processing. *Arab. J. Sci. Eng.* **2016**, *41*, 1757–1769. [CrossRef]
329. Adetunla, A.; Akinlabi, E. Fabrication of Aluminum Matrix Composites for Automotive Industry Via Multipass Friction Stir Processing Technique. *Int. J. Automot. Technol.* **2019**, *20*, 1079–1088. [CrossRef]
330. Dinaharan, I.; Akinlabi, E.T. Low cost metal matrix composites based on aluminum, magnesium and copper reinforced with fly ash prepared using friction stir processing. *Compos. Commun.* **2018**, *9*, 22–26. [CrossRef]
331. Azimi-Roeen, G.; Kashani-Bozorg, S.F.; Nosko, M.; Nagy, Š.; Mat'ko, I. Correction to: Formation of Al/(Al13Fe4 + Al2O3) Nano-composites via Mechanical Alloying and Friction Stir Processing. *J. Mater. Eng. Perform.* **2018**, *27*, 6800. [CrossRef]
332. Huang, C.W.; Aoh, J.N. Friction stir processing of copper-coated SiC particulate-reinforced aluminum matrix composite. *Materials* **2018**, *11*, 599. [CrossRef]
333. Fotoohi, H.; Lotfi, B.; Sadeghian, Z.; Byeon, J. Microstructural characterization and properties of in situ Al-Al3Ni/TiC hybrid composite fabricated by friction stir processing using reactive powder. *Mater. Charact.* **2019**, *149*, 124–132. [CrossRef]
334. Kumar, P.A.; Madhu, H.C.; Pariyar, A.; Perugu, C.S.; Kailas, S.V.; Garg, U.; Rohatgi, P. Friction stir processing of squeeze cast A356 with surface compacted graphene nanoplatelets (GNPs) for the synthesis of metal matrix composites. *Mater. Sci. Eng. A* **2020**, *769*, 138517. [CrossRef]
335. Zhang, Q.; Xiao, B.L.; Wang, Q.Z.; Ma, Z.Y. In situ Al3Ti and Al2O3 nanoparticles reinforced Al composites produced by friction stir processing in an Al-TiO2 system. *Mater. Lett.* **2011**, *65*, 2070–2072. [CrossRef]
336. Kalashnikova, T.A.; Gusarova, A.V.; Chumaevskii, A.V.; Knyazhev, E.O.; Shvedov, M.A.; Vasilyev, P.A. Regularities of composite materials formation using additive electron-beam technology, friction stir welding and friction stir processing. *Met. Work. Mater. Sci.* **2019**, *21*, 94–112. [CrossRef]
337. Gusarova, A.V.; Chumaevskii, A.V.; Osipovich, K.S.; Kalashnikov, K.N.; Kalashnikova, T.A. Regularities of structural changes after friction stir processing in materials obtained by the additive method. *Nanosci. Technol. An Int. J.* **2020**, *11*, 195–205. [CrossRef]
338. Fernandez, G.J.; Murr, L.E. Characterization of Tool Wear and Weld Optimization in the Friction-Stir Welding of Cast Aluminum 359+20% SiC Metal-Matrix Composite. *Mater. Charact.* **2004**, *52*, 65–75. [CrossRef]

339. Zuo, L.; Shao, W.; Zhang, X.; Zuo, D. Investgation on Tool Wear in Friction Stir Welding of SiCp/Al Composites. *Wear* **2022**, *498–499*, 204331. [CrossRef]
340. Eliseev, A.A.; Fortuna, S.V.; Kalashnikova, T.A.; Chumaevskii, A.V.; Kolubaev, E.A. Structural Phase Evolution in Ultrasonic-Assisted Friction Stir Welded 2195 Aluminum Alloy Joints. *Russ. Phys. J.* **2017**, *60*, 1022–1026. [CrossRef]
341. Sato, Y.S.; Park, S.H.C.; Matsunaga, A.; Honda, A.; Kokawa, H. Novel production for highly formable Mg alloy plate. *J. Mater. Sci.* **2005**, *40*, 637–642. [CrossRef]
342. Kalashnikova, T.A.; Kalashnikov, K.N.; Shvedov, M.A.; Vasilyev, P.A. Structure and properties of copper compensator joints obtained by hybrid friction stir welding technology. *Met. Work. Mater. Sci.* **2019**, *21*, 85–93. [CrossRef]
343. Fall, A.; Fesharaki, M.H.; Khodabandeh, A.R.; Jahazi, M. Tool Wear Characteristics and Effect on Microstructure in Ti-6Al-4V Friction Stir Welded Joints. *Metals* **2016**, *6*, 275. [CrossRef]
344. Reynolds, A.P.; Hood, E.; Tang, W. Texture in Friction Stir Welds of Timetal 21S. *Scr. Mater.* **2005**, *52*, 491–494. [CrossRef]
345. Ramulu, M.; Gangwar, K.; Cantrell, A.; Laxminarayana, P. Study of Microstructural Characteristics and Mechanical Properties of Friction Stir Welded Three Titanium Alloys. *Mater. Today Proc.* **2018**, *5*, 1082–1092. [CrossRef]
346. Kumarsingh, A.; Kumar, D. Thermo-Mechanical Analysis of Friction Stir Welding Tool (W-Alloy and Ti-Alloy). *REST J. Emerg. Trends Model. Manuf.* **2017**, *3*, 37–43.
347. John, R.; Jata, K.V.; Sadananda, K. Residual Stress Effects on Near-Threshold Fatigue Crack Growth in Friction Stir Welds in Aerospace Alloys. *Int. J. Fatigue* **2003**, *25*, 939–948. [CrossRef]
348. Kosturek, R.; Wachowski, M.; Szak, T.; Sek, L.; Mierzyński, J.; Sobczak, U. Research on the Friction Stir Welding of Titanium Grade 1. *MATEC Web Conf.* **2018**, *242*, 1–5. [CrossRef]
349. Karna, S.; Cheepu, M.; Venkateswarulu, D.; Srikanth, V. Recent Developments and Research Progress on Friction Stir Welding of Titanium Alloys: An Overview. *IOP Conf. Ser. Mater. Sci. Eng.* **2018**, *330*, 012068. [CrossRef]
350. Kim, J.-D.; Jin, E.-G.; Murugan, S.P.; Park, Y.-D. Recent Advances in Friction-Stir Welding Process and Microstructural Investigation of Friction Stir Welded Pure Titanium. *J. Weld. Join.* **2017**, *35*, 6–15. [CrossRef]
351. Charit, I.; Mishra, R.S.; Mahoney, M.W. Multi-Sheet Structures in 7475 Aluminum by Friction Stir Welding in Concert with Post-Weld Superplastic Forming. *Scr. Mater.* **2002**, *47*, 631–636. [CrossRef]
352. Gangwar, K.; Ramulu, M.; Cantrell, A.; Sanders, D.G. Microstructure and Mechanical Properties of Friction Stir Welded Dissimilar Titanium Alloys: TIMET-54M and ATI-425. *Metals* **2016**, *6*, 252. [CrossRef]
353. Liu, H.J.; Zhou, L. Microstructural Zones and Tensile Characteristics of Friction Stir Welded Joint of TC4 Titanium Alloy. *Trans. Nonferrous Met. Soc. China* **2010**, *20*, 1873–1878. [CrossRef]
354. Lee, W.B.; Lee, C.Y.; Chang, W.S.; Yeon, Y.M.; Jung, S.B. Microstructural Investigation of Friction Stir Welded Pure Titanium. *Mater. Lett.* **2005**, *59*, 3315–3318. [CrossRef]
355. Mashinini, P.M.; Dinaharan, I.; Raja, J.D.; Hattingh, D.G. Microstructure Evolution and Mechanical Characterization of Friction Stir Welded Titanium Alloy Ti–6Al–4V Using Lanthanated Tungsten Tool. *Mater. Charact.* **2018**, *139*, 328–336. [CrossRef]
356. Shinde, G.; Gajghate, S.; Dabeer, P.S.; Seemikeri, C.Y. Low Cost Friction Stir Welding: A Review. *Mater. Today Proc.* **2017**, *4*, 8901–8910. [CrossRef]
357. Mironov, S.; Sato, Y.S.; Kokawa, H. Journal of Materials Science & Technology Friction-Stir Welding and Processing of Ti-6Al-4V Titanium Alloy: A Review. *J. Mater. Sci. Technol.* **2018**, *34*, 58–72. [CrossRef]
358. Seighalani, K.R.; Givi, M.K.B.; Nasiri, A.M.; Bahemmat, P. Investigations on the Effects of the Tool Material, Geometry, and Tilt Angle on Friction Stir Welding of Pure Titanium. *J. Mater. Eng. Perform.* **2010**, *19*, 955–962. [CrossRef]
359. Liu, F.C.; Liao, J.; Gao, Y.; Nakata, K. Influence of Texture on Strain Localization in Stir Zone of Friction Stir Welded Titanium. *J. Alloys Compd.* **2015**, *626*, 304–308. [CrossRef]
360. Mironov, S.; Sato, Y.S.; Kokawa, H. Grain Structure Evolution during Friction-Stir Welding. *Phys. Mesomech.* **2020**, *23*, 21–31. [CrossRef]
361. Ramulu, M.; Greenwell, T.; Labossiere, P. Full-Field Strain Behavior Of Friction Stir-Welded Titanium Alloy By Digital Image Correlation. *Appl. Mech. Mater.* **2014**, *692*, 490–496. [CrossRef]
362. Sanders, D.G.; Edwards, P.; Cantrell, A.M.; Gangwar, K.; Ramulu, M. Friction Stir-Welded Titanium Alloy Ti-6Al-4V: Microstructure, Mechanical and Fracture Properties. *JOM* **2015**, *67*, 1054–1063. [CrossRef]
363. Lauro, A. Friction Stir Welding of Titanium Alloys. *Weld. Int.* **2012**, *26*, 8–21. [CrossRef]
364. Amirov, A.I.; Eliseev, A.A.; Beloborodov, V.A.; Chumaevskii, A.V.; Gurianov, D.A. Formation of α′ Titanium Welds by Friction Stir Welding. *J. Phys. Conf. Ser.* **2020**, 1611. [CrossRef]
365. Amirov, A.I.; Chumaevskii, A.V.; Vorontsov, A.V. Formation of (α + β) Titanium Welds by Friction Stir Welding Using Heat-Resistant Alloy Tool. *AIP Conf. Proc.* **2020**, *2310*, 020017. [CrossRef]
366. Amirov, A.; Moskvichev, E.; Ivanov, A.; Chumaevskii, A.; Beloborodov, V. Formation Features of a Welding Joint of Alloy Ti-5Al-3Mo-1V by the Friction Stir Welding Using Heat-Resistant Tool from ZhS6 Alloy. *Obrab. Met.* **2022**, *24*, 53–63. [CrossRef]
367. Amirov, A.; Utyaganova, V.; Beloborodov, V.; Eliseev, A. Formation Features of a Welding Joint of Alloy Grade2 by the Friction Stir Welding Using Temperature Resistant Tools. Met. Work. *Mater. Sci.* **2019**, *21*, 72–82. [CrossRef]
368. Amirov, A.; Chumaevskii, A.; Savchenko, N.; Gurianov, D.; Nikolaeva, A.; Krasnoveykin, V.; Ivanov, A.; Rubtsov, V.; Kolubaev, E. Features of Permanent Joints of Titanium (α + β)-Alloys Obtained by Friction Stir Welding Using a Nickel Superalloy Tool. *Metals* **2023**, *13*, 222. [CrossRef]

369. Ramulu, M.; Labossiere, P.; Greenwell, T. Elastic-Plastic Stress/Strain Response of Friction Stir-Welded Titanium Butt Joints Using Moiré Interferometry. *Opt. Lasers Eng.* **2010**, *48*, 385–392. [CrossRef]
370. Du, S.; Liu, H.; gao, Y.; Hu, Y.; Zhou, L. Effects of Process Parameters on Joint Formation and Tool Wear Behavior in Friction Stir Welded TA5 Alloy. *Int. J. Adv. Manuf. Technol.* **2022**, *123*, 2531–2547. [CrossRef]
371. Mironov, S.; Zhang, Y.; Sato, Y.S.; Kokawa, H. Development of Grain Structure in β-Phase Field during Friction Stir Welding of Ti-6Al-4V Alloy. *Scr. Mater.* **2008**, *59*, 27–30. [CrossRef]
372. Mironov, S.; Sato, Y.S.; Kokawa, H. Development of Grain Structure during Friction Stir Welding of Pure Titanium. *Acta Mater.* **2009**, *57*, 4519–4528. [CrossRef]
373. Amirov, A.I.; Eliseev, A.A.; Rubtsov, V.E.; Utyaganova, V.R. Butt Friction Stir Welding of Commercially Pure Titanium by the Tool from a Heat-Resistant Nickel Alloy. *AIP Conf. Proc.* **2019**, *2167*, 020016. [CrossRef]
374. Brassington, W.D.P.; Colegrove, P.A. Alternative Friction Stir Welding Technology for Titanium–6Al–4V Propellant Tanks within the Space Industry. Sci. Technol. *Weld. Join.* **2017**, *22*, 300–318. [CrossRef]
375. Raut, N.; Yakkundi, V.; Sunnapwar, V.; Medhi, T.; Jain, V.K.S. A Specific Analytical Study of Friction Stir Welded Ti-6Al-4V Grade 5 Alloy: Stir Zone Microstructure and Mechanical Properties. *J. Manuf. Process.* **2022**, *76*, 611–623. [CrossRef]
376. Eliseev, A.A.; Amirov, A.I.; Filippov, A.V. Influence of Axial Force on the Pure Titanium Surface Relief during Friction Stir Processing. *AIP Conf. Proc.* **2019**, *2167*, 020077. [CrossRef]
377. Farias, A.; Batalha, G.F.; Prados, E.F.; Magnabosco, R.; Delijaicov, S. Tool Wear Evaluations in Friction Stir Processing of Commercial Titanium Ti-6Al-4V. *Wear* **2013**, *302*, 1327–1333. [CrossRef]
378. Jiang, L.; Huang, W.; Liu, C.; Chai, L.; Yang, X.; Xu, Q. Microstructure, Texture Evolution and Mechanical Properties of Pure Ti by Friction Stir Processing with Slow Rotation Speed. *Mater. Charact.* **2019**, *148*, 1–8. [CrossRef]
379. Costa, A.M.S.; Oliveira, J.P.; Pereira, V.F.; Nunes, C.A.; Ramirez, A.J.; Tschiptschin, A.P. Ni-Based Mar-M247 Superalloy as a Friction Stir Processing Tool. *J. Mater. Process. Technol.* **2018**, *262*, 605–614. [CrossRef]
380. Rodelas, J.; Lippold, J. Characterization of Engineered Nickel-Base Alloy Surface Layers Produced by Additive Friction Stir Processing. *Metallogr. Microstruct. Anal.* **2013**, *2*, 1–12. [CrossRef]
381. Singh, A.K.; Ratrey, P.; Astarita, A.; Franchitti, S.; Mishra, A.; Arora, A. Enhanced Cytocompatibility and Mechanical Properties of Electron Beam Melted Ti-6Al-4V by Friction Stir Processing. *J. Manuf. Process.* **2021**, *72*, 400–410. [CrossRef]
382. Singh, A.K.; Kaushik, L.; Singh, J.; Das, H.; Mondal, M.; Hong, S.T.; Choi, S.H. Evolution of Microstructure and Texture in the Stir Zone of Commercially Pure Titanium during Friction Stir Processing. *Int. J. Plast.* **2022**, *150*, 103184. [CrossRef]
383. Zhang, Y.; Sato, Y.S.; Kokawa, H.; Park, S.H.C.; Hirano, S. DuStir zone microstructure of commercial purity titanium friction stir welded using pcBN tool. *Mater. Sci. Eng. A* **2008**, *488*, 25–30. [CrossRef]
384. Edwards, P.D.; Ramulu, M. Investigation of microstructure, surface and subsurface characteristics in titanium alloy friction stir welds of varied thicknesses. *Sci. Technol. Weld. Join.* **2009**, *14*, 476–483. [CrossRef]
385. Liu, H.J.; Zhou, L.; Liu, Q.W. Microstructural evolution mechanism of hydrogenated Ti–6Al–4V in the friction stir welding and post-weld dehydrogenation process. *Scr. Mater.* **2009**, *61*, 1008–1011. [CrossRef]
386. Zhou, L.; Liu, H.J. Effect of 0.3 wt.% hydrogen addition on microstructural evolution of Ti–6Al–4V alloy in the friction stir welding and post-weld dehydrogenation process. *Mater. Charact.* **2011**, *62*, 1036–1041. [CrossRef]
387. Wu, L.H.; Xue, P.; Xiao, B.L.; Ma, Z.Y. Achieving superior low-temperature superplasticity for lamellar microstructure in nugget of a friction stir welded Ti-6Al-4V joint. *Scr. Mater.* **2016**, *122*, 26–30. [CrossRef]
388. Li, B.; Shen, Y.; Hu, W.; Luo, L. Surface modification of Ti–6Al–4V alloy via friction-stir processing: Microstructure evolution and dry sliding wear performance. *Surf. Coat. Technol.* **2014**, *239*, 160–170. [CrossRef]
389. Pilchak, A.L.; Tang, W.; Sahiner, H.; Reynolds, A.P.; Williams, J.C. Microstructure Evolution during Friction Stir Welding of Mill-Annealed Ti-6Al-4V. *Metall. Mater. Trans. A* **2010**, *42*, 745–762. [CrossRef]
390. Wang, J.; Su, J.; Mishra, R.S.; Xu, R.; Baumann, J.A. A Preliminary Study of Deformation Behavior of Friction Stir Welded Ti-6Al-4V. *J. Mater. Eng. Perform.* **2014**, *23*, 3027–3033. [CrossRef]
391. Lippold, J.C.; Livingston, J.J. Microstructure Evolution During Friction Stir Processing and Hot Torsion Simulation of Ti-6Al-4V. *Metall. Mater. Trans. A* **2013**, *44*, 3815–3825. [CrossRef]
392. Edwards, P.D.; Ramulu, M. Comparative study of fatigue and fracture in friction stir and electron beam welds of 24mm thick titanium alloy Ti-6Al-4V. *Fatigue Fract. Eng. Mater. Struct.* **2016**, *39*, 1226–1240. [CrossRef]
393. Muzvidziwa, M.; Okazaki, M.; Suzuki, K.; Hirano, S. Role of microstructure on the fatigue crack propagation behavior of a friction stir welded Ti–6Al–4V. *Mater. Sci. Eng. A* **2016**, *652*, 59–68. [CrossRef]
394. Yoon, S.; Ueji, R.; Fujii, H. Effect of initial microstructure on Ti–6Al–4V joint by friction stir welding. *Mater. Des.* **2015**, *88*, 1269–1276. [CrossRef]
395. Zhang, W.; Ding, H.; Cai, M.; Yang, W.; Li, J. Low-temperature superplastic deformation mechanism in Ti–6Al–4V alloy processed by friction stir processing. *Mater. Sci. Eng. A* **2019**, *764*, 138261. [CrossRef]
396. Zhang, W.; Liu, H.; Ding, H.; Fujii, H. Superplastic deformation mechanism of the friction stir processed fully lamellar Ti-6Al-4V alloy. *Mater. Sci. Eng. A* **2020**, *785*, 139390. [CrossRef]
397. Zhang, W.; Ding, H.; Cai, M.; Yang, W.; Li, J. Ultra-grain refinement and enhanced low-temperature superplasticity in a friction stir-processed Ti-6Al-4V alloy. *Mater. Sci. Eng. A* **2018**, *727*, 90–96. [CrossRef]

398. Zykova, A.P.; Vorontsov, A.V.; Chumaevskii, A.V.; Gurianov, D.A.; Gusarova, A.V.; Savchenko, N.L.; Kolubaev, E.A. The Influence of Multipass Friction Stir Processing on Formation of Microstructure and Mechanical Properties of Ti6Al4V Alloy. *Russ. J. Non-Ferrous Met.* **2022**, *63*, 167–176. [CrossRef]
399. Zhang, C.; Ding, Z.; Xie, L.; Zhang, L.-C.; Wu, L.; Fu, Y.; Wang, L.; Lu, W. Electrochemical and in vitro behavior of the nanosized composites of Ti-6Al-4V and TiO2 fabricated by friction stir process. *Appl. Surf. Sci.* **2017**, *423*, 331–339. [CrossRef]
400. Xie, L.; Wang, L.; Wang, K.; Yin, G.; Fu, Y.; Zhang, D.; Lu, W.; Hua, L.; Zhang, L.-C. TEM characterization on microstructure of Ti–6Al–4V/Ag nanocomposite formed by friction stir processing. *Materialia* **2018**, *3*, 139–144. [CrossRef]
401. da Silva, M.V.; Bruno, S.; Freitasa, X.; da Silva, A.M.; Ferrinho, C.V.; Nabil, P.; Ismênia, C.M.; Fariaa, S.T.; Coelhoa, G.C.; Nunes, C.A. Processing and characterization of high aluminum multicomponent (Co,Ni)-based superalloys for friction stir welding (FSW) tools. *Mater. Today Commun.* **2020**, *25*, 101282.
402. Maniscalco, J.; Elmustafa, A.A.; Bhukya, S.; Wu, Z. Numerical Simulation of the Donor-Assisted Stir Material for Friction Stir Welding of Aluminum Alloys and Carbon Steel. *Metals* **2023**, *13*, 164. [CrossRef]
403. Li, J.; Cao, F.; Shen, Y. Effect of welding parameters on friction stir welded Ti–6Al–4V joints: Temperature, microstructure and mechanical properties. *Metals.* **2020**, *10*, 940. [CrossRef]
404. Wu, L.H.; Wang, D.; Xiao, B.L.; Ma, Z.Y. Tool wear and its effect on microstructure and properties of friction stir processed Ti–6Al–4V. *Mater. Chem. Phys.* **2014**, *146*, 512–522. [CrossRef]
405. Mironov, S.; Zhang, Y.; Sato, Y.S.; Kokawa, H. Crystallography of transformed b microstructure in friction stir welded Ti–6Al–4V alloy. *Scr. Mater.* **2008**, *59*, 511–514. [CrossRef]
406. Mochizuki, N.; Takasugi, T.; Kaneno, Y.; Oki, S.; Hirata, T. Friction Stir Welding of 430 Stainless Steel and Pure Titanium Using Ni3Al-Ni3V Dual Two-Phase Intermetallic Alloy Tool. In Proceedings of the 1st International Joint Symposium on Joining and Welding, Osaka, Japan, 6–8 November 2013; Elsevier: Amsterdam, The Netherlands, 2013; pp. 465–471.
407. Zhang, Y.; Sato, Y.S.; Kokawa, H.; Park, S.H.C.; Hirano, S. Microstructural characteristics and mechanical properties of Ti–6Al–4V friction stir welds. *Mater. Sci. Eng. A* **2008**, *485*, 448–455. [CrossRef]
408. Adesina, A.Y.; Iqbal, Z.; Al-Badour, F.A.; Gasem, Z.M. Mechanical and Tribological Characterization of AlCrN Coated Spark Plasma Sintered W–25%Re–Hfc Composite Material for FSW Tool Application. *J. Mater. Res. Technol.* **2019**, *8*, 436–446. [CrossRef]